



TESTING COSMOLOGICAL MODELS

WILL THE REAL NON-GAUSSIANITY PLEASE STAND UP

Jeppe Trøst Nielsen

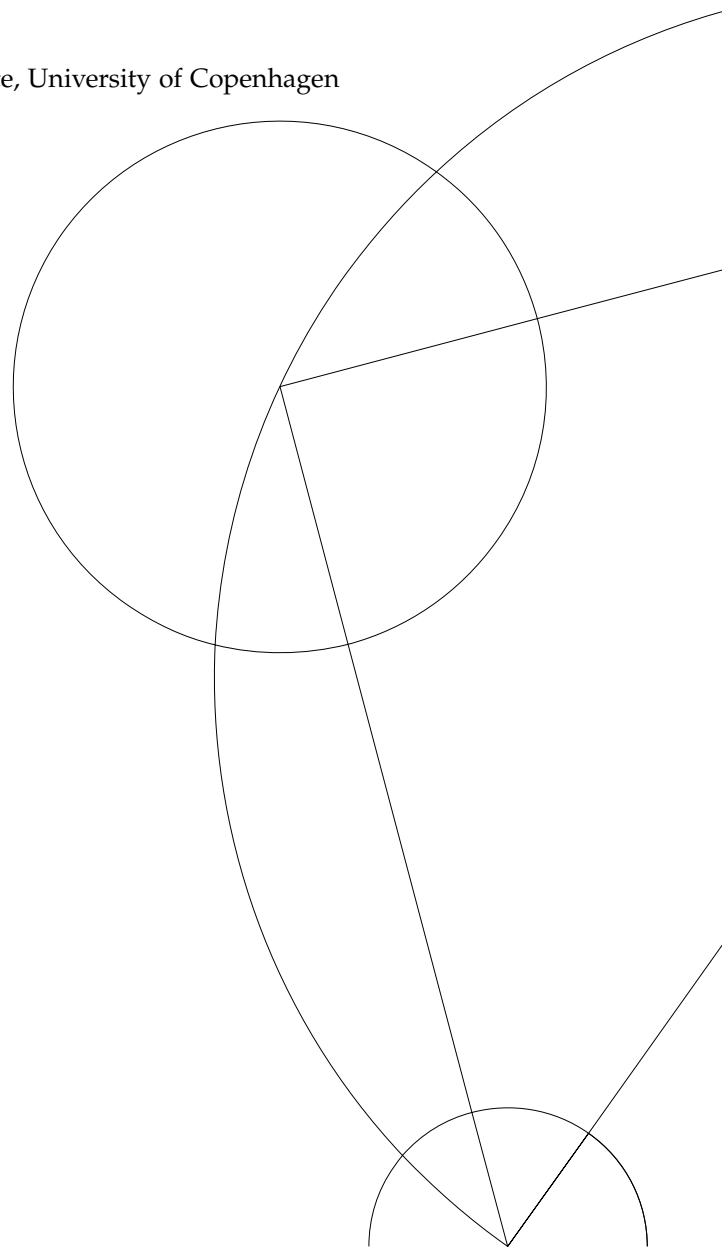
Niels Bohr International Academy, Niels Bohr Institute, University of Copenhagen

July 3rd, 2017

Academic supervisor:

Subir Sarkar

This thesis has been submitted to the PhD School
of The Faculty of Science, University of Copenhagen



I am resolved; 'tis but a three years' fast:
The mind shall banquet, though the body pine:
Fat paunches have lean pates, and dainty bits
Make rich the ribs, but bankrupt quite the wits.

Love's labour's lost

ABSTRACT

The concordance model of cosmology is remarkable for its apparent simplicity, and vast range of predictions. Yet its two most well known and infamous ingredients, dark energy and inflation, have so far avoided all attempts at direct observation. Even so, theorists invent ever more exotic models, and experiments must keep up at an ever increasing pace, preserving both precision and accuracy in the analysis.

In this thesis I compute corrections to large scale structure observables, corrections we expect solely due to general relativity. The calculations can be perceived in two ways. The pessimist will say these effects are unwanted systematics in the search for primordial physics, the optimist will see it as a chance to test general relativity to ever increasing precision. Regardless, these effects must be computed as part of the interpretation of coming observations.

I calculate the predicted bispectrum in galaxy number counts from general relativistic effects. This includes in particular lensing, which will systematically shift the observed bispectrum for observations of large scale structure. Furthermore, I develop and explore a scheme for fast computation of the galaxy number count spectra, in the flat-sky approximation.

The last part of the work is a numerical analysis of the resulting spectra. I analyse both the potential observability of individual bispectra, and their correction due to general relativistic effects. It is clear from the results that lensing must be carefully included in any attempt at accurately extracting primordial bispectra.

SAMMENFATNING

Den kosmologiske overensstemmelsesmodel er bemærkelsesværdig på grund af sin tilsyneladende enkelhed og samtidige lange række af forudsigelser. Modellens to mest berømte og berygtede ingredienser, mørk energi og inflation, har hidtil undvejet alle vores forsøg på direkte observation. Alligevel opfinder teoretikere mere og mere eksotiske modeller, og eksperimenter skal således holde trit med stadigt stigende tempo, og samtidigt bevare både præcision og nøjagtighed i deres analyse.

I denne afhandling beregner jeg korrektioner til observable i storskala struktur, korrektioner vi forventer udelukkende fra generel relativitetsteori. Beregningerne kan således ses fra to vinkler. Pessimisten vil sige, at disse effekter er uønskede systematiske fejl i vores jagt efter 'big bang' fysik. Optimisten derimod ser det som en chance for at teste generel relativitetsteori mere præcist end nogensinde. Uanset hvad må disse korrektioner beregnes som led i fortolkningen af kommende observationer.

Jeg beregner det forudsagte bispektrum i galakseantallet fra generel relativitetsteori. Dette omfatter især linseffekter, som systematisk vil ændre det observerede bispektrum for observationer af storskala struktur. Desuden udvikler og udforsker jeg et system til hurtig beregning af galakseantalsspektrene, hvor jeg gør brug af at tilnærme himlen som værende flad.

Den sidste del af arbejdet er en numerisk analyse af de resulterende spektre. Jeg analyserer både den potentielle synlighed af individuelle bispektre og deres korrektioner på grund af generel relativitetsteori. Det fremgår klart af resultaterne, at linseffekter omhyggeligt må inddrages i vores forsøg på nøjagtigt at bestemme bispektre fra big bang.

PREFACE

Many people in many places have contributed to the completion of this thesis. First and foremost I am very happy to have had Subir Sarkar supervise me and invariably cheer me on, both when things go according to plan, and when they do not. Without his patience and insistence, my work the last four years would have been very dull indeed.

I would also like to thank professor Ruth Durrer who introduced me to the calculations of galaxy number counts. Working with Ruth and the group at the Université de Genève was a great one hundred days.

Some of my work in the last four years is not included here. In particular the paper I wrote with Laure Berthier on a possible treatment of theoretical uncertainties in fitting data to for example effective field theories (Berthier and Nielsen, 2016). I am very proud of this work, but its subject is very different from the cosmological calculations presented here, and therefore I chose to leave it out. I recommend reading *her* thesis for an in-depth presentation of these results.

I have also chosen to not discuss further my work with Subir Sarkar and Alberto Guffanti, showing that the evidence for cosmic acceleration from type Ia supernovae is marginal (Nielsen et al., 2016), as it is presented in my Master's thesis (Nielsen, 2015).

My work would not have been possible without the continued support from both old and new at the Niels Bohr Institute, in particular Andy, Chris, Alberto, Subir, Sebastian, Amel, Meera, and finally and most notably Laure *qui me supporte toujours*.

I hope you will enjoy reading.

CONTENTS

| | |
|--|----|
| ABSTRACT | iv |
| SAMMENFATNING | v |
| PREFACE | vi |
| 1 INTRODUCTION | 1 |
| 2 IMMEDIATE MATHEMATICAL ASIDE | 5 |
| 2.1 Random fields | 5 |
| 2.1.1 Fourier transforming random fields | 8 |
| 2.2 Random fields on the sky | 9 |
| 2.2.1 Spin-weighted spherical harmonics | 12 |
| 2.3 The flat sky approximation | 14 |
| 2.3.1 Results about $3j$ symbols | 15 |
| 3 COSMOLOGICAL PERTURBATIONS | 19 |
| 3.1 Generation of perturbations | 20 |
| 3.2 Evolution of perturbations | 21 |
| 3.2.1 The Newtonian universe | 22 |
| 3.2.2 The early universe | 24 |
| 4 OBSERVATIONS ON THE SKY | 27 |
| 4.1 Cosmic microwave background | 29 |
| 4.1.1 Cosmic variance | 30 |
| 4.1.2 Computing the primordial bispectrum in the CMB on a flat sky | 34 |
| 4.2 Large scale structure | 36 |
| 4.2.1 Geodesic lightcone coordinates | 38 |
| 4.2.2 Galaxy number count perturbation from GLC to Poisson gauge | 41 |
| 4.2.3 All-order result at small scales | 46 |
| 4.2.4 Comparison with Bertacca et al. (2014b) | 51 |
| 4.2.5 Comparison with Yoo and Zaldarriaga (2014) | 52 |
| 4.2.6 Explicit extension to higher perturbative orders | 54 |
| 4.2.7 Galaxy count power spectrum | 55 |
| 4.2.8 Galaxy count bispectrum | 56 |
| 4.2.9 Computing the primordial bispectrum of the galaxy number count | 59 |

| | | |
|--------|---|-----|
| 4.2.10 | Computing the bispectrum of the galaxy number count on a flat sky | 60 |
| 4.2.11 | Computing the primordial galaxy bispectrum on a flat sky | 77 |
| 4.2.12 | Redshift binning and shot noise | 81 |
| 4.2.13 | Next-to-leading order corrections | 84 |
| 5 | A THEORETICIAN'S EXPERIMENT | 89 |
| 5.1 | The model | 90 |
| 5.2 | Computational observations | 91 |
| 5.3 | General relativistic pollution of simple galaxy bispectra | 96 |
| 6 | FINAL REMARKS | 101 |

INTRODUCTION

The concordance model of cosmology is well equipped to explain numerous observations of large experiments. The standard model of cosmology has two main components: dark energy, denoted by Λ , and cold dark matter (CDM). Λ CDM, the combination of the two on a homogeneous and isotropic background, is able to explain observations from the very early universe to the very late. The spectrum of the cosmic microwave background, the earliest photons we can ever observe, can be fitted by just *six* important parameters (Ade et al., 2016). With only few additions, the same parameters seem to be able to explain the large scale structure in the late universe – the clumps of galaxies, galaxy groups, and the large filaments stretching across the universe. As such, the detailed structure on these largest scales in the universe become an important probe for our understanding beyond the six parameters. Perhaps the small neutrino masses will be observed as a minute effect in the clustering of galaxies, or exotic theories of gravity may show themselves as small effects beyond Einstein’s relativity. Common to the observation of physics beyond the standard cosmology is its small effects – the gross features of the universe have been observed, and Λ CDM is *de facto* the reigning theory, despite its theoretical shortcomings (Sarkar, 2008). Given the small size of the higher order effects, we must compute the predictions of the theories more and more precisely. Indeed to distinguish two theories from each other – even very different theories – can come down to the small contributions in higher order observables. To test which is the better description of nature requires precision calculations.

A well-known higher-order observable is the three point correlation, or the bispectrum of the perturbations in the universe. Observing *truly primordial* non-gaussianities in the three point correlator has the potential to be a great guide to the physics just moments after the big bang. Inflation in all its incarnations, to be predictive, will dictate certain slightly non-gaussian statistics in the early quantum fluctuations of the universe. The observation of such non-gaussianities, although not a smoking gun, will guide the hand of theorists for the coming waves of theories of primordial physics. As with all higher order observables, it does unfortunately hide behind unwanted noise, both terrestrial, astrophysical and cosmic. The cosmic microwave background is literally at the edge of the universe, and we must be sure we are not seeing the effects of the dust on its way, be it in the Milky Way, our more distant neighbours, or the enormous clouds of dust spanning the cosmos.

Recently Tutusaus et al. (2017) questioned the direct evidence for the model from low-redshift probes, and found that there is little to no preference for Λ CDM over non-accelerated universes.

Correlators are the quantities describing the expectation value of fluctuations. Three-point correlators describe the expectation value of the product of the value of a field evaluated at three points. Since the quantum fluctuations are very small, the n -point correlators of the primordial field shrink as n grows – therefore the three-point correlator is a higher order observable, ie. higher order in the initial, small field.

The large scale structure on the other hand, we *know*, has three-point correlations – general relativity predicts them. It is therefore necessary to calculate these predictions with the same precision one hopes to observe the primordial prediction. Non-linear evolution of the cosmic structure formation along with gravitational lensing effects are just some of the effects that must be understood to exquisite precision if we hope to see deviations from the standard theory.

Three point correlations are far from the only interesting thing to look for. In recent news, gravitational waves, both primordial and astrophysical, have featured on a lot of frontpages – and for good reason. Observation of primordial gravitational waves – or more practically, a particular pattern of polarization in the cosmic microwaves – is a so far unverified prediction of inflation, and one that would put it on a much more solid foundation (Krauss et al., 2010). Unfortunately general relativity predicts contamination of this signal. As the light travels through the universe, it is *lensed*, and this creates the same patterns as the primordial gravitational waves. Foregrounds such as dust may also pollute the observed signal, and so far has prevented detection of primordial gravitational waves – if they exist (Ade et al., 2015).

Astrophysical gravitational waves, on the other hand, are not just swirly patterns in the observed photon polarization, but rather are the direct detection of space-time perturbations. All information we have about the universe so far has been carried by light. Whether it be the light from the early primordial plasma, light from supernovae or simply starlight, it has always been electromagnetic radiation which kept us informed. If the observations of gravitational waves live up to their hype, they will be not just new observations, but a new way of observing altogether (Abbott et al., 2016a). A large amount of work has gone into the detection and understanding of these *very* tiny undulations of space-time. However it is still not clear that the signals and the detector noise have been completely understood (Creswell et al., 2017; Liu and Jackson, 2016; Naselsky et al., 2016).

In the meantime, we must explore all available options. If higher-order correlators carry information, we must find it. To distinguish it from known physics, we must weed out *all traces* of the old. In this thesis I focus on the bispectrum of galaxies and the cosmic microwaves. While the latter has been thoroughly explored (Ade et al., 2014b), the former is still in development (Bertacca et al., 2014a; Di Dio et al., 2014; Yoo and Zaldarriaga, 2014). The main contributions presented in this work are the development of the flat sky approximation to galaxy surveys, and the extension of the calculation of dominant terms in the galaxy distribution, at small scales, to all orders in perturbation theory. The long calculation of the flat sky quantities and their comparison with the full sky calculation allows for a significant decrease in computation time. The *proof* of the all-order calculation of dominating terms at small scales is also included, as it was only conjectured in the earlier paper on the matter. The explicit comparison of the three calculations in the recent literature has already been published (Nielsen and Durrer, 2017), the rest has not.

There are indeed papers dating back to before the COBE years talking about primordial bispectra. Komatsu and Spergel (2000) already comment that even Planck would not be able to see the bispectrum from the most vanilla, single-field slow-roll inflation. Naturally, one may hope for even more exotic theories – ones that Planck might just see – or for galaxy surveys to come to the rescue.

These two developments – flat sky and the use of dominant terms – combined allow me to do realistic galaxy survey computations, including redshift binning, for higher multipoles than has been done before. The flat sky calculations I do are not restricted to the dominating terms however. One proviso is that one expects the flat sky approximation to hold at relatively high multipoles, where in any case the remaining terms are small. The calculational technique, however, is generic. These calculations help both in the computation of the general relativistic effects *and* the effects of a primordial bispectrum.

I try throughout to combine mathematics and physical insight. Especially the flat-sky approximation will give us a great deal of intuition on the physics, which is easily lost in the full-sky calculation. Certain terms will have a very natural interpretation, which will be clear only when comparing the results of the two methods.

This work should be seen in continuation of my previous thesis, written two years ago ([Nielsen, 2015](#)). It served as the extension of our work on supernova analyses ([Nielsen et al., 2016](#)). In it, I introduced basic concepts of probability theory, the evolution of the perfectly homogeneous and isotropic universe, and various discussions on non-standard theories of the cosmos. All of these topics are also useful in the current context, but will not be repeated. That means the level of discussion in the following starts beyond these topics.

The following chapters are ordered chronologically, according to the universe. The necessary mathematics comes first, in chapter 2. Chapter 3 introduces cosmological perturbations, their generation, and evolution. Observing these perturbations is the main part of the work, and chapter 4 is the tour de force through the calculations of both signal and noise in these observations. Finally, chapter 5 presents some computations showing what we can expect to find, and chapter 6 the concluding remarks.

IMMEDIATE MATHEMATICAL ASIDE

The purpose of the current chapter is two-fold. The first is to set in stone the notations and conventions I will be using, and the second to keep a record of results I will use, so expect to see references back to this chapter in the following. It is my hope that a dive into the mathematics will help give you a clearer physical picture of what is going on. Doing it this way the mathematics will be set, and excessive derivations can be kept out of the way of physical results in the rest of the work. The nature of this chapter does not entice new results, although I hope a number of approximations I find are new to some.

The following sections will go through random fields, in particular random gaussian fields and small excursions from these; we will put the random fields on the sky and study the spherical harmonics and related identities; and lastly we take a look at how to simplify the computations by employing the flat sky approximation, and to which degree we can trust the results.

For an introduction to basic probability theory, see eg. the first chapter of [Nielsen \(2015\)](#).

2.1 RANDOM FIELDS

The great tragedy of cosmology is our inability to make exact predictions about the state of the universe. The physical laws we follow only predict the behavior of space and matter. The only way we know how to set the boundary conditions are by way of statistical methods, ie. randomness. However, given knowledge about the probability distributions of the initial conditions, and the deterministic evolution, we may still predict eg. moments of distributions of matter and radiation in the early and late universe. To treat this, we need to look at the concept of a *random field*.

Random fields are the natural evolution of random variables and stochastic processes. The random variable does not have a sense of place or distance to other random variables. It may be the observation of light from a distant source, or the blip in a detector. The random field is putting a random variable at every point in eg. a vector space. Now the variables have an intimate relation to each other, and we may talk of the distance between them. For standard cosmology the interesting fields are homogeneous and isotropic – fields for which the statistical properties depend

neither on the exact location nor the orientation of the observer. As always, this puts enormous constraints on the allowed structures.

Just as the gaussian distribution is the go-to distribution for random variables, the gaussian random field is a good starting point for us. Just as the gaussian random variable is completely described by its mean and covariance, the gaussian random field is completely described by its mean and two-point correlator. The two-point correlator of the random field $f(\mathbf{x})$ is defined just like the covariance

$$\zeta(\mathbf{x}, \mathbf{y}) = \langle f(\mathbf{x})f(\mathbf{y}) \rangle \quad (2.1.1)$$

where $\langle \dots \rangle$ is the ensemble average. In general, this is a function of both variables and is the function describing completely the gaussian field. However, imposing isotropy and homogeneity on f has great effect on the correlator. Homogeneity means only the relative positions of \mathbf{x} and \mathbf{y} can be important, and isotropy means the result cannot depend on an absolute angle. Homogeneity removes three degrees of freedom, the three dimensions of translational invariance, and isotropy removes a further two, the angles. We can write up all three scenarios

$$\zeta(\mathbf{x}, \mathbf{y}) = \begin{cases} \zeta(0, \mathbf{x} - \mathbf{y}) & \text{homogeneous} \\ \zeta(\mathbf{x}, |\mathbf{x} - \mathbf{y}|) & \text{isotropic around } \mathbf{x} \\ \zeta(0, |\mathbf{x} - \mathbf{y}|) & \text{both} \end{cases} \quad (2.1.2)$$

So as long as we are dealing with the case of the (assumed) homogeneous and isotropic universe, the two-point correlator is a function of only one variable, the distance $r = |\mathbf{x} - \mathbf{y}|$ between the points of interest $\zeta = \zeta(r)$. All higher point correlators of the gaussian field are, analogously to the case of a random variable, completely specified by this function. In the case of a zero-mean random gaussian field, we have

$$\zeta(\mathbf{x}_1, \dots, \mathbf{x}_n) = \begin{cases} \langle f(\mathbf{x}_1) \dots f(\mathbf{x}_n) \rangle = 0 & \text{for } n \text{ odd} \\ \langle f(\mathbf{x}_1) \dots f(\mathbf{x}_n) \rangle = \sum_{\text{pairings}} \prod \zeta(r_{ij}) & \text{for } n \text{ even} \end{cases} \quad (2.1.3)$$

where the sum goes over all possible pairings of the n random variables, the product goes over all the pairs, and $r_{ij} = |\mathbf{x}_i - \mathbf{x}_j|$. It is customary to define a *connected* correlator or, in a sense, the non-gaussian part of the correlator. We may define them recursively as follows,

$$\zeta_c(\mathbf{x}) = \zeta(\mathbf{x}) \quad (2.1.4)$$

$$\sum_{\text{partitions}} \prod \zeta_c(\mathbf{x}_i, \dots, \mathbf{x}_j) = \zeta(\mathbf{x}_1, \dots, \mathbf{x}_n) \quad (2.1.5)$$

where the sum goes over all partitions (not just pairs) of the \mathbf{x}_i , and the product over all the terms in the partition. This means in particular for us,

$$\zeta_c(\mathbf{x}, \mathbf{y}) = \zeta(\mathbf{x}, \mathbf{y}) - \zeta(\mathbf{x})\zeta(\mathbf{y}) \quad (2.1.6)$$

$$\zeta_c(\mathbf{x}, \mathbf{y}, \mathbf{z}) = \zeta(\mathbf{x}, \mathbf{y}, \mathbf{z}) - \zeta(\mathbf{x}, \mathbf{y})\zeta(\mathbf{z}) - \zeta(\mathbf{x})\zeta(\mathbf{y}, \mathbf{z}) - \zeta(\mathbf{z}, \mathbf{x})\zeta(\mathbf{y}) + 2\zeta(\mathbf{x})\zeta(\mathbf{y})\zeta(\mathbf{z}) \quad (2.1.7)$$

This already sounds a lot like the cosmological principle – and it is! We will indeed assume the matter distribution of the Universe is homogeneous and isotropic. Without these assumptions, the analysis becomes much harder.

This is known as Isserlis' theorem, (Isserlis, 1916), or in the context of particle physics as Wick's theorem, (Wick, 1950).

In statistical mechanics, this is known as the Ursell function, (Ursell, 1927). It was initially constructed to compute thermodynamic observables in imperfect gases.

Note that the connected correlator takes care of removing the mean of the field for us. The combinations of Isserlis' theorem and connected correlators will prove very useful in the computation of cosmological bispectra. In particular we will encounter random fields, which are not exactly gaussian, but whose non-gaussian part can be written as the product of gaussian fields. Say we have the random field f given by

$$f^{(2)}(\mathbf{x}) = af_0(\mathbf{x}) + a^2 f_1(\mathbf{x})f_2(\mathbf{x}) \quad (2.1.8)$$

where all f_i are zero-mean gaussian fields with correlation function $\langle f_i(\mathbf{x})f_j(\mathbf{y}) \rangle = \xi_{ij}(\mathbf{x}, \mathbf{y})$ and a is a small parameter. Let us see what the connected three-point function looks like to lowest order in a . Employing directly equation (2.1.7) we get

$$\begin{aligned} \xi_c^{(2)}(\mathbf{x}, \mathbf{y}, \mathbf{z}) = a^4 & [\xi_{10}(\mathbf{x}, \mathbf{y})\xi_{20}(\mathbf{x}, \mathbf{z}) + \xi_{10}(\mathbf{y}, \mathbf{z})\xi_{20}(\mathbf{y}, \mathbf{x}) + \xi_{10}(\mathbf{z}, \mathbf{x})\xi_{20}(\mathbf{z}, \mathbf{y}) \\ & + \xi_{20}(\mathbf{x}, \mathbf{y})\xi_{10}(\mathbf{x}, \mathbf{z}) + \xi_{20}(\mathbf{y}, \mathbf{z})\xi_{10}(\mathbf{y}, \mathbf{x}) + \xi_{20}(\mathbf{z}, \mathbf{x})\xi_{10}(\mathbf{z}, \mathbf{y})] + \mathcal{O}(a^6) \end{aligned} \quad (2.1.9)$$

It should now be clearer why it is called the *connected* correlator: each term above connects the three points, and there is no term like $\xi(\mathbf{x}, \mathbf{x})\xi(\mathbf{y}, \mathbf{z})$, where one coordinate is left alone. This calculation is illustrated in figure 1, where the diagrams appear in the same order as the terms in the equation.

In light of the above, we also see that the connected three-point function of a homogeneous, isotropic field is only a function of the lengths of the three distances between the points, $\xi_c = \xi_c(|\mathbf{x} - \mathbf{y}|, |\mathbf{z} - \mathbf{y}|, |\mathbf{x} - \mathbf{z}|)$.

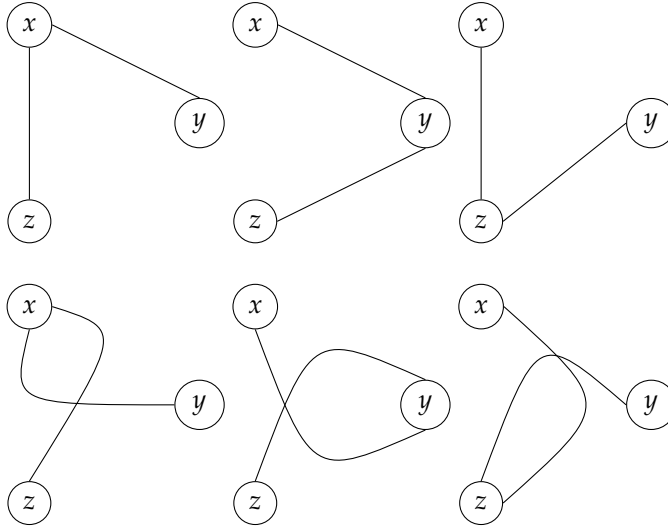


Figure 1: Illustration of the different terms of the *connected* three-point correlator. A line between two points designates a two-point correlator. In any figure here, any point can be reached by any other by walking along connecting lines. Permuting the lines here corresponds to permuting the indices 1 and 2 in the correlators.

2.1.1 Fourier transforming random fields

All the previous discussion was in real-space. The correlator tells us something about correlations between different points in space. Given the correlator of a gaussian field we showed that all other properties of the field were fixed. What happens when we Fourier transform the random field, and what can we say about its Fourier coefficients?

Given a homogeneous, isotropic random field f , we construct the Fourier transform

$$\hat{f}(\mathbf{k}) = \int d^n x f(x) \exp(ix \cdot \mathbf{k}) \quad (2.1.10)$$

where n is the dimension of the space. We now ask what are the properties of the correlators of \hat{f} . They turn out, not surprisingly, to be very simple,

$$\begin{aligned} \langle \hat{f}(\mathbf{k}) \hat{f}(\mathbf{k}') \rangle &= \int d^n x d^n x' \langle f(x) f(x') \rangle \exp(ix' \cdot \mathbf{k}' + ix \cdot \mathbf{k}) \\ &= \int d^n (x' - x) \xi(|x - x'|) \exp(i(x' - x) \cdot \mathbf{k}') \int d^n x' \exp(ix \cdot (\mathbf{k} + \mathbf{k}')) \\ &= (2\pi)^n \delta^{(n)}(\mathbf{k} + \mathbf{k}') \int d^n X \xi(x) \exp(-iXk \cos \theta) \equiv (2\pi)^n \delta^{(n)}(\mathbf{k} + \mathbf{k}') P(k) \end{aligned} \quad (2.1.11)$$

where $P(k)$ is called the *power spectrum*. This last integral can be solved in general in terms of hypergeometric functions. Writing the volume element in spherical coordinates as $d^n X = r^{n-1} dr d\Omega_{n-1}$, where Ω_{n-1} is the solid angle in n dimensions, we can recursively generate the next dimension by adding another angle, call it θ_{n-1} , going from 0 to π . We must then extend the measure as $d^{n+1} X = d^n X r \sin^{n-1} \theta_{n-1} d\theta_{n-1}$. In these coordinates, we fix the angle between the two vectors to be θ_{n-1} and integrate all the others out. That leaves us the volume of the unit ball in $n - 1$ dimensions. The rest of the integral is ugly, but can be written down in terms of a hypergeometric function:

$$\int d^n X \xi(X) \exp(-iXk \cos \theta) = \Omega_{n-2} \sqrt{\pi} \frac{\Gamma(\frac{1+n}{2})}{\Gamma(1 + \frac{n}{2})} \int dr r^{n-1} \xi(r) {}_0F_1(1 + \frac{n}{2}; kr) \quad (2.1.12)$$

It is now explicit that $P(k)$ is only a function of the size of k , not its direction. In three dimensions the result takes the form

$$P(k) = 4\pi \int dr r^2 \frac{\sin(kr)}{kr} \xi(r) \quad (2.1.13)$$

An analogous argument shows that the bispectrum, the Fourier transform of the three-point function, is only a function of the lengths of the three k s, just like the three point correlator is a function of the lengths between the coordinates,

$$\langle \hat{f}(\mathbf{k}_1) \hat{f}(\mathbf{k}_2) \hat{f}(\mathbf{k}_3) \rangle \equiv (2\pi)^n \delta^{(n)}(\mathbf{k}_1 + \mathbf{k}_2 + \mathbf{k}_3) B(k_1, k_2, k_3) \quad (2.1.14)$$

This fixes my Fourier convention: I include the $(2\pi)^{-n}$ and the minus in the exponential when doing the integral over k -space. That means there are no factors here.

This is again due to the fact that only the sides of the triangle of ks matter, not the orientation or location of the triangle.

The different bispectra of the universe is what will concern us for the most part of this work, and as such I will not go to higher cumulants here. The next thing that will concern us is how this all translates to observations made in the sky.

2.2 RANDOM FIELDS ON THE SKY

Just as we defined random fields in \mathbb{R}^n before, we now would like to know how the results translate into things we observe. As cosmological observations typically take place on the sky, we need to know how our functions behave on the sky. A particularly well-suited set of functions are the spherical harmonics, $Y_{\ell m}$. These are the simultaneous eigenfunctions of the Laplacian and the ∂_ϕ differential operator on the 2-sphere,

$$\nabla^2 Y_{\ell m} = -\ell(\ell + 1)Y_{\ell m} \quad \partial_\phi Y_{\ell m} = imY_{\ell m} \quad (2.2.1)$$

I will use the convention that the functions integrate to 1 over the sphere. The spherical harmonics will be our sines and cosines, or rather complex exponentials, of the 2-sphere. Just as we expanded the functions in \mathbb{R}^3 in Fourier modes, we would like to expand functions on S^2 in spherical harmonics.

Since the $Y_{\ell m}$ were constructed to be orthogonal on the sphere, we have immediately that the expansion parameters for a function f , which we call $a_{\ell m}$, are

$$f(\mathbf{n}) = \sum_{\ell m} a_{\ell m} Y_{\ell m} \quad \text{where} \quad a_{\ell m} = \int d^2n f(\mathbf{n}) Y_{\ell m}^*(\mathbf{n}) \quad (2.2.2)$$

These are completely analogous to fourier components, and so the results from the previous section will carry over rather straight forwardly. A homogeneous random field on the sky will have a correlation function which only depends on the *angle* between the two directions, $\zeta = \zeta(\mathbf{n} \cdot \mathbf{n}')$. In the case of spherical harmonics, we again get a power spectrum, this time dependent only on ℓ , not m . I take for physical reasons the field to be real, and we get

$$\langle a_{\ell m} a_{\ell' m'}^* \rangle = \int d^2n d^2n' \zeta(\mathbf{n} \cdot \mathbf{n}') Y_{\ell m}^*(\mathbf{n}) Y_{\ell' m'}(\mathbf{n}') \quad (2.2.3)$$

To do the integrals we expand the correlator in Legendre polynomials. These are real, orthogonal polynomials on $[-1; 1]$ which we label by $\ell = 0 \dots \infty$,

$$\int_{-1}^1 P_\ell(x) P_{\ell'}(x) dx = \frac{2\delta_{\ell\ell'}}{2\ell + 1} \quad (2.2.4)$$

We then expand the correlation function in these functions, with a conventional prefactor,

$$\zeta(\mathbf{n} \cdot \mathbf{n}') = \sum_{\ell} \frac{2\ell + 1}{4\pi} C_\ell P_\ell(\mathbf{n} \cdot \mathbf{n}') \quad \text{where} \quad C_\ell = 2\pi \int_{-1}^1 dx \zeta(x) P_\ell(x) \quad (2.2.5)$$

In the case of satellite and balloon experiments, even the observer is in the sky!

A beautiful property of the Legendre polynomials is an expansion of the polynomial in terms of products of spherical harmonics

$$P_\ell(\mathbf{n} \cdot \mathbf{n}') = \sum_m \frac{4\pi}{2\ell + 1} Y_{\ell m}(\mathbf{n}) Y_{\ell m}^*(\mathbf{n}') \quad (2.2.6)$$

Now putting the identity in equation (2.2.6) into equation (2.2.5), putting the whole thing into our expression in equation (2.2.3) and using the orthogonality of the spherical harmonics we get the nice result

$$\langle a_{\ell m} a_{\ell' m'}^* \rangle = \delta_{mm'} \delta_{\ell\ell'} C_\ell \quad (2.2.7)$$

So the expectation value of the product of expansion coefficients is only a function of ℓ , and its power spectrum C_ℓ is simply the expansion parameters of the correlation function. If we compare with equation (2.1.11) this should not be surprising. This can also be interpreted as an effect of rotational invariance. Since rotations mix m but not of different ℓ , it is clear that the power spectrum cannot have explicit dependence on the m – that would break the rotational invariance.

We find similar result for the bispectrum. Using that the correlator is only a function of the three angles between the three directions, write

$$\langle a_{\ell_1 m_1} a_{\ell_2 m_2} a_{\ell_3 m_3} \rangle = \int d^2 n_1 d^2 n_2 d^2 n_3 \zeta(\mathbf{n}_1 \cdot \mathbf{n}_2, \mathbf{n}_1 \cdot \mathbf{n}_3, \mathbf{n}_2 \cdot \mathbf{n}_3) Y_{\ell_1 m_1}^*(\mathbf{n}_1) Y_{\ell_2 m_2}^*(\mathbf{n}_2) Y_{\ell_3 m_3}^*(\mathbf{n}_3) \quad (2.2.8)$$

As before, we expand the correlation function in Legendre polynomials, this time with a sum over three different indices, one for each argument of the function.

$$\zeta(\mathbf{n}_1 \cdot \mathbf{n}_2, \mathbf{n}_1 \cdot \mathbf{n}_3, \mathbf{n}_2 \cdot \mathbf{n}_3) = \quad (2.2.9)$$

$$\sum_{\ell\ell'\ell'' mm'm''} C_{\ell\ell'\ell''} Y_{\ell m}(\mathbf{n}_1) Y_{\ell m}^*(\mathbf{n}_2) Y_{\ell' m'}(\mathbf{n}_1) Y_{\ell' m'}^*(\mathbf{n}_3) Y_{\ell'' m''}(\mathbf{n}_2) Y_{\ell'' m''}^*(\mathbf{n}_3) \quad (2.2.10)$$

$$C_{\ell\ell'\ell''} = \int dx dy dz \zeta(x, y, z) P_\ell(x) P_{\ell'}(y) P_{\ell''}(z)$$

Now we need to know the integral over three spherical harmonics. The explicit form is not very enlightening, and I will simply call it the Gaunt integral, \mathcal{G} , with three lower ℓ indices and three upper m indices. It can be written in terms of Wigner $3j$ symbols, which are closely related to *Clebsch-Gordan coefficients*. The $3j$ symbols are written as a matrix of three upper numbers and three lower numbers, but evaluate to just a single number. The integral over three spherical harmonics is then, by definition

$$\int d^2 n Y_{\ell_1 m_1}(\mathbf{n}) Y_{\ell_2 m_2}(\mathbf{n}) Y_{\ell_3 m_3}(\mathbf{n}) \equiv \mathcal{G}_{\ell_1 \ell_2 \ell_3}^{m_1 m_2 m_3} \quad (2.2.11)$$

$$\mathcal{G}_{\ell_1 \ell_2 \ell_3}^{m_1 m_2 m_3} = \sqrt{\frac{(2\ell_1 + 1)(2\ell_2 + 1)(2\ell_3 + 1)}{4\pi}} \begin{pmatrix} \ell_1 & \ell_2 & \ell_3 \\ 0 & 0 & 0 \end{pmatrix} \begin{pmatrix} \ell_1 & \ell_2 & \ell_3 \\ m_1 & m_2 & m_3 \end{pmatrix} \quad (2.2.12)$$

This is also the expansion coefficient of the product of spherical harmonics in terms of a single spherical harmonic,

$$Y_{\ell_1 m_1}(\mathbf{n}) Y_{\ell_2 m_2}(\mathbf{n}) = \sum_{\ell_3} \mathcal{G}_{\ell_1 \ell_2 \ell_3}^{m_1 m_2 m_3} Y_{\ell_3 m_3}^*(\mathbf{n}) \quad \text{where} \quad m_3 = -m_1 - m_2, \quad (2.2.13)$$

The constraints on the arguments here present a problem for the general case. We assume for a moment the correlation function can be split in three independent pieces, and the correlation function can be regarded simply as a function of three arguments x, y, z . This is not general, but will nonetheless prove useful later.

from which the result of the triple integral is apparent. In terms of the Gaunt integrals, the correlator is

$$\langle a_{\ell_1 m_1} a_{\ell_2 m_2} a_{\ell_3 m_3} \rangle = \sum_{\ell' \ell'' m, m', m''} C_{\ell' \ell''} \mathcal{G}_{\ell_1 \ell' \ell''}^{m_1, -m, m''} \mathcal{G}_{\ell_2 \ell' \ell}^{m_2, -m', m} \mathcal{G}_{\ell_3 \ell'' \ell'}^{m_3, -m'', m'} \quad (2.2.14)$$

Using Equation (12.1.3.6) of [Varshalovich et al. \(1988\)](#) we can do the sum over the three m s. That gives us a $6j$ symbol along with just the geometric factor we are looking for,

$$\langle a_{\ell_1 m_1} a_{\ell_2 m_2} a_{\ell_3 m_3} \rangle = \mathcal{G}_{\ell_1 \ell_2 \ell_3}^{m_1 m_2 m_3} b_{\ell_1 \ell_2 \ell_3} \quad \text{where} \quad (2.2.15)$$

$$b_{\ell_1 \ell_2 \ell_3} = \sum_{\ell' \ell''} \frac{(2\ell + 1)(2\ell' + 1)(2\ell'' + 1)}{4\pi} C_{\ell' \ell''} \begin{pmatrix} \ell_1 & \ell_2 & \ell_3 \\ 0 & 0 & 0 \end{pmatrix}^{-1} \\ \times \begin{pmatrix} \ell_1 & \ell & \ell' \\ 0 & 0 & 0 \end{pmatrix} \begin{pmatrix} \ell_2 & \ell' & \ell'' \\ 0 & 0 & 0 \end{pmatrix} \begin{pmatrix} \ell_3 & \ell'' & \ell \\ 0 & 0 & 0 \end{pmatrix} \left\{ \begin{matrix} \ell_1 & \ell_2 & \ell_3 \\ \ell & \ell' & \ell'' \end{matrix} \right\} \quad (2.2.16)$$

where $B_{\ell_1 \ell_2 \ell_3}^{m_1 m_2 m_3} = \mathcal{G}_{\ell_1 \ell_2 \ell_3}^{m_1 m_2 m_3} b_{\ell_1 \ell_2 \ell_3}$ is the bispectrum and $b_{\ell_1 \ell_2 \ell_3}$ is called the reduced bispectrum. Again, the precise form of it is not as interesting as the fact that the physics of the bispectrum only depends on the ℓ s, not the m s. There are however certain selection rules, like the $\delta_{mm'}$ for the power spectrum. The Gaunt integral is non-zero only if $\sum \ell$ is even, $\sum m = 0$ and the ℓ s fulfill the triangle condition: no ℓ may be bigger than the sum of the others.

It is now interesting to know how a 3 dimensional field with a particular power spectrum, or bispectrum, projects onto the 2 dimensional sky, and how these relate to the angular power spectrum and bispectrum. Take a random field in three dimensions, $f(\mathbf{x})$ and look at only the points on the 2-sphere at a distance r from the origin. Equating the fourier expansion of the field on the sphere with the expansion in spherical harmonics we see that the coefficients are given by

$$a_{\ell m} = \frac{1}{2\pi^2 i^\ell} \int d^3 k j_\ell(kr) Y_{\ell m}(\hat{\mathbf{k}}) \hat{f}(\mathbf{k}) \quad (2.2.17)$$

where j_ℓ is a spherical Bessel function. I used here the expansion of the exponential function,

$$\exp(-i\mathbf{k} \cdot \mathbf{n}r) = 4\pi \sum_{\ell m} i^{-\ell} j_\ell(kr) Y_{\ell m}(\mathbf{n}) Y_{\ell m}^*(\hat{\mathbf{k}}) \quad (2.2.18)$$

From this expression for the $a_{\ell m}$ we derive

$$C_\ell = \frac{2}{\pi} \int dk k^2 P(k) j_\ell(kr)^2 \quad (2.2.19)$$

So evidently there is a direct translation between the full three dimensional field and the projection, as expected. We will need many more expressions like this for derivatives of fields and integrated fields, later.

The same calculation for the bispectrum can be found in [Fergusson and Shellard \(2008\)](#) in great detail. One takes the delta function of k s coming from the expectation

value and writes it in integral form, $\delta(x) = 2\pi \int dk \exp(ikx)$, and performs the expansion in equation (2.2.18) to get the very cumbersome – analytically as well as numerically – expression

$$b_{\ell_1 \ell_2 \ell_3} = \frac{8}{\pi^3} \int dk_1 dk_2 dk_3 (k_1 k_2 k_3)^2 B(k_1, k_2, k_3) \int dx x^2 j_{\ell_1}(xk_1) j_{\ell_2}(xk_2) j_{\ell_3}(xk_3) \quad (2.2.20)$$

The last integral over x can be found in [Jackson and Maximon \(1972\)](#). Numerically it is quite impossible to solve.

One soon realises that full sky calculations are entirely intractable. Analytically it is beautiful, but tedious, numerically it is almost impossible, and even on the data side of things, there is simply not enough computer power to make use of it all. It is therefore interesting for us to see if there is a way to speed up things. Before doing that, we need to do a further, short detour to look at spin-weighted spherical harmonics.

2.2.1 Spin-weighted spherical harmonics

The spin-weighted spherical harmonics are a generalization of the ordinary spherical harmonics, as derived by eg. [Newman and Penrose \(1966\)](#). For our purposes, we do not need the deep mathematical details about how these functions are really $U(1)$ gauge fields and how they transform. More explanations on their definition and further properties can be found in eg. [Boyle \(2016\)](#); [Durrer \(2008\)](#).

We simply need some grasp of their construction, and we are going to use that when looking at derivatives of fields on the sphere. Let us then simply write down a way to construct spin-weighted spherical harmonics. As a start, the ordinary spherical harmonics are simply the spin-weighted, with weight zero. We denote the spin-weight with a small subscript s before the function. Therefore we have

$${}_0Y_{\ell m}(\mathbf{n}) = Y_{\ell m}(\mathbf{n}) \quad (2.2.21)$$

The spin-weight, like the ordinary projection of the angular momentum m , takes values between $-\ell$ and ℓ . We may now act on such a function with a differential operator to lower or raise the spin. Take a function η with spin weight s . We now construct the following functions,

$$\bar{\partial}\eta = -(\sin \theta)^s \left(\frac{\partial}{\partial \theta} + \frac{i}{\sin \theta} \frac{\partial}{\partial \phi} \right) (\sin \theta^{-s} \eta) \quad (2.2.22)$$

$$\partial\eta = -(\sin \theta)^{-s} \left(\frac{\partial}{\partial \theta} - \frac{i}{\sin \theta} \frac{\partial}{\partial \phi} \right) (\sin \theta^s \eta) \quad (2.2.23)$$

which have spin-weights $s + 1$ and $s - 1$ respectively. Combined with the fact that we know the spherical harmonic with spin weight zero, we can this way generate the rest of them. We define the following

$$\bar{\partial}(s Y_{\ell m}) = \sqrt{(\ell - s)(\ell + s + 1)}_{s+1} Y_{\ell m} \quad (2.2.24)$$

$$\bar{\partial}(s Y_{\ell m}) = -\sqrt{(\ell + s)(\ell - s + 1)}_{s-1} Y_{\ell m} \quad (2.2.25)$$

Like the ordinary spherical harmonics, the spin-weighted spherical harmonics form an orthonormal basis on the sphere. Any function with spin-weight s may be written as a sum of ${}_s Y_{\ell m}$. Furthermore the product of two functions of spin-weights s, s' is $s + s'$. It is therefore interesting to find an expression like the Gaunt integral for the functions with spin-weights. Indeed, we may write the product of two spin-weighted spherical harmonics as the following sum – compare equation (2.2.13)

$${}_s Y_{\ell_1 m_1}(\mathbf{n}) {}_{s_2} Y_{\ell_2 m_2}(\mathbf{n}) = \sum_{\ell_3} \sum_{s_1 s_2 s_3} \mathcal{G}_{\ell_1 \ell_2 \ell_3}^{m_1 m_2 m_3} {}_{s_3} Y_{\ell_3 m_3}^*(\mathbf{n}) \quad \text{where} \quad \begin{array}{l} m_3 = -m_1 - m_2 \\ s_3 = -s_1 - s_2 \end{array} \quad (2.2.26)$$

where I have defined the spin-weighted Gaunt integral

$${}_{s_1 s_2 s_3} \mathcal{G}_{\ell_1 \ell_2 \ell_3}^{m_1 m_2 m_3} = \sqrt{\frac{(2\ell_1 + 1)(2\ell_2 + 1)(2\ell_3 + 1)}{4\pi}} \begin{pmatrix} \ell_1 & \ell_2 & \ell_3 \\ -s_1 & -s_2 & -s_3 \end{pmatrix} \begin{pmatrix} \ell_1 & \ell_2 & \ell_3 \\ m_1 & m_2 & m_3 \end{pmatrix} \quad (2.2.27)$$

We are going to use these functions when looking at derivatives of random fields on the sky. Writing the normal partial derivatives as the vectors $(e_1, e_2) = (\partial_\theta, \sin \theta^{-1} \partial_\phi)$, we introduce the helicity basis $e_\pm = \frac{1}{\sqrt{2}}(e_1 \pm ie_2)$. The derivatives with respect to these may be identified proportional to the derivatives defined in equations (2.2.22) and (2.2.23). In terms of these, the product of covariant derivatives is

$$\nabla_a f \nabla^a g = \nabla_+ f \nabla_- g + \nabla_- f \nabla_+ g = \frac{1}{2} (\bar{\partial} f \bar{\partial} g + \bar{\partial} f \bar{\partial} g) \quad (2.2.28)$$

This raises and lowers the spin weights of f, g , and allows us to use equation (2.2.26) to perform integrals. We may for example be interested in the spherical harmonic coefficients of the function $\nabla f \nabla g$. This can be found as follows

$$\begin{aligned} a_{\ell m}^{\nabla f \nabla g} &= \int d^2 n Y_{\ell m}^* \sum_{\ell_2 m_2 \ell_3 m_3} (a_{\ell_2 m_2}^f)^* (a_{\ell_3 m_3}^g)^* \nabla_a Y_{\ell_2 m_2}^* \nabla^a Y_{\ell_3 m_3}^* \\ &= -\frac{1}{2} \int d^2 n Y_{\ell m}^* \sum_{\ell_2 m_2 \ell_3 m_3} (a_{\ell_2 m_2}^f)^* (a_{\ell_3 m_3}^g)^* \sqrt{\ell_2(\ell_2 + 1)\ell_3(\ell_3 + 1)} \\ &\quad \times ({}_1 Y_{\ell_2 m_2 - 1}^* {}_{-1} Y_{\ell_3 m_3}^* + {}_{-1} Y_{\ell_2 m_2 1}^* {}_1 Y_{\ell_3 m_3}^*) \\ &= -\frac{1}{2} \sum_{\ell_2 m_2 \ell_3 m_3} (a_{\ell_2 m_2}^f)^* (a_{\ell_3 m_3}^g)^* \sqrt{\ell_2(\ell_2 + 1)\ell_3(\ell_3 + 1)} ({}_{01-1} \mathcal{G}_{\ell_2 \ell_3}^{m m_2 m_3} + {}_{0-11} \mathcal{G}_{\ell_2 \ell_3}^{m m_2 m_3}) \end{aligned} \quad (2.2.29)$$

We thus succeed in writing the $a_{\ell m}$ solely in terms of the coefficients of the original functions f, g and geometrical factors. Manipulations like these will be useful when

we need to calculate the bispectrum of galaxy number counts. These perturbations also have derivatives of different fields, and need to be treated similar to what we just did. Naturally the calculation is slightly different since we will be calculating bispectra, and not power spectra, but the idea is the same. Derivatives on the sphere are translated into spin spherical harmonics, which are integrated by the use of equation (2.2.26).

2.3 THE FLAT SKY APPROXIMATION

A popular approximation is to only treat a small part of the sky, or rather to treat the full sky as a patchwork of many small, flat pieces. We may restrict ourselves to a part that is so small, it seems to not curve. Remember, the trouble with the full sky is that it curves in on itself. Taking only a part of the sky, we have no such restriction, and can again do a simple Fourier analysis. We only need to build up a dictionary between the flat sky and the full sky, and we need to keep in mind how well one approximates the other. The results here rely heavily on [Bernardeau et al. \(2011\)](#) and their references.

For my purposes, the first order approximation suffices. However, to have a handle on the accuracy, it is good to have a bound on the following order. Some interesting insight appears if we take the naive construction of the flat sky to its limit. We will see this later, when we start constructing the observable galaxy distribution.

First let us construct the simple flat sky. It is simply the two dimensional fourier transform,

$$f(\mathbf{n}) = (2\pi)^{-2} \int d^2\ell a(\ell) \exp(-i\ell \cdot \mathbf{n}) \quad \text{where} \quad a(\ell) = \int d^2n f(\mathbf{n}) \exp(i\ell \cdot \mathbf{n}) \quad (2.3.1)$$

where I choose to call the Fourier modes $a(\ell)$ instead of $\hat{f}(\mathbf{k})$ – the reason being its close connection to the $a_{\ell m}$ from the full sky. What we need is a relation between the power spectrum of $a(\ell)$ and the $a_{\ell m}$, in the limit $\theta \ll 1$ - for very small patches. With this definition, we apply equation (2.1.12) and find the power spectrum, which we call $C(\ell)$, not $P(k)$, is

$$C(\ell) = 2\pi \int J_0(\ell\theta) \theta \zeta(\theta) d\theta \quad (2.3.2)$$

Keeping only lowest orders in θ we can write $\sin \theta \approx \theta$ and as shown by [Bernardeau et al. \(2011\)](#)

$$P_\ell(\cos \theta) = J_0(L\theta) + \mathcal{O}(\theta^2) \quad \text{where} \quad L = \sqrt{\ell(\ell+1)} \quad (2.3.3)$$

With these two identifications, we see that the computations of equations (2.2.5) and (2.3.2) match. That means our construction with exponentials works, and because of the slightly off definition of L , we even get rid of the first order correction to P_ℓ .

This simple observation makes for incredible simplification in the computations of power spectra and bispectra.

The most important quantities to take with us are of course $C(\ell)$ and $b(\ell_1, \ell_2, \ell_3)$ which are given by

$$\langle a(\ell)a^*(\ell') \rangle = (2\pi)^2 \delta(\ell - \ell') C(\ell) \quad (2.3.4)$$

$$\langle a(\ell_1)a(\ell_2)a(\ell_3) \rangle = (2\pi)^2 \delta(\ell_1 + \ell_2 + \ell_3) b(\ell_1, \ell_2, \ell_3), \quad (2.3.5)$$

and which, as we just saw are completely analogous to the corresponding quantities on the full sky. I will, when computing this, strictly use the flat sky approximation. However, I find it instructive to derive the results in both ways and compare the different expressions. That will turn out to not only verify our flat sky calculations, but also teach us the physics content of the full sky calculation. Many physical effects lie hidden behind complex expressions. Usually, the flat sky approximation guides the way to a better understanding of these expressions.

2.3.1 Results about $3j$ symbols

Because of the many bispectrum calculations, we will encounter $3j$ symbols en masse. In an effort to thwart computing time, various approximations for these have been necessary. For completeness, I list here the more important ones.

Case: All $m_i = 0$

In this case, a simple analytic expression can be written down, and is listed in eg. [Nielsen and Durrer \(2017\)](#),

$$\begin{pmatrix} \ell & \ell' & L \\ 0 & 0 & 0 \end{pmatrix} = \sqrt{\frac{[(\ell - \ell' + L - 1)!!][(\ell' - \ell + L - 1)!!][(\ell + \ell' - L - 1)!!][(\ell + \ell' + L)/2!]}{[(\ell - \ell' + L)/2]![\ell' - \ell + L)/2]![\ell + \ell' - L)/2]![\ell + \ell' + L - 1]!!(\ell + \ell' + L + 1)}} \quad (2.3.6)$$

With the usual selection rules. The expression is, however neither enlightening nor simple to put on a computer – factorials usually are not. By using Stirling's approximation, it is however possible to reduce all the factorials to exponentials and polynomials. The exponentials all cancel out, and we are left with the delightfully simple expression for the squared $3j$ symbol,

$$\begin{pmatrix} \ell & \ell' & L \\ 0 & 0 & 0 \end{pmatrix}^2 = \frac{2}{\pi \sqrt{(\ell + \ell' + L + 1)(\ell + \ell' - L)(\ell - \ell' + L)(-\ell + \ell' + L)}} \quad (2.3.7)$$

which has corrections of order $1/\min(\ell, \ell', L)$. This number can be interpreted as the inverse area of the triangle with sides ℓ, ℓ', L times 2π . This interpretation will

naturally be handy as a way of comparing the expressions of full sky calculations with those of a flat sky.

Case: $m_1 = 0, m_2 = -m_3$

This scenario appears when in the computation of galaxy bispectra we run into terms differentiated with respect to the angle, as we will encounter the spin-spherical harmonics above. In [Di Dio et al. \(2016\)](#) the ratio of the first to the zeroth is called A , the second to the zeroth C . Here, I will simply refer to them as

$$A_{\ell_1 \ell_2 \ell_3}^{(m)} = \frac{\begin{pmatrix} \ell_1 & \ell_2 & \ell_3 \\ 0 & m & -m \end{pmatrix} + \begin{pmatrix} \ell_1 & \ell_2 & \ell_3 \\ 0 & -m & m \end{pmatrix}}{2 \begin{pmatrix} \ell_1 & \ell_2 & \ell_3 \\ 0 & 0 & 0 \end{pmatrix}} = \frac{\begin{pmatrix} \ell_1 & \ell_2 & \ell_3 \\ 0 & m & -m \end{pmatrix}}{\begin{pmatrix} \ell_1 & \ell_2 & \ell_3 \\ 0 & 0 & 0 \end{pmatrix}} \text{ or } 0 \quad (2.3.8)$$

Note that when the three ℓ_i sum to an odd number, the $3j$ symbol changes sign when flipping the m . That means we end up with the same selection rules as we started with for the $3j$ symbol with all $m_i = 0$. When the ℓ_i sum to an even number, the A is given by this expression, and when the ℓ sum to an odd number, it is zero.

I have here used that for the relevant ℓ , changing the signs of the m leaves $A^{(m)}$ invariant. It is clear that $A^{(0)} = 1$. To compute it for higher m we need the recursive results of [Luscombe and Luban \(1998\)](#). For illustration, I first do the case $m = 1$ explicitly. We use the formula for $g(m)$ in their table 1 and insert it in their equation (1). After replacement, it reads

$$C(1)A^{(1)} + D(0)A^{(0)} + C(0)A^{(1)} = 0 \quad \text{where} \quad (2.3.9)$$

$$C(0) = C(1) = \sqrt{(\ell_2 + 1)\ell_2(\ell_3 + 1)\ell_3} \quad \text{and} \quad (2.3.10)$$

$$D(0) = -\ell_1(\ell_1 + 1) + \ell_2(\ell_2 + 1) + \ell_3(\ell_3 + 1) \quad (2.3.11)$$

where I have quietly dropped the ℓ subscripts. It is now clear that we can write, analytically,

$$A^{(1)} = -\frac{D(0)}{2C(0)} = \frac{\ell_1(\ell_1 + 1) - \ell_2(\ell_2 + 1) - \ell_3(\ell_3 + 1)}{2\sqrt{(\ell_2 + 1)\ell_2(\ell_3 + 1)\ell_3}} \quad (2.3.12)$$

We may even want to keep the subleading powers, just as we in the flat sky approximation use $\sqrt{\ell(\ell + 1)}$ as the length of the L , as this actually makes the approximation better. It is curious that the same thing happens here.

Dropping subleading powers of ℓ_i , this is

$$A_{\ell_1 \ell_2 \ell_3}^{(1)} \approx -\frac{\ell_2^2 + \ell_3^2 - \ell_1^2}{2\ell_2 \ell_3} = -\hat{\ell}_2 \cdot \hat{\ell}_3 \quad (2.3.13)$$

where the vectors ℓ_i form a triangle, which is exactly the case for our bispectrum calculations. With this result, we can go ahead and write down the answer for any $m \ll \ell_i$.

Note first that in this limit the functions $C(m), D(m)$ reduce to constants, and in particular we can write

$$A^{(m+2)} + 2xA^{(m+1)} + A^{(m)} = 0, \quad (2.3.14)$$

where $x \equiv D/C$. This difference equation, with boundary conditions $A^{(0)} = 1$ and $A^{(1)} = -x/2$, is solved by

$$A^{(m)} = -\frac{1}{2} \left[\left(-\sqrt{x^2 - 1} - x \right)^m + \left(\sqrt{x^2 - 1} - x \right)^m \right] \quad (2.3.15)$$

Writing $x = \cos \theta$, we immediately recognise $-\sin^2 \theta$ in the square roots, and may expand

$$\begin{aligned} A^{(m)} &= -\frac{1}{2} [(-i \sin \theta - \cos \theta)^m + (i \sin \theta - \cos \theta)^m] = (-1)^m \frac{1}{2} [e^{im\theta} + e^{-im\theta}] \\ &= (-1)^m \cos m\theta = (-1)^m T_m(x) \end{aligned} \quad (2.3.16)$$

The cognizant reader may already from the difference equation have recognised the solutions are the Chebyshev polynomials T_m . So in the asymptotic limit, the expression can be written as

$$A_{\ell_1 \ell_2 \ell_3}^{(m)} \equiv \frac{\begin{pmatrix} \ell_1 & \ell_2 & \ell_3 \\ 0 & m & -m \end{pmatrix}}{\begin{pmatrix} \ell_1 & \ell_2 & \ell_3 \\ 0 & 0 & 0 \end{pmatrix}} \approx (-1)^m T_m(\hat{\ell}_2 \cdot \hat{\ell}_3) \quad (2.3.17)$$

where the product $\hat{\ell}_2 \cdot \hat{\ell}_3$ is defined in equation (2.3.13). This approximation is shown in figure 2 for various combinations of ℓ_i . We see clearly that small ℓ_1 compared to $\ell_{2,3}$ and m make for a better approximation.

We will need the exact expression for $A^{(2)}$. Keeping the m dependence in the formulas, we have, in the notation of [Luscombe and Luban \(1998\)](#)

$$A^{(2)}C(2) + A^{(1)}D(1) + C(1) = 0 \Rightarrow \quad (2.3.18)$$

$$\begin{aligned} A_{\ell_1 \ell_2 \ell_3}^{(2)} &= \frac{D(0)D(1) - 2C(1)^2}{2C(1)C(2)} \quad (2.3.19) \\ &= \frac{(\ell_2(\ell_2 + 1) + \ell_3(\ell_3 + 1) - \ell_1(\ell_1 + 1))(\ell_2(\ell_2 + 1) + \ell_3(\ell_3 + 1) - \ell_1(\ell_1 + 1) - 2) - 2(\ell_2 + 1)\ell_2(\ell_3 + 1)\ell_3}{2\sqrt{(\ell_2 - 1)\ell_2(\ell_2 + 1)(\ell_2 + 2)(\ell_3 - 1)\ell_3(\ell_3 + 1)(\ell_3 + 2)}} \end{aligned}$$

All the notation and vocabulary presented here is going to be put to extensive use in chapter 4, where I will calculate the observed cosmological bispectra. Before that happens, we need to know how the primordial perturbations are created and what happens to them as the universe grows old.

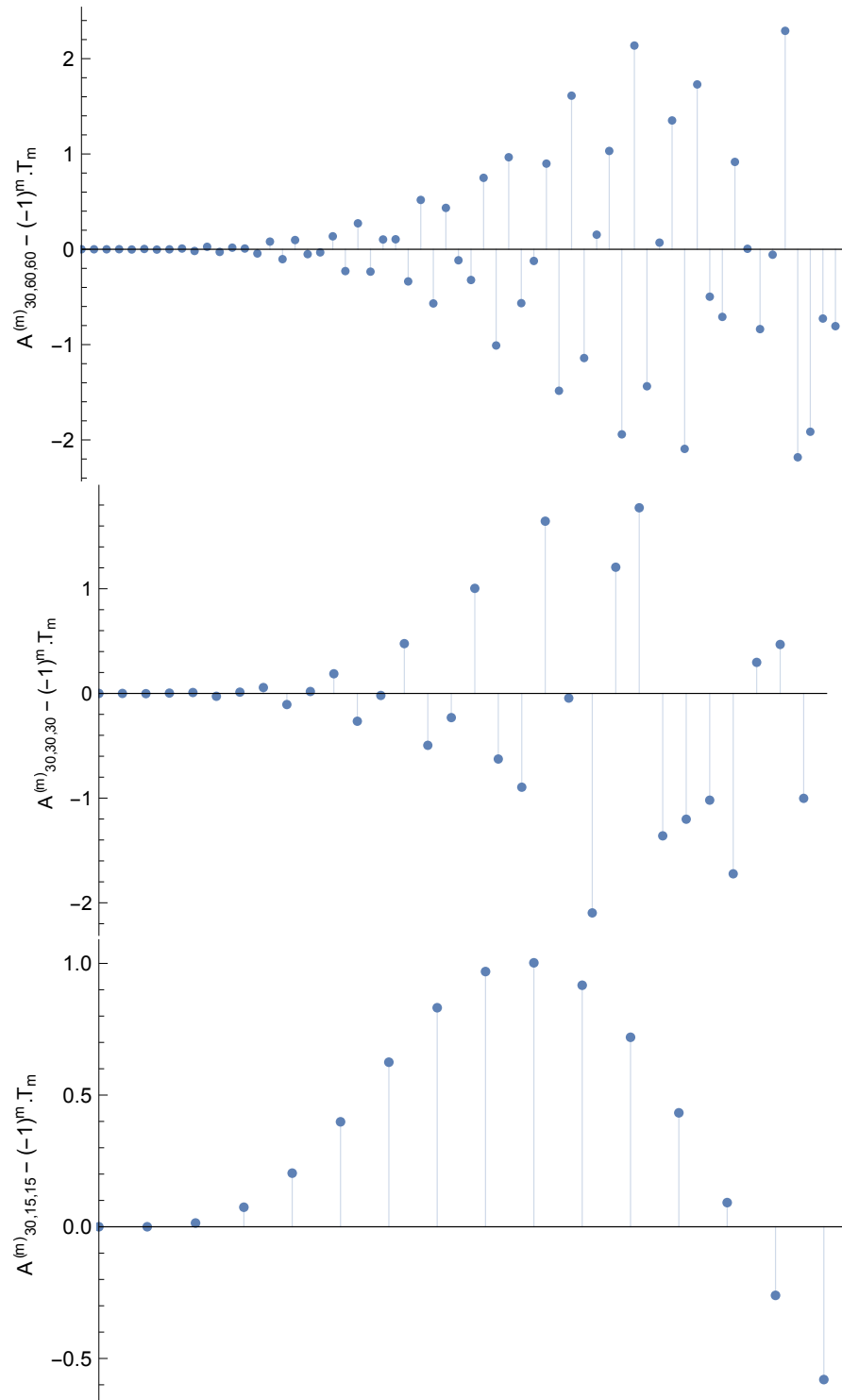


Figure 2: Plots of the approximation of equation (2.3.17) subtracted from the exact value for different angles $\ell_2 \cdot \ell_3$, as indicated on the axes. We see that the smaller the angle is – ie. the smaller ℓ_1 is – the better the approximation. The x-axis goes from $m = 0$ to the maximal m allowed.

COSMOLOGICAL PERTURBATIONS

This chapter is intended to be a boiled-down introduction to the structures of the universe and where they come from. The seeds of cosmic structures are usually assumed to be quantum fluctuations which have undergone inflation, which I briefly describe. Following that, we will have a look at how the initial seeds evolve in the expanding universe, and how they become the *cosmic microwave background* (CMB) with its intricate anisotropies we see in the early universe, and the *cosmic large scale structures* (LSS) we see in the old universe.

I cannot hope to make this a fully fledged introduction to cosmological perturbation theory. Instead, I will focus on the things that are important for the following chapters. Further details can be found in the literature or text books, eg. [Dodelson \(2003\)](#); [Durrer \(2008\)](#); [Mukhanov \(2005\)](#) from which these sections draw inspiration.

An introduction to the macroscopic evolution of the *Friedmann-Lemaître-Robertson-Walker* (FLRW) universe can be found in [Nielsen \(2015\)](#).

It is standard belief that the macroscopic evolution of the universe can be decoupled from the perturbative calculations. Any effect of the perturbations is called *backreaction*, and whether or not this effect is important is not quite settled yet, see eg. [Bolejko and Korzyński \(2016\)](#) and their references for a review and survey. For our purposes I will simply assume perturbation theory works, and do the calculations.

The perturbed universe is comprised of two parts: space-time and fields. As always, fields – matter and radiation – dictate how space-time curves, while the space-time tells the fields how to move. Perturbation theory treats the universe at large as small excursions away from the FLRW model, in terms of field contents and space-time. The simplest case of such a perturbed universe is one with *scalar* perturbations. This is described by the simple metric

$$g_{\mu\nu} = \bar{g}_{\mu\nu} + h_{\mu\nu} \quad \text{where} \quad h_{\mu\nu} = a^2 \text{diag}(-2\Psi, -2\Psi) \quad (3.0.1)$$

and the barred $\bar{g}_{\mu\nu}$ fulfills the unperturbed Einstein Equations, a is the cosmological scale factor and Ψ is the scalar perturbation, or loosely the gravitational potential. I stress that this is *not* general, but will serve us well for the approximations we make. The most general scalar perturbation has two degrees of freedom instead of one, while the most general perturbation has ten degrees of freedom – all of them! For our purposes, one degree of freedom suffices. The difference between using one and

This particular choice of how to write the scalar degree of freedom is called Poisson or Newtonian gauge. In this gauge, there is a simple translation of Ψ in the Newtonian limit, since it is simply the classical Newtonian gravitational potential. I will not dive deeper into the (many) problems of gauge invariance.

two is going to be suppressed in the limit we will work in, for standard cosmological parameters.

For CMB calculations, we will need linear relativistic perturbation theory, while for the calculations of the LSS, we will take a simpler approach to get higher order corrections. To calculate the LSS perturbations in section 3.2.1, we will work in the Newtonian limit, that is, Newtonian physics in an expanding universe. The CMB calculation can be summarised as expanding the Einstein field equations (EFE) and the Boltzmann equations around their homogeneous solutions, to calculate simultaneously the space-time and field perturbations. The calculation is long, and is done in many text books on the subject, and I summarize the major points in section 3.2.2.

3.1 GENERATION OF PERTURBATIONS

The generation of cosmological perturbations is usually assumed to happen by quantum fluctuations of a scalar field filling the universe. The details of the behavior of this field can be more or less complicated, but the basic point remains: The scalar field is supposed to fill the universe with energy – making the inflationary scenario happen – and is also going to decay into ordinary matter and radiation when inflation ends. The perturbations of the scalar field during inflation are therefore taken over by the resulting decay products – matter and radiation. That means a particular spectrum of scalar field perturbations give a predictable spectrum of ordinary fields. This spectrum is what we take as the initial condition for our later calculations.

While the principle started off rather clean – a scalar degree of freedom filling up the universe – the details get messy. I will not go deep into the machinery of inflation, but choose to just outline the calculations. I loosely follow the derivations of [Baumann \(2011\)](#); [Chluba et al. \(2015\)](#).

The simplest toy model that provides an inflationary scenario is a scalar field coupled minimally to gravity. This is described by the action

$$S = \frac{1}{2} \int d^4x \sqrt{g} [R - (\nabla\phi)^2 - 2V(\phi)] \quad (3.1.1)$$

The first term gives the EFE, while the last two are the usual terms in the action for the scalar field, except for the fact that they now multiply the jacobian \sqrt{g} . This is the minimal coupling. Skipping right over all the gauge invariance problems, we define the comoving curvature perturbation $\mathcal{R} = \Psi - H\delta q / (\bar{\rho} + \bar{p})$, a combination of the scalar metric perturbation Ψ and the density, pressure and momentum density ρ, p, q . This quantity has the nice property that it is approximately time-independent on super-horizon scales, $k \ll aH$. It therefore makes sense to expand this quantity in Fourier modes. These Fourier modes have a power spectrum. The spectrum is

Whether or not the theory of inflation actually works has for some years been up for debate, notably by Paul Steinhardt, see eg. [Steinhardt \(2004, 2011\)](#). It seems whether or not it does is either a philosophical or political issue. I do not mean to take any stance on the subject, except to say if inflation works, I look at the potential observable outcome.

interesting, because these adiabatic perturbations will decay to ordinary matter, and this matter will inherit the power spectrum.

As it turns out, the power spectrum arises from quantum fluctuations of the scalar field. We can take the action in equation (3.1.1) and write it as an expansion in \mathcal{R} – a perturbative quantity. Doing this and finding the equations of motion gives independent equations for each Fourier mode of $v = z\mathcal{R}$ where $z = a\dot{\phi}/H$,

$$v_k'' + (k^2 - z''/z)v_k = 0 \quad (3.1.2)$$

This is the equation for a harmonic oscillator with time dependent frequency. Quantizing this harmonic oscillator while setting reasonable boundary conditions – even *earlier* than inflation – one can solve for the modes of v , which in turn give the modes of the curvature perturbation. For this single field model the resulting power spectrum of the curvature perturbations is

$$\mathcal{P}_{\mathcal{R}} = \frac{H^2}{8\pi^2\epsilon M_{pl}^2} (k/H)^{n_s-1} \quad (3.1.3)$$

where ϵ is the slow-roll parameter describing the change of the Hubble constant during inflation, and n_s is the famous *tilt* of the spectrum. This tilt depends on how quickly inflation happens, and the various parameters of the field theory.

When inflation ends, the *inflaton field* – with its perturbation as we just outlined – will decay to ordinary matter. This is usually called *reheating*, since the inflaton decay heats up the universe by providing a bath of radiation and matter. For the small perturbations we have in the early plasma of the universe, all the physics can be approximated as linear. This means that the power spectrum of the curvature perturbations carry over with a simple multiplicative function to eg. density perturbations. We have eg.

$$\mathcal{P}_{\text{matter}}(k, z) \approx T_{\text{matter}}(k, z)\mathcal{P}_{\mathcal{R}}(k) \quad (3.1.4)$$

where T is a transfer function. This transfer function and its relatives for radiation are the topic of the next section.

3.2 EVOLUTION OF PERTURBATIONS

To get from the initial conditions to our observables, we need to have a grasp of how perturbative quantities in the universe evolve. We will have a look at two approaches. For the CMB, we need the full relativistic machinery going in order to get all the details of the power spectrum out. For LSS however, we can get by using just Newtonian theory in an expanding universe.

Remember inflation happens in not quite de Sitter space. Had it been exact de Sitter, then inflation would never end. So, in an effort to make the actual universe happen, we must have a slowly changing Hubble parameter. How slow this change is determines how much the power spectrum is tilted.

3.2.1 The Newtonian universe

Let us see how Newtonian physics in an expanding universe can give us a first look at cosmological structures. We will do the calculation in a universe consisting of just normal matter. Regardless of whether the cosmological constant shows up at late times, the 'early old' universe – ie. at redshifts above, say 1, but long after recombination – is practically only matter and dark matter. Any corrections to the structure formation will be small.

First we need to set up the Newtonian dynamics. This can be written as a set of three equations. They are the continuity equation, Euler equation and Poisson equation, as given by [Bernardeau et al. \(2002\)](#)

$$\rho' + 3\mathcal{H}\rho + \nabla \cdot (\rho\mathbf{v}) = 0 \quad (3.2.1)$$

$$\mathcal{H}'\mathbf{x} + \mathbf{v}' + \mathcal{H}\mathbf{v} + (\mathbf{v} \cdot \nabla)\mathbf{v} = -\nabla\phi \quad (3.2.2)$$

$$\nabla^2\phi = 4\pi G a^2 \rho \quad (3.2.3)$$

Where $\rho = \bar{\rho}(1 + \delta)$ is the matter density, $\mathbf{v} = \mathcal{H}\mathbf{x} + \mathbf{u}$ is the velocity, split into Hubble expansion $\mathcal{H}\mathbf{x}$ and the peculiar velocity \mathbf{u} , and $\phi = \bar{\Psi} + \Psi$ is the gravitational potential. We are interested in the perturbative departures from these. Taking the zeroth-order part to be solutions of the zero-order equations, we can write down the equations for the perturbations. These are

$$\delta' + \nabla \cdot ([1 + \delta]\mathbf{u}) = 0 \quad (3.2.4)$$

$$\mathbf{u}' + \mathcal{H}\mathbf{u} + (\mathbf{u} \cdot \nabla)\mathbf{u} = -\nabla\Psi \quad (3.2.5)$$

$$\nabla^2\Psi = \frac{3}{2}\mathcal{H}^2\delta \quad (3.2.6)$$

where I neglect anisotropic stress and I remind that $\Omega_m = 1$. The last equation here can be used to find Ψ once the density contrast δ has been obtained. Neglecting vorticity, which quickly decays away if it were present, we need to specify only the divergence of the velocity field, $\theta = \nabla \cdot \mathbf{u}$. We may also define the velocity potential v through $\mathbf{u} = \nabla v$. It is clear that in Fourier space, the two are related by $-k^2 v = \theta$.

Let us now rewrite equation (3.2.4) in Fourier modes. We may write the equation as

$$\delta' + \theta = -\nabla \cdot (\delta\mathbf{u}) \quad (3.2.7)$$

Fourier expanding the left hand side is straight forward. The right hand side may be written as

$$\begin{aligned} & -(2\pi)^{-6} \nabla \cdot \int d^3k_1 d^3k_2 \exp(-i(\mathbf{k}_1 + \mathbf{k}_2) \cdot \mathbf{x}) \delta(\mathbf{k}_1) \mathbf{u}(\mathbf{k}_2) = \\ & (2\pi)^{-6} \int d^3k_1 d^3k_2 \exp(-i(\mathbf{k}_1 + \mathbf{k}_2) \cdot \mathbf{x}) \delta(\mathbf{k}_1) i(\mathbf{k}_1 + \mathbf{k}_2) \mathbf{u}(\mathbf{k}_2) = \\ & -(2\pi)^{-6} \int d^3k_1 d^3k_2 \exp(-i(\mathbf{k}_1 + \mathbf{k}_2) \cdot \mathbf{x}) \delta(\mathbf{k}_1) \frac{(\mathbf{k}_1 + \mathbf{k}_2) \cdot \mathbf{k}_2}{k_2^2} \theta(\mathbf{k}_2) \end{aligned} \quad (3.2.8)$$

Note the Jeans' swindle going on here: For a homogeneous universe, $\bar{\Psi}$ formally diverges. We will simply subtract it.

where I have used that \mathbf{u} is curl free, and so $\mathbf{u} = ik^{-2}\mathbf{k}\theta$. Fourier transforming this expression, we get from equation (3.2.7),

$$\delta'(\mathbf{k}) + \theta(\mathbf{k}) = -(2\pi)^{-3} \int d^3k_1 d^3k_2 \delta(\mathbf{k}_1 + \mathbf{k}_2 - \mathbf{k}) \frac{(\mathbf{k}_1 + \mathbf{k}_2) \cdot \mathbf{k}_2}{k_2^2} \delta(\mathbf{k}_1) \theta(\mathbf{k}_2) \quad (3.2.9)$$

Now taking the gradient of equation (3.2.5), inserting equation (3.2.6) and rearranging we get

$$\theta' + \mathcal{H}\theta + \frac{3}{2}\mathcal{H}^2\delta = -\nabla \cdot [(\mathbf{u} \cdot \nabla)\mathbf{u}] \quad (3.2.10)$$

We have again an easy left hand side and a tricky right hand side. Replacing gradients by momenta, we find

$$\begin{aligned} \nabla \cdot [(\mathbf{u} \cdot \nabla)\mathbf{u}] &= i\delta(\mathbf{k}_1 + \mathbf{k}_2 - \mathbf{k})(\mathbf{k}_1 + \mathbf{k}_2) \cdot \left[\left(-i \frac{\theta(\mathbf{k}_1)\mathbf{k}_1}{k_1^2} \right) \cdot i\mathbf{k}_2 \left(-i \frac{\theta(\mathbf{k}_2)\mathbf{k}_2}{k_2^2} \right) \right] \\ &= \delta(\mathbf{k}_1 + \mathbf{k}_2 - \mathbf{k})\theta(\mathbf{k}_1)\theta(\mathbf{k}_2) \frac{(\mathbf{k}_1 + \mathbf{k}_2) \cdot \mathbf{k}_2 \mathbf{k}_1 \cdot \mathbf{k}_2}{k_1^2 k_2^2} \end{aligned} \quad (3.2.11)$$

by symmetrisation, we then get for the Fourier transformed Euler equation

$$\theta' + \mathcal{H}\theta + \frac{3}{2}\mathcal{H}^2\delta = -(2\pi)^{-3} \int d^3k_1 d^3k_2 \delta(\mathbf{k}_1 + \mathbf{k}_2 - \mathbf{k}) \frac{(\mathbf{k}_1 + \mathbf{k}_2)^2 \mathbf{k}_1 \cdot \mathbf{k}_2}{2k_1^2 k_2^2} \theta(\mathbf{k}_1) \theta(\mathbf{k}_2) \quad (3.2.12)$$

Let us now expand the Fourier modes of the density contrast and velocity field as

$$\delta(\mathbf{k}) = \sum a^n \delta_n(\mathbf{k}) \quad (3.2.13)$$

$$\theta(\mathbf{k}) = -\mathcal{H} \sum a^n \theta_n(\mathbf{k}) \quad (3.2.14)$$

Here, higher order terms x_n include more and more powers of the initial fields, eg. δ_2 is quadratic in the initial density field. It is clear that the mode coupling terms of equations (3.2.9) and (3.2.12) couple different terms in these series. The general solution can in our approximation be written down:

$$\delta_n = (2\pi)^{-3} \int d^3k_1 \dots d^3k_n \delta(\mathbf{k} - \sum \mathbf{k}_n) F_n(\mathbf{k}_1, \dots, \mathbf{k}_n) \delta_1(\mathbf{k}_1) \dots \delta_1(\mathbf{k}_n) \quad (3.2.15)$$

$$\theta_n = (2\pi)^{-3} \int d^3k_1 \dots d^3k_n \delta(\mathbf{k} - \sum \mathbf{k}_n) G_n(\mathbf{k}_1, \dots, \mathbf{k}_n) \delta_1(\mathbf{k}_1) \dots \delta_1(\mathbf{k}_n) \quad (3.2.16)$$

where F and G are homogeneous functions of the momenta with degree zero, ie. scaling the momenta up or down leaves the functions invariant. They are given by

$$\begin{aligned} F_n(\mathbf{q}_1, \dots, \mathbf{q}_n) &= \sum_{m=1}^{n-1} \frac{G_m(\mathbf{q}_1, \dots, \mathbf{q}_m)}{(2n+3)(n-1)} [(2n+1)\alpha(\mathbf{k}_1, \mathbf{k}_2) F_{n-m}(\mathbf{q}_{m+1}, \dots, \mathbf{q}_n) \\ &\quad + 2\beta(\mathbf{k}_1, \mathbf{k}_2) G_{n-m}(\mathbf{q}_{m+1}, \dots, \mathbf{q}_n)] \end{aligned} \quad (3.2.17)$$

$$\begin{aligned} G_n(\mathbf{q}_1, \dots, \mathbf{q}_n) &= \sum_{m=1}^{n-1} \frac{G_m(\mathbf{q}_1, \dots, \mathbf{q}_m)}{(2n+3)(n-1)} [3\alpha(\mathbf{k}_1, \mathbf{k}_2) F_{n-m}(\mathbf{q}_{m+1}, \dots, \mathbf{q}_n) \\ &\quad + 2n\beta(\mathbf{k}_1, \mathbf{k}_2) G_{n-m}(\mathbf{q}_{m+1}, \dots, \mathbf{q}_n)] \end{aligned} \quad (3.2.18)$$

It should be clear why we must be careful when the density field becomes 'big', $\delta_1 \approx 1$! I will not delve into the details of convergence or non-linearity, suffice it to say that it is a big problem.

where $k_1 = q_1 + \dots + q_m, k_2 = q_{m+1} + \dots + q_n$. The starting point is of course $F_1 = G_1 = 1$. The case which we need for the bispectra is the first corrections to the linear evolution. They are

$$F_2(\mathbf{q}_1, \mathbf{q}_2) = \frac{5}{7} + \frac{1}{2} \frac{\mathbf{q}_1 \cdot \mathbf{q}_2}{q_1 q_2} (q_1/q_2 + q_2/q_1) + \frac{2}{7} \frac{(\mathbf{q}_1 \cdot \mathbf{q}_2)^2}{q_1^2 q_2^2} \quad (3.2.19)$$

$$G_2(\mathbf{q}_1, \mathbf{q}_2) = \frac{3}{7} + \frac{1}{2} \frac{\mathbf{q}_1 \cdot \mathbf{q}_2}{q_1 q_2} (q_1/q_2 + q_2/q_1) + \frac{4}{7} \frac{(\mathbf{q}_1 \cdot \mathbf{q}_2)^2}{q_1^2 q_2^2} \quad (3.2.20)$$

With these, we now have the expressions for perturbative non-linearity of structure formation. We simply need the starting point – everything is given in terms of $\delta_1(\mathbf{k}, \tau)$. To find this, we differentiate the continuity equation with respect to conformal time, and insert the Euler equation – everything cut at first order. This gives us

$$\delta'' + \theta' = 0 \Rightarrow \delta'' + \mathcal{H}\delta' = \frac{3}{2}\mathcal{H}^2\delta \quad (3.2.21)$$

Let us factorise the density contrast, $\delta(\mathbf{x}, \tau) = \delta(\mathbf{x}, 0)D_1(\tau)$ where τ is conformal time, and solve this equation for D_1 . In the universe we are considering, the conformal hubble rate is $\mathcal{H} = Ha = a^{-1/2} \Rightarrow \mathcal{H}' = -1/(2a)$. Inserting this, and the ansatz $D_1 = a^n$ we get the following equation for the power n ,

$$n^2 + n/2 = 3/2 \quad (3.2.22)$$

This equation is solved by $n = 1$, corresponding to a *growing* mode, and $n = -3/2$, corresponding to a *decaying* mode. In the simple case we have covered so far, evidently we can describe the perturbed density, velocity and potential in terms of the initial density perturbation, scaled by the cosmological scale factor $a(\tau)$. However, we still need that seeding first order density fluctuation – not the primordial, but the one which results from the plasma in the early universe. We did this calculation assuming only matter. However, in the very early universe, radiation played a large role, and we will have to do the relativistic calculation to get the evolution right at these very early times.

3.2.2 The early universe

I will simply try to outline the calculations, and cannot give enough credit to the massive amount of work that lies behind. More details can be found in [Dodelson \(2003\)](#), which I follow. The basic equation to be solved – to put it lightly, is the Boltzmann equation. For some collection of particle species, we provide distribution functions $f_i(\mathbf{x}, \mathbf{p}, t)$, and the Boltzmann equation then describes the evolution of said particles,

$$\frac{df}{dt} = C[f_1, \dots, f_n], \quad (3.2.23)$$

where C describes all interactions between the particles. In the case of the entire universe, in principle all particles shall be taken into account. Luckily, some are more important than others – though the importance of particles changes during the course of history. In the beginning – not the *very* beginning – at a temperature of around 1 MeV, photons and charged particles are very important, and all behave like radiation. After recombination – when the primordial plasma recombines, ie. forms neutral atoms – photons start becoming less important. In the very late universe, the gravitational potential is very simple. All these things help us to make approximate solutions at different times. To appreciate how messy things quickly become, let us write down the collisionless Boltzmann equation for photons in an inhomogeneous universe,

$$\frac{df}{dt} = \frac{\partial f}{\partial t} + \frac{\hat{p}^i}{a} \frac{\partial f}{\partial x^i} - p \frac{\partial f}{\partial p} \left(H + \frac{\partial \Phi}{\partial t} + \frac{\hat{p}^i}{a} \frac{\partial \Psi}{\partial x^i} \right) = 0 \quad (3.2.24)$$

This describes the continuity, Euler equation, the cosmological redshifting and gravitational pull on photons – we have yet to put in charged particles! Important collisions in the primordial plasma are the result of Compton scattering. This is the simple elastic scattering of photons off electrons,

$$e^- + \gamma \leftrightarrow e^- + \gamma \quad (3.2.25)$$

To describe this with the Boltzmann equation, we need to know the distribution function of both electrons and photons, and then for the collision subtract the disappearing left hand side above, and replace it with the right hand side, where the momenta have changed. This can be written as

$$\begin{aligned} C[f(\mathbf{p})]_{\text{Compton}} &= p^{-1} \int d^3 q_{LIPS} \int d^3 q'_{LIPS} \int d^3 p'_{LIPS} |\mathcal{M}|^2 (2\pi)^4 \\ &\delta^{(4)}(p_\mu + q_\mu - p'_\mu - q'_\mu) (f_e(\mathbf{q}')f(\mathbf{p}') - f_e(\mathbf{q})f(\mathbf{p})) \end{aligned} \quad (3.2.26)$$

where \mathcal{M} is the amplitude which can be calculated from quantum field theory, and the measures are *Lorentz Invariant Phase Space* differentials, that is, they have been normalised by the energy and suitable factors of π . The point being, a collision term like this simply transports the particles around in the distribution functions – the two particles on the left of equation (3.2.25) with momenta \mathbf{q}, \mathbf{p} become particles with momenta \mathbf{q}', \mathbf{p}' .

After including baryons, dark matter and potentially even the slight effect of neutrinos, one must simultaneously solve a number of equations,

$$\dot{\Theta} + ik\mu\Theta = -\dot{\Phi} - ik\mu\Psi - \dot{\tau} \left[\Theta_0 - \Theta + \mu v_b - \frac{1}{2}P_2(\mu)\Pi \right] \quad (3.2.27)$$

$$\Pi = \Theta_2 + \Theta_{P2} + \Theta_{P0} \quad (3.2.28)$$

$$\dot{\Theta}_P + ik\mu\Theta_P = -\dot{\tau} \left[-\Theta_P + \frac{1}{2}(1 - P_2(\mu))\Pi \right] \quad (3.2.29)$$

$$\dot{\delta} + ikv = -3\dot{\Phi} \quad (3.2.30)$$

$$\dot{v} + Hv = -ik\Psi \quad (3.2.31)$$

$$\dot{\delta}_b + ikv_b = -3\dot{\Phi} \quad (3.2.32)$$

$$\dot{v}_b + Hv_b = -ik\Psi + \frac{\dot{\tau}}{R}[v_b + 3i\Theta_1] \quad (3.2.33)$$

$$\dot{\mathcal{N}} + ik\mu\mathcal{N} = -\dot{\Phi} - ik\mu\Psi \quad (3.2.34)$$

where equations (3.2.27) to (3.2.29) describe the photon temperature and polarization, equations (3.2.30) and (3.2.31) describe dark matter interactions, equations (3.2.32) and (3.2.33) describe the baryon evolution and finally equation (3.2.34) describes the neutrinos. The density and velocity fields are $\delta, v, \mu = \cos\theta$, τ is the optical depth and R is the ratio of photon to baryon density.

All these are cogs in the machinery to calculate two things important to us: the temperature anisotropies at recombination – the anisotropies we now see as CMB – and the linear density inhomogeneities which seed our Newtonian calculation from before.

Lucky for us, solving these equations has never been easier: software packages like CAMB (Lewis, 2013; Lewis and Bridle, 2002) and CLASS (Blas et al., 2011; Lesgourgues, 2011) can solve the systems to percent level accuracy within a matter of seconds. These programs use various approximation schemes to speed up computations, and can be coerced into providing both transfer functions for different species and power spectra of various observables. The true beginning of these kinds of programs were with CMBFAST by Seljak and Zaldarriaga (1996), which utilised a trick to get tremendous speed-up when going from the temperature field to the observable CMB power spectrum. Although, as time goes by, the physics gets hidden in what essentially becomes a black-box of CMB computations. Perhaps that is why Mukhanov (2004) developed CMBLOW – a way to bring back at least approximations for what is going on, and how one may interpret constraints on cosmological parameters as consequences of physical phenomena.

Equipped with the knowledge of the universe and its structures, we now need to find out how to observe them, and what our limited observations can tell us. That is the subject of the next chapter.

*Given more time, the precision
will even reach sub-percent
levels.*

4

OBSERVATIONS ON THE SKY

For all the perturbative quantities described in the previous chapter, we have to observe them. This is in principle simple – just look at the sky! – but in practice all but impossible.

Take first the CMB. Place the earth in the middle of the observable universe. From all sides, photons stream to us from the edge of the visible universe and from every small pixel of a detector we can determine the temperature of exactly that one spot on the sky. Each photon received has been on the way to our eyes since about 380 thousand years after the big bang, which is when it was last scattered in the hot early plasma. The temperature and movement of the plasma *then*, determines the photon energy distribution, which we observe *today*. In NASA's illustration in figure 3, this is compared to looking into the cloudy Danish sky – we know there is space and universe above the clouds, however, the photons we observe have last been scattered in the cloud, and that means our view of what is beyond is obscured.

All the observations of CMB photons put together give us a temperature field of the CMB sky,

$$T(\mathbf{n}) = T_0(1 + \Theta(\mathbf{n})) \quad (4.0.1)$$

where observationally, $T_0 \approx 2.726$ (Fixsen, 2009), and $\Theta \approx 10^{-5}$ (Bennett et al., 2003), except the dipole, which is presumably of kinematic origin. This temperature field on the sky is then interpreted as photons arriving from the perturbed radiation field just around recombination, when the photons start free-streaming – the two are not exactly coincidental, but are very close. The difficult part comes now: to see the edge of the universe, there is an enormous amount of universe to see through, a universe full of dust and galaxies and most notably *our own* galaxy. All these things pollute observations of the CMB, and always will. In the most recent space-borne mission, the *Planck satellite*, these problems are circumvented by mapping in many frequencies and assuming the shape of the spectra of foregrounds. It is no wonder that one needs a firm grasp of foreground pollution to determine just how much of the observed light really is the CMB. It is therefore no surprise that observations of polarisation spectra, which are even further suppressed, are that much harder. One bad example is the 2014 press release from BICEP2 (Ade et al., 2014a), which hardly did any foreground cleaning and as a consequence was dead on arrival. Further analysis indeed showed that the polarisation spectra they had found were compatible with being *only* foreground (Ade et al., 2015).

There is a slight difference between the visible and the observable universe. The visible universe is all the way up to redshift ≈ 1080 , when the primordial plasma recombines. Earlier than that, all photons are bouncing around on the plasma, and the universe is completely opaque. However, all observations need not be optical. Should one find a way to observe for instance the cosmic neutrino background, this would be an observation inside the opaque universe. Similarly, primordial gravitational waves, if they exists, will let us look all the way to the big bang. Hence I find it reasonable to distinguish the two.

Foregrounds in this regard is different types of dust and gasses between us and the surface of last scattering.

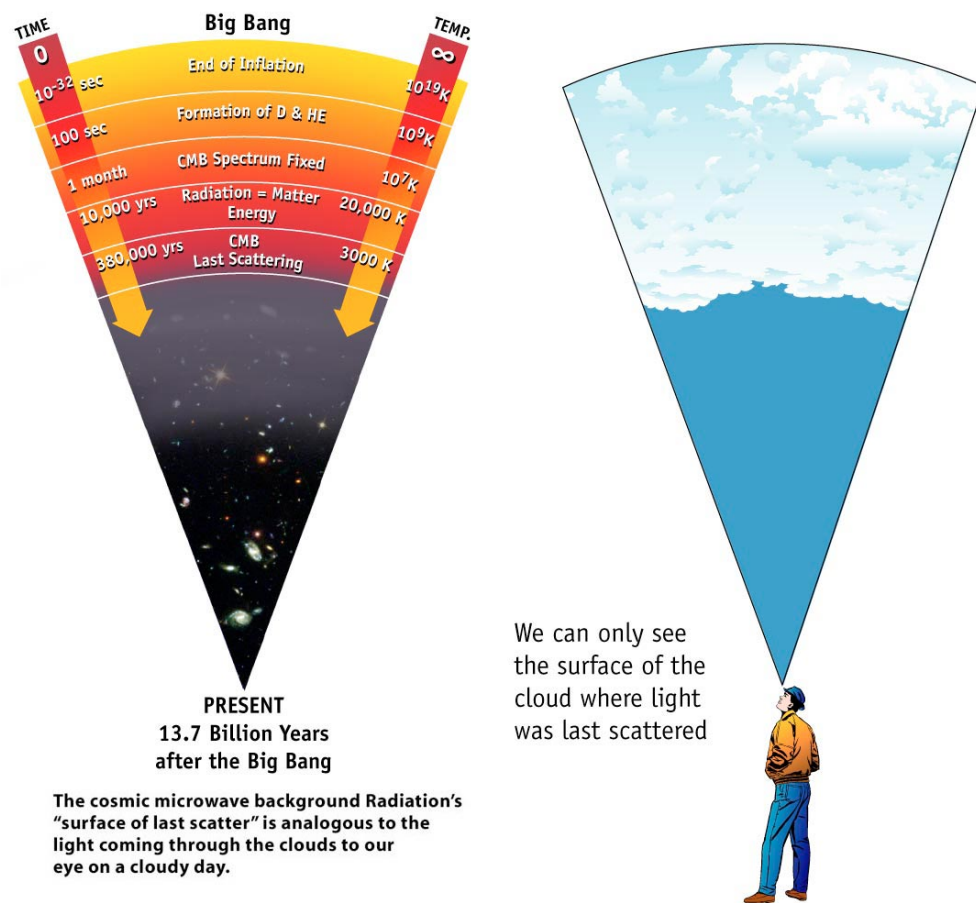


Figure 3: Illustration of *last scattering* by the NASA/WMAP Science Team. The sky, like the primordial plasma, is literally clouded, and we only see the surface on which the photons were last scattered. From <https://map.gsfc.nasa.gov/media/990053/index.html>, last updated 1st April 2011.

In that sense, galaxy surveys are simpler. An observed galaxy is after all a galaxy. Another great complication arises immediately though. What is the distribution of galaxies in the universe? Our calculations so far concerned the density field of baryons and dark matter. To which degree can we really say that galaxies follow the distribution of dark matter? This problem is known under the umbrella term *galaxy bias*. One way about it is to scale the predicted galaxy density by a bias factor b , and include this factor in the analysis. More sophisticated analyses will introduce even second and higher order biasing, as described by eg. [McDonald and Roy \(2009\)](#). I will not treat the problem of bias in the following. For the simple procedure of linear or quadratic bias, these effects are simple to include later. There is also the trouble that galaxies move around. Since the light from moving galaxies is Doppler shifted, there is no one-to-one correspondence between the redshift of a galaxy and the cosmological redshift at the time the galaxy emitted the light. Furthermore the light is lensed as it traverses the universe. This effect changes the perceived location of the galaxy, so one cannot even be sure of the observed angular position. These effects, and many more, can be taken into account however. We will do so in the sections below. Using a special set of coordinates, it is possible to predict *not just* the galaxy distribution, but rather the *perceived* distribution.

The following sections first introduce the calculations of the CMB observations on the sky, and its cosmic noise. We will use the same language to describe the galaxy number counts on the sky. The calculations of the number counts in various limits are very long, and very detailed. The main result is the proof of equation (4.2.94), the derivation and verification of equations (4.2.163) to (4.2.165), including the expressions of all their individual terms, and finally the flat-sky expression for the bispectrum in equations (4.2.194) to (4.2.200).

4.1 COSMIC MICROWAVE BACKGROUND

Given the mathematics of chapter 2, it should come as no surprise that we wish to Fourier transform the observed temperature anisotropies on the sky. The great leap forward by [Seljak and Zaldarriaga \(1996\)](#) was writing the temperature field transfer function as a line-of-sight integral

$$\Theta(k, \mu \equiv \hat{n} \cdot \hat{k}) = \int_0^{\eta_0} S(k, \eta) \exp(ik\mu(\eta - \eta_0)) \quad (4.1.1)$$

where $S(k, \eta)$ is called the *source function*. The important part being that the source function by partial integration can be written as a function of just k and η – *not* of μ . This allows a simple decomposition onto Legendre polynomials. Expanding this

exponential as equation (2.2.18) and inserting equation (2.2.6) we see by orthogonality that

$$\int_{-1}^1 d\mu P_\ell(\mu) \exp(ik\mu(\eta - \eta_0)) = 2i^\ell j_\ell(k[\eta - \eta_0]) \quad (4.1.2)$$

$$\Rightarrow \Theta_\ell(k) = 4\pi i^\ell \int d\eta S(k, \eta) j_\ell(k[\eta - \eta_0]) \quad (4.1.3)$$

To compute the observable CMB sky we put ourselves at $\mathbf{x} = 0$ and compute the expansion coefficients of the spherical harmonics,

$$\begin{aligned} a_{\ell m} &= \int d^2n Y_{\ell m}^*(\mathbf{n}) \Theta(\mathbf{x} = 0, \mu) = \int d^2n Y_{\ell m}^*(\mathbf{n}) \int \frac{d^3k}{(2\pi)^3} \Theta(\mathbf{k}, \mu) \\ &= \int \frac{d^3k}{(2\pi)^3} d^2n Y_{\ell m}(\mathbf{n}) \sum_{\ell' m'} \Theta_{\ell'}(\mathbf{k}) Y_{\ell' m'}(\mathbf{n}) Y_{\ell' m'}^*(\hat{\mathbf{k}}) \\ &= 4\pi i^\ell \int \frac{d^3k}{(2\pi)^3} \Delta_\ell(k) \Phi(\mathbf{k}) Y_{\ell m}(\hat{\mathbf{k}}) \end{aligned} \quad (4.1.4)$$

where I have defined the transfer function $\Delta_\ell(k) = \int d\eta S(k, \eta) j_\ell(k[\eta - \eta_0])$, which takes the initial perturbations to the observed anisotropies, $\Theta_\ell(\mathbf{k}) = 4\pi i^\ell \Delta_\ell(k) \Phi(\mathbf{k})$. Given a power spectrum and bispectrum of the primordial fluctuations we use this to translate to observed anisotropies. Taking the primordial power spectrum to be $\langle \Phi \Phi^* \rangle = (2\pi)^3 \delta(\mathbf{k} - \mathbf{k}') P(k)$ we get

$$C_\ell \equiv \langle |a_{\ell m}|^2 \rangle = \frac{2}{\pi} \int dk k^2 |\Delta_\ell(k)|^2 P(k) \equiv 4\pi \int \frac{dk}{k} |\Delta_\ell(k)|^2 \mathcal{P}(k) \quad (4.1.5)$$

where I write the *dimensionless* primordial power spectrum, $\mathcal{P}(k) = P(k)k^3 / (2\pi^2)$.

We also want to calculate the observed bispectrum. All I need to insert in equation (2.2.20) is the transfer functions $\Delta_\ell(k)$, since I am correlating temperature anisotropies, not primordial perturbations. That makes the reduced bispectrum

$$\begin{aligned} b_{\ell_1 \ell_2 \ell_3} &= \frac{8}{\pi^3} \int dk_1 dk_2 dk_3 (k_1 k_2 k_3)^2 B(k_1, k_2, k_3) \\ &\quad \Delta_{\ell_1}(k_1) \Delta_{\ell_2}(k_2) \Delta_{\ell_3}(k_3) \int dx x^2 j_{\ell_1}(k_1 x) j_{\ell_2}(k_2 x) j_{\ell_3}(k_3 x) \end{aligned} \quad (4.1.6)$$

4.1.1 Cosmic variance

The $a_{\ell m}$ are *random variables* whose variance is C_ℓ . That means that even from the cleanest map of the CMB sky, we can never be completely sure exactly which power spectrum we are seeing. A tell-tale sign of dark energy for example shows up at very low ℓ . However, as the $a_{\ell m}$ here have a relatively large variance, we cannot say for sure that we are seeing the so-called *Sachs-Wolfe plateau*. As we get to larger ℓ , this effect wears off, and the variances becomes much smaller than the squared mean. Since the theoretical predictions is the power spectrum – not the $a_{\ell m}$ – we need to determine this quantity. Our best estimator is simply the average of $|a_{\ell m}|^2$.

Since the $a_{\ell m}$ are gaussianly distributed, our estimator will be distributed as a scaled chi-squared with $2\ell + 1$ degrees of freedom,

$$\hat{C}_\ell = (2\ell + 1)^{-1} \sum_m |\hat{a}_{\ell m}|^2 \quad (4.1.7)$$

It is simple to show this has mean C_ℓ and variance $2C_\ell^2(2\ell + 1)^{-1}$ (Nielsen, 2015). This unbeatable uncertainty is called *cosmic variance*. This property of the measurements can be seen in figure 4. The plot shows $D_\ell = \ell(\ell + 1)C_\ell / (2\pi)$ and the difference to the best fit model.

We can do a similar analysis for the cosmic variance of the bispectrum in a gaussian universe. The mean of the bispectrum is simply zero, since it is the expectation value of an odd number of gaussian variables. The variance of the bispectrum however, is not. By Isserlis' theorem we get 15 different pairings of the six terms, each of which potentially contributes, depending on the different m_i values. The result can be found in eg. Gangui and Martin (2000); Luo (1994) and is

$$\begin{aligned} \langle a_{\ell_1 m_1} a_{\ell_2 m_2} a_{\ell_3 m_3} a_{\ell_1 m_1}^* a_{\ell_2 m_2}^* a_{\ell_3 m_3}^* \rangle = & \quad (4.1.8) \\ C_{\ell_1} C_{\ell_2} C_{\ell_3} + 2\delta_{\ell_1 \ell_2 \ell_3} (\delta_{m_1 m_3} + \delta_{m_1, -m_3}) (\delta_{m_1 m_2} + \delta_{m_1, -m_2}) C_{\ell_1}^3 + \\ \delta_{\ell_1 \ell_2} [\delta_{m_1, m_2} + \delta_{m_1, -m_2}] C_{\ell_1}^2 C_{\ell_3} + \delta_{\ell_3 \ell_2} [\delta_{m_3, m_2} + \delta_{m_3, -m_2}] C_{\ell_2}^2 C_{\ell_1} + \\ \delta_{\ell_3 \ell_1} [\delta_{m_3, m_1} + \delta_{m_3, -m_1}] C_{\ell_1}^2 C_{\ell_2} \end{aligned}$$

To get an estimator of the bispectrum, we will have to do something like equation (4.1.7), a sum over many products of $a_{\ell m}$ to get a reliable estimate of their origin. To get rid of the m dependence of the full bispectrum in equation (2.2.15), we use the orthogonality of the $3j$ symbols and define the *rotationally invariant reduced bispectrum*, as defined by Ade et al. (2014b)

$$B_{\ell_1 \ell_2 \ell_3} = h_{\ell_1 \ell_2 \ell_3} \sum_{m_i} \begin{pmatrix} \ell_1 & \ell_2 & \ell_3 \\ m_1 & m_2 & m_3 \end{pmatrix} B_{\ell_1 \ell_2 \ell_3}^{m_1 m_2 m_3} = h_{\ell_1 \ell_2 \ell_3}^2 b_{\ell_1 \ell_2 \ell_3} \quad \text{where} \quad (4.1.9)$$

$$h_{\ell_1 \ell_2 \ell_3} = \sqrt{\frac{(2\ell_1 + 1)(2\ell_2 + 1)(2\ell_3 + 1)}{4\pi}} \begin{pmatrix} \ell_1 & \ell_2 & \ell_3 \\ 0 & 0 & 0 \end{pmatrix} \quad (4.1.10)$$

Taking now our best estimate of the individual B_ℓ^m to be the corresponding product of three $a_{\ell m}$, we take as an estimate of B_ℓ the corresponding sum of \hat{B}_ℓ^m ,

$$\hat{B}_{\ell_1 \ell_2 \ell_3} = h_{\ell_1 \ell_2 \ell_3} \sum_{m_i} \begin{pmatrix} \ell_1 & \ell_2 & \ell_3 \\ m_1 & m_2 & m_3 \end{pmatrix} \hat{a}_{\ell_1 m_1} \hat{a}_{\ell_2 m_2} \hat{a}_{\ell_3 m_3} \quad (4.1.11)$$

It is clear from orthogonality of the $3j$ symbols, $\sum_{m_i} (G_\ell^m)^2 = h_\ell^2$, that $\langle \hat{B}_\ell \rangle = h_\ell^2 b_\ell$. The exact cosmic variance of the bispectrum is difficult to get. We can, however get a reasonable approximation for high ℓ_i if we simply discard all terms in equation (4.1.8) except the first. It is clear that this is exact for all different ℓ , and an approximation if some are equal. With just this first term we see that the variance becomes

$$V_{\ell_1 \ell_2 \ell_3} \equiv \langle \hat{B}_{\ell_1 \ell_2 \ell_3} \hat{B}_{\ell_1 \ell_2 \ell_3} \rangle = h_{\ell_1 \ell_2 \ell_3}^2 C_{\ell_1} C_{\ell_2} C_{\ell_3} g_{\ell_1 \ell_2 \ell_3} \quad (4.1.12)$$

I am always assuming full sky coverage. Without this, the spherical harmonics are not orthogonal, and the variance on the $a_{\ell m}$ increases. The simplest way to salvage this for the C_ℓ estimator is to just scale it down by the fraction of the sky covered. This does introduce correlations among the C_ℓ . The C_ℓ obtained this way can be called pseudo- C_ℓ .

This definition differs by a factor of h_ℓ from some recent papers. We will mostly use b_ℓ , and will not notice this difference much.

I will use the shorthand notation $B_{\ell_1 \ell_2 \ell_3}^{m_1 m_2 m_3} \rightarrow B_\ell^m$ when the ℓ or m values are not important. It should be clear from the context that there are actually three ℓ values hiding behind the one explicitly written down.

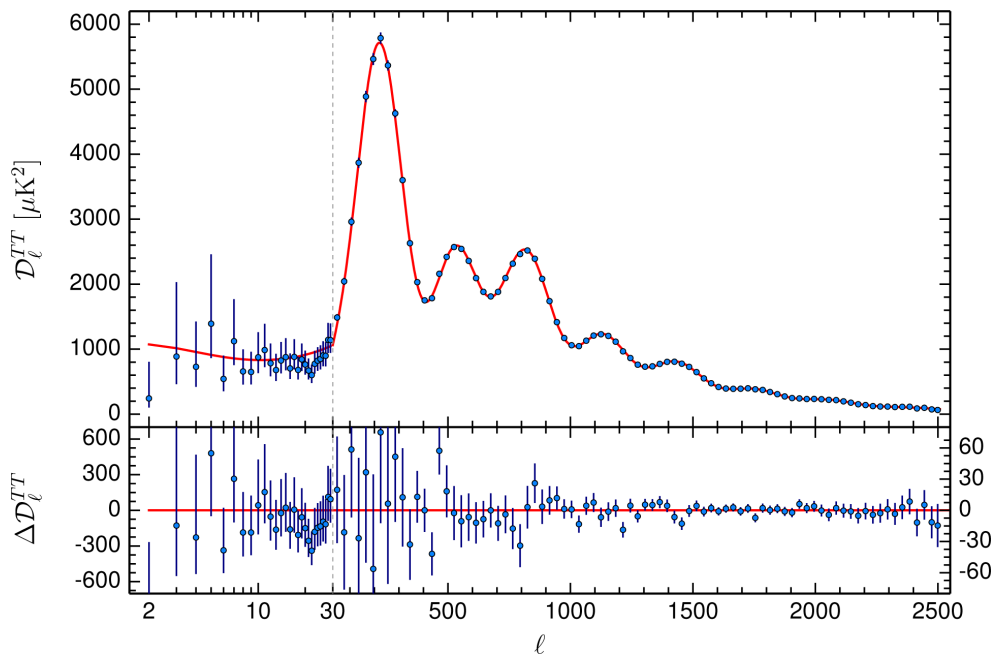


Figure 4: The 2015 Planck temperature power spectrum from [Aghanim et al. \(2016\)](#). Two things to note: the first 28 multipoles are plotted logarithmically, while the rest are plotted linearly and the higher multipoles have been binned. The error bars include – but are not limited to – cosmic variance. The binning visibly helps beat down cosmic variance, but comes at the cost of washing out features. It can therefore only be done for the parts of the power spectrum that are relatively slowly varying. We see clearly here how for the very low multipoles ℓ , cosmic variance ruins our chances for making very precise comparisons. For the difference plot, the left y-axis corresponds to the first 28 multipoles, and the right y-axis to the rest.

where the factor g is 1 for all different ℓ , 2 if two are equal, and 6 if all three are equal. The reason it enters is the two sums over m_i in the B_ℓ – eg. if $\ell_1 = \ell_2$, then both $m_1 = m'_1, m_2 = m'_2$ and $m_1 = m'_2, m_2 = m'_1$ contribute, giving an overall factor 2. If all three ℓ are equal, then this factor is 6, for the six combinations of pairs of (m_i, m'_i) . This does neglect terms like (here for $\ell_1 = \ell_2$)

$$h_{\ell_1 \ell_2 \ell_3}^2 C_{\ell_1} C_{\ell_2} C_{\ell_3} \sum_{m_1} \left(\begin{matrix} \ell_1 & \ell_1 & \ell_3 \\ m_1 & -m_1 & 0 \end{matrix} \right)^2 + \left(\begin{matrix} \ell_1 & \ell_1 & \ell_3 \\ m_1 & m_1 & -2m_1 \end{matrix} \right)^2 \quad (4.1.13)$$

for the high ℓ we are interested in, these terms are practically percent level corrections – and only correction to equal- ℓ bispectra, which are very rare. As is usual, we will completely neglect these terms.

Doing the sum to obtain all observed B_ℓ is in practice very limiting, as the computational time scales as ℓ_{max}^5 – one sum over m_i drops out due to the selection rules on \mathcal{G}_ℓ^m . For the resolutions in Planck, $\ell_{max} \approx 2500$. Suffice it to say this cannot be done in reasonable time – especially when accounting for error analysis on simulations! Various techniques have been developed to cope with this fact. Common for all of them is a degree of approximation, usually motivated ones. For that reason, different approximate estimators will have different use cases.

Since we are *not* doing data analysis, we are free from these computations. We only need to compute the predicted bispectrum, which scales as ℓ_{max}^3 – one power for each index. Assuming full sky coverage and no foreground – which is absurd! – we will instead estimate to which degree we see a particular *template* B_ℓ of non-gaussianity as follows. Put a parameter f_{NL} in front of the template, and do a simple χ^2 analysis with the variance V_ℓ we found before,

$$\chi^2 = \sum_{\ell_1 \geq \ell_2 \geq \ell_3} \frac{(\hat{B}_{\ell_1 \ell_2 \ell_3} - f_{NL} B_{\ell_1 \ell_2 \ell_3})^2}{V_{\ell_1 \ell_2 \ell_3}} \quad (4.1.14)$$

where \hat{B}_ℓ is the observed bispectrum and B_ℓ is the predicted bispectrum. This tells us to which degree the observed \hat{B}_ℓ shows the template B_ℓ . Clearly, this linear model has a minimal χ^2 at

$$\hat{f}_{NL} = \frac{\sum_{\ell_1 \geq \ell_2 \geq \ell_3} \hat{B}_{\ell_1 \ell_2 \ell_3} (V_{\ell_1 \ell_2 \ell_3})^{-1} B_{\ell_1 \ell_2 \ell_3}}{\sum_{\ell_1 \geq \ell_2 \geq \ell_3} B_{\ell_1 \ell_2 \ell_3} (V_{\ell_1 \ell_2 \ell_3})^{-1} B_{\ell_1 \ell_2 \ell_3}} \quad (4.1.15)$$

From equation (4.1.12) we get directly that, in a gaussian universe, the estimator \hat{f}_{NL} will have a cosmic variance of

$$\begin{aligned} \sigma_{\hat{f}_{NL}}^2 &= \left(\sum_{\ell_1 \geq \ell_2 \geq \ell_3} B_{\ell_1 \ell_2 \ell_3} (V_{\ell_1 \ell_2 \ell_3})^{-1} B_{\ell_1 \ell_2 \ell_3} \right)^{-1} \\ &= \left(\sum_{\ell_1 \geq \ell_2 \geq \ell_3} h_{\ell_1 \ell_2 \ell_3}^2 b_{\ell_1 \ell_2 \ell_3}^2 / (g_{\ell_1 \ell_2 \ell_3} C_{\ell_1} C_{\ell_2} C_{\ell_3}) \right)^{-1} \end{aligned} \quad (4.1.16)$$

I have here rewritten it in terms of the reduced bispectrum, which is the quantity we compute. The interesting number to calculate for one's favourite model with a

characteristic bispectrum is of course the signal-to-noise ratio of the expected f_{NL} . Let us without loss of generality expect it to be unity. The crucial number to get *low* in order to have a chance of observing the bispectrum is then

$$\begin{aligned} \frac{S}{N} &= \sqrt{\sum_{\ell_1 \geq \ell_2 \geq \ell_3} B_{\ell_1 \ell_2 \ell_3} (V_{\ell_1 \ell_2 \ell_3})^{-1} B_{\ell_1 \ell_2 \ell_3}} \\ &= \sqrt{\sum_{\ell_1 \geq \ell_2 \geq \ell_3} h_{\ell_1 \ell_2 \ell_3}^2 b_{\ell_1 \ell_2 \ell_3}^2 / (g_{\ell_1 \ell_2 \ell_3} C_{\ell_1} C_{\ell_2} C_{\ell_3})} \end{aligned} \quad (4.1.17)$$

As long as the bispectrum is small, and the approximation in equation (4.1.12) holds, the variance, or signal-to-noise is fixed. If we are to directly observe this quantity, we must have noise considerably smaller than the signal. The computation of this number will be the aim of the coming chapter.

These computations assume a full sky all the way through, which ensures rotational invariance, and in turn gets rid of a lot of problems. In a more realistic analysis, where eg. the galaxy takes up almost 25% of the sky, one has to include more terms to take good care of the incomplete sky coverage. [Creminelli et al. \(2006\)](#) show that including a linear term, besides the bispectrum triplets we include, saves the estimator. This term, on a full sky, will obviously average to zero, but on the incomplete sky, it makes sure one is not biased simply because the sky is not being observed in a particular direction.

4.1.2 Computing the primordial bispectrum in the CMB on a flat sky

The expression in equation (4.1.6) is in principle very limiting. I will now derive a simpler way to calculate it on a flat sky, following the derivation of [Babich et al. \(2004\)](#); [Fergusson and Shellard \(2008\)](#).

We first write the temperature field on the sky as

$$T(\mathbf{n}) = (2\pi)^{-2} \int d^2\ell a(\ell) \exp(-i\ell \cdot \mathbf{n}) \Rightarrow a(\ell) = \int d^2n T(n) \exp(i\ell \cdot \mathbf{n}) \quad (4.1.18)$$

Note that the vector \mathbf{n} is now a two-dimensional vector in the plane of the sky, it is no longer pointing in the direction of the sky from us. The vector $(0,0)$ is then a special direction picked by us, eg. the z direction, in which the coordinate system originates. We now write out the temperature field in Fourier space and instead of equation (4.1.4) we now have

$$\begin{aligned} a(\ell) &= \int d^2n \exp(i\ell \cdot \mathbf{n}) \int \frac{d^3k}{(2\pi)^3} \int_0^{\eta_0} d\eta S(k, \eta) \exp(-i\mathbf{k} \cdot \mathbf{n}(\eta_0 - \eta)) \\ &= \int \frac{d^3k}{2\pi} \Phi(\mathbf{k}) \int_0^{\eta_0} d\eta S(k, \eta) \exp(-ik_z[\eta_0 - \eta]) \delta(\mathbf{k}_\perp(\eta_0 - \eta) - \ell) \end{aligned} \quad (4.1.19)$$

where \mathbf{k}_\perp is the momentum perpendicular to the line of sight, and k_z is along it.

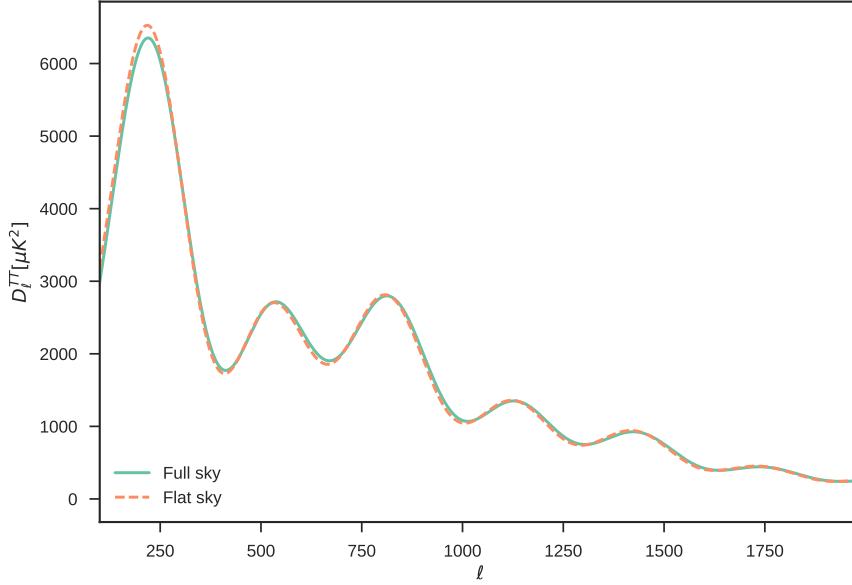


Figure 5: Comparison of the flat sky computation with the full sky computation from CLASS for a run-of-the-mill Λ CDM universe. The result is noticeably worse around the first acoustic peak, as we get into low- ℓ territory. For high ℓ , evidently this is a reasonable approximation.

The power spectrum and bispectrum are defined by equations (2.3.4) and (2.3.5). Let us first compute the power spectrum. It is

$$(2\pi)^2 \delta(\ell - \ell') C(\ell) = (2\pi) \int d^3k P(k) \int_0^{\eta_0} d\eta S(k, \eta) \exp(-ik_z[\eta_0 - \eta]) \delta(\mathbf{k}_\perp(\eta_0 - \eta) - \ell) \int_0^{\eta_0} d\eta' S(k, \eta') \exp(ik_z[\eta_0 - \eta']) \delta(\mathbf{k}_\perp(\eta_0 - \eta') - \ell') \quad (4.1.20)$$

Now we use that the source function mainly has contributions around the last scattering surface, at η_R . This is known as the *thin shell approximation*. We therefore put $\eta \rightarrow \eta_R$ each time we calculate the momentum k_\perp above, and use $\eta \approx \eta' \approx \eta_R$ to set the other delta function to $\delta(\ell - \ell')$. This leaves us with

$$C(\ell) = \int_0^\infty \frac{dk_z}{\pi} P(\sqrt{k_z^2 + \ell^2 / (\eta_0 - \eta_R)^2}) (\eta_0 - \eta_R)^{-2} |\Delta(k_z, \ell)|^2 \quad (4.1.21)$$

where I change the integral to start at zero in exchange for a factor two, and define the flat sky transfer function

$$\Delta(k_z, \ell) = \int_0^{\eta_0} d\eta S(\sqrt{k_z^2 + \ell^2 / (\eta_0 - \eta_R)^2}, \eta) \exp(ik_z \eta) \quad (4.1.22)$$

This approximation of the power spectrum is shown in figure 5.

Next, let us go through the same procedure for the bispectrum, as [Fergusson and Shellard \(2008\)](#) do. We may again simply write down the correlator

$$\begin{aligned}
(2\pi)^2 \delta(\sum \ell) b_{\ell_1 \ell_2 \ell_3} &= \int d^3 k_1 d^3 k_2 d^3 k_3 \delta(\sum \mathbf{k}) B(k_1, k_2, k_3) \\
&\int_0^{\eta_0} d\eta S(k, \eta_1) \exp(-ik_{1z}[\eta_0 - \eta_1]) \delta(\mathbf{k}_{1\perp}(\eta_0 - \eta_1) - \ell_1) \\
&\int_0^{\eta_0} d\eta' S(k, \eta_2) \exp(ik_{2z}[\eta_0 - \eta_2]) \delta(\mathbf{k}_{2\perp}(\eta_0 - \eta_2) - \ell_2) \\
&\int_0^{\eta_0} d\eta' S(k, \eta_3) \exp(ik_{3z}[\eta_0 - \eta_3]) \delta(\mathbf{k}_{3\perp}(\eta_0 - \eta_3) - \ell_3)
\end{aligned} \tag{4.1.23}$$

Under the same approximations we integrate out the three k_{\perp} and insert them in the $\delta(\sum \mathbf{k}_{\perp})$ to get a delta function on the ℓ_i , which leaves us with

$$b_{\ell_1 \ell_2 \ell_3} = \left(\frac{1}{2\pi(\eta_0 - \eta_R)^2} \right)^2 \int_{-\infty}^{\infty} dk_{1z} dk_{2z} dk_{3z} \delta(\sum k_{iz}) B(k_1, k_2, k_3) \Delta(k_{1z}, \ell_1) \Delta(k_{2z}, \ell_2) \Delta(k_{3z}, \ell_3) \tag{4.1.24}$$

where the k_i in the bispectrum are given by $k_i = \sqrt{k_{iz}^2 + \ell_i^2 / (\eta_0 - \eta_R)^2}$. We can get rid of 'half' of these three integrals. The k_{3z} takes the delta function, and the lower half of the k_{2z} integral can be found by the symmetry $\Delta(k_z, \ell) = \Delta(-k_z, \ell)^*$. We therefore get $\Delta(k_{3z}, \ell_3) \rightarrow \Delta(k_{1z} + k_{2z}, \ell_3)^*$. We can use to our advantage that the integral is invariant under simultaneous complex conjugation and sending both $k_{iz} \rightarrow -k_{iz}$. We therefore only need to integrate eg. the positive k_{2z} values, and the negative part of the integral will just be the complex conjugate of the result. This also makes manifest the fact that our integral is real – we are adding a number and its complex conjugate. This frees us from numerical mistakes, which might otherwise have introduced accidental imaginary parts in the integration procedure. Writing this out, we have the final result

$$\begin{aligned}
b_{\ell_1 \ell_2 \ell_3} &= \left(\frac{1}{2\pi(\eta_0 - \eta_R)^2} \right)^2 \int_{-\infty}^{\infty} dk_{1z} \int_0^{\infty} dk_{2z} B(k_1, k_2, k_3) \\
&\times 2\text{Re}(\Delta(k_{1z}, \ell_1) \Delta(k_{2z}, \ell_2) \Delta^*(k_{1z} + k_{2z}, \ell_3))
\end{aligned} \tag{4.1.25}$$

4.2 LARGE SCALE STRUCTURE

We will in this analysis treat observations of galaxies similar to the previous analysis of the CMB. To do this, we must know the *perceived* galaxy distribution across the sky, for all relevant redshifts. The wrong answer is to simply take the galaxy distribution and write it in terms of spherical harmonics, as we will be missing terms like doppler shifting and lensing effects.

Three different groups have recently done this analysis to second order ([Bertacca, 2015](#); [Bertacca et al., 2014b,a](#); [Di Dio et al., 2014](#); [Yoo and Zaldarriaga, 2014](#)). I will follow the derivation of [Di Dio et al. \(2014\)](#), which uses the so-called geodesic light

cone coordinates. These are coordinates in which geodesics are easy to work with. In return, however, the translation back to Poisson gauge is a bit tricky. We need the translation back to Poisson gauge because it is here we know how the perturbations evolve. We will afterwards try to make sense of the small differences in the results of the three different calculations, largely following the work of [Nielsen and Durrer \(2017\)](#).

The galaxy number count is defined as

$$\Delta(\mathbf{n}, z) = \frac{N(\mathbf{n}, z) - N(z)}{N(z)} \quad (4.2.1)$$

where $N(\mathbf{n}, z)$ is the number of galaxies in a differential volume dzd^2n and $N(z) = (4\pi)^{-1} \int d^2n N(\mathbf{n}, z)$. Now, both the density and the volume element will be perturbed by general relativistic effects. It is these effects we want to clarify. I will here first do the calculation to first order in an attempt to let the physics be clear in spite of the calculations. A cursory glance at [Di Dio et al. \(2014\)](#) shows that the final answer to second order takes up several pages. There is, however a particular limit in which I will calculate the result to all orders. This will help us in the identification of discrepancies of different calculations. This means I will be spelling out a lot of details, which will be necessary to calculate the higher orders – even though it will seem excessive for the calculation of the first order.

We define for the density field and the jacobian the following

$$\rho(\mathbf{n}, z) = \bar{\rho}(\eta_s^{(0)}) \left(1 + \sum_n \delta^{(n)}\right) \quad (4.2.2)$$

$$V(\mathbf{n}, z) = \bar{V}(z) \left(1 + \frac{\sum_n \delta V^{(n)}}{\bar{V}}\right) \quad (4.2.3)$$

where the superscript (n) signifies the order of the contribution. It is clear that the first order contribution to Δ is

$$\Delta = \frac{\rho V - \langle \rho V \rangle}{\langle \rho V \rangle} \quad (4.2.4)$$

$$\Rightarrow \Delta^{(1)}(\mathbf{n}, z) = \delta^{(1)} + \frac{\delta V^{(1)}}{\bar{V}} \quad (4.2.5)$$

Background values have a superscript (0) , such that the fiducial conformal time and distance of a source at observed redshift z are defined by

$$1 + z_s = \frac{a(\eta_o)}{a(\eta_s^{(0)})} \quad \text{and} \quad r_s^{(0)} = \eta_o - \eta_s^{(0)} \quad (4.2.6)$$

To find the corrections, we will first calculate them exactly in the geodesic lightcurve coordinates and then do an approximate translation to Poisson gauge.

4.2.1 Geodesic lightcone coordinates

The geodesic lightcone (GLC) coordinates were first introduced by [Gasperini et al. \(2011\)](#) in relation to the problem of averaging in inhomogeneous cosmology, and can be seen as a gauge fixing of the historical *observational coordinates* of [Ellis et al. \(1985\)](#). They As it turns out, they will be very useful to our somewhat different purpose. Instead of the normal (η, r, θ, ϕ) we call them $(\tau, w, \tilde{\theta}_1, \tilde{\theta}_2)$. τ is a timelike coordinate, w is a null coordinate, and the remaining two $\tilde{\theta}_a$ are angular variables. We write the line element in these coordinates as

$$ds^2 = Y^2 dw^2 - 2Y dw d\tau + \gamma_{ab}(d\tilde{\theta}^a - U^a dw)(d\tilde{\theta}^b - U^b dw) \quad (4.2.7)$$

where as is usual there is an implicit sum over repeat indices, here a and b . In an exact FRW universe, the coordinates and metric functions translate trivially as $\tau^{(0)} = t$, $w^{(0)} = \eta + r$, $\tilde{\theta}^{(0)} = (\theta, \phi)$, $Y^{(0)} = a$, $U_a^{(0)} = 0$, $\gamma_{ab} = a^2 r^2 \text{diag}(1, \sin^2 \theta)$. We can also write the metric in matrix form as

$$g_{\mu\nu} = \begin{pmatrix} 0 & -Y & 0 \\ -Y & Y^2 + U^2 & -U_b \\ 0 & -U_a & \gamma_{ab} \end{pmatrix}, \quad g^{\mu\nu} = \begin{pmatrix} -1 & -Y^{-1} & -U^b/Y \\ -Y^{-1} & 0 & 0 \\ -U^a/Y & 0 & \gamma^{ab} \end{pmatrix} \quad (4.2.8)$$

We see that w is null by $\partial_\mu w \partial^\mu w = g^{ww} = 0$. We may also check that $-\partial_\mu \tau$ describes geodesic flow by verifying the following is zero,

$$\begin{aligned} \partial^\nu \tau \nabla_\nu (\partial_\mu \tau) &= -\frac{1}{2} g^{\nu\tau} g^{\sigma\tau} (g_{\sigma\nu,\mu} + g_{\mu\sigma,\nu} - g_{\mu\nu,\sigma}) = -\frac{1}{2} g^{\nu\tau} g^{\sigma\tau} g_{\sigma\nu,\mu} \\ &= -2 \frac{\partial_\mu Y}{Y} + \frac{\partial_\mu (Y^2 + U^2)}{Y^2} - 2 \frac{U^a \partial_\mu U_a}{Y^2} + \frac{U^a U^b \partial \gamma_{ab}}{Y^2} = 0 \end{aligned} \quad (4.2.9)$$

where the last equality follows from $U^a \partial_\mu U_a = U_a \partial_\mu U^a + U^a U^b \partial \gamma_{ab}$ and $\partial_\mu U^2 = U_a \partial_\mu U^a + U^a \partial_\mu U_a$. We can similarly show that the null rays $\partial_\mu w$ are geodesic, and so the lighttrays emitted by sources travel to the observer along these, on the observer's lightcone. The change in energy – the redshift – is then calculated as the product of the source/observer velocity and the photon momentum, $k^\mu \propto Y^{-1} \delta_\tau^\mu$, ([Gasperini et al., 2011](#))

$$1 + z_s = \frac{(k^\mu u_\mu)_s}{(k^\mu u_\mu)_o} = \frac{(Y^{-1} \delta_\tau^\mu \partial_\mu \tau)_s}{(Y^{-1} \delta_\tau^\mu \partial_\mu \tau)_o} = \frac{Y(\tau_o, w_o, \tilde{\theta}^a)}{Y(\tau_s, w_o, \tilde{\theta}^a)} \quad (4.2.10)$$

Note that the arguments $w_o, \tilde{\theta}^a$ are fixed along the geodesic. In the homogeneous universe this is the known result $1/a(t)$. In the inhomogeneous universe this is no longer true, however equation (4.2.10) is still exact, since the meaning of Y changes.

The angular diameter and luminosity distances may also be written down exactly in the GLC coordinates, [Fanizza et al. \(2013\)](#)

$$d_L^2 = (1 + z_s)^4 d_A^2 = (1 + z_s)^4 \frac{4\sqrt{\gamma_s}}{(\det(u_\tau^{-1} \partial_\tau \gamma^{ab}) \gamma^{3/2})_o} \quad (4.2.11)$$

where $\gamma = \det \gamma_{ab}$.

We now wish to translate these results into coordinates for which we can solve the behavior, here I choose Poisson coordinates. To do this, we must expand the expressions for the GLC coordinates in terms of the Poisson coordinates – specifically in powers of the first-order potential $\Psi^{(1)}$, which comes from the expansion of the full potential, $\Psi = \sum_n \Psi^{(n)}$. This is done via the transformation

$$g_{GLC}^{\mu\nu} = g_{PG}^{\sigma\rho} \partial_\sigma^{PG} x_{GLC}^\mu \partial_\rho^{PG} x_{GLC}^\nu \quad (4.2.12)$$

with suitable boundary conditions (Marozzi, 2015). We will take advantage of the many zeros in the inverse GLC metric. To repeat equation (3.0.1), the Poisson metric is, using conformal time and neglecting anisotropic stress, a useful approximation in the late universe,

$$g_{\mu\nu}^{PG} = a(\eta)^2 \begin{pmatrix} -1 - 2\Psi & 0 & 0 \\ 0 & 1 - 2\Psi & 0 \\ 0 & 0 & (1 - 2\Psi)\gamma_{ab}^{PG} \end{pmatrix} \quad (4.2.13)$$

where $\gamma_{ab}^{PG} = r^2 \text{diag}(1, \sin^2 \theta)$. Remember from the identification in the homogeneous universe, we already have the zeroth-order of the coordinate transformation. We first look at the $\tau - \tau$ component of equation (4.2.12), which gives

$$-a^2 = \frac{(\partial_\eta \tau)^2}{-1 - 2\Psi} + \frac{(\partial_r \tau)^2}{1 - 2\Psi} + \frac{\partial_a \tau \partial^a \tau}{1 - 2\Psi} \quad (4.2.14)$$

Here the partial derivatives ∂_a refer to the Poisson variables θ_a (with no tilde), whose indices are raised and lowered using γ_{ab}^{PG} . We know of course that the zeroth order must match, $\tau = t = \int d\eta a$. Taking only the first order of this equation, we get only contributions from the first term on the right-hand side

$$2\Psi a^2 = 2a \partial_\eta \tau^{(1)} \Rightarrow \tau^{(1)} = \int^\eta d\eta' a(\eta') \Psi(\eta', r, \theta^a) \equiv a(\eta) P(\eta, r, \theta^a) \quad (4.2.15)$$

which also defines the shorthand function P . For the null coordinate w we get, using the $w - w$ part of equation (4.2.12),

$$0 = \frac{(\partial_\eta w)^2}{-1 - 2\Psi} + \frac{(\partial_r w)^2}{1 - 2\Psi} + \frac{\partial_a w \partial^a w}{1 - 2\Psi} \quad (4.2.16)$$

Again, we may insert the zeroth order result, which gets rid of the angular part,

$$(1 - 2\Psi)(\partial_\eta w)^2 = (1 + 2\Psi)(\partial_r w)^2 \Rightarrow 2\partial_\eta w^{(1)} - 2\Psi = 2\partial_r w + 2\Psi \quad (4.2.17)$$

Let me now define zeroth order lightcone variables $\eta_\pm = \eta \pm r$, with the partial derivatives $\partial_\pm = (\partial_\eta \pm \partial_r)/2$. With these we write the previous equation as

$$\partial_- w^{(1)} = \Psi \Rightarrow w^{(1)}(\eta_+, \eta_-, \theta^a) = \int_{\eta_0}^{\eta_-} dx \Psi(\eta_+, x, \theta^a) \quad (4.2.18)$$

where the integral goes along the observer lightcone. This integral can also be written as

$$w^{(1)} = -2 \int_{\eta_s}^{\eta_0} d\eta' \Psi(\eta', \eta + r - \eta') \equiv -2 \int_{\eta_s}^{\eta_0} d\eta' \Psi[\eta'] \quad (4.2.19)$$

Keep good track of the factors of a when manipulating angular indices. For the Poisson coordinate angles, I take the indices to be raised and lowered using the scale-factor free γ . Also note that it means we have $\gamma^{(0)} = a^2 \gamma^{PG}$.

where the square brackets around the argument η' define a shorthand notation for the past lightcone at conformal time η' . Finally, looking at the $w - a$ part of equation (4.2.12) we have – after having already found the expression for w

$$0 = \frac{\partial_\eta w \partial_\eta \tilde{\theta}^a}{-1 - 2\Psi} + \frac{\partial_r w \partial_r \tilde{\theta}^a}{1 - 2\Psi} + \frac{\partial_b w \partial^b \tilde{\theta}^a}{1 - 2\Psi} \quad (4.2.20)$$

This equation is trivially satisfied at zeroth order, and the first order is

$$2\partial_- \tilde{\theta}^{(1)a} = \partial^b w^{(1)} \Rightarrow \tilde{\theta}^{(1)a}(\eta_+, \eta_-, \theta^a) = \frac{1}{2} \int_{\eta_0}^{\eta_-} dx \partial^a w^{(1)}(\eta_+, x, \theta^a) \quad (4.2.21)$$

equations (4.2.15), (4.2.18) and (4.2.21) define for us the first order translation to GLC coordinates from Poisson gauge. We are now in a position to translate the functions of the GLC metric as well. The $\tau - w$ part of equation (4.2.12) gives

$$Y^{-1} = a^{-2} \left(\frac{\partial_\eta \tau \partial_\eta w}{1 + 2\Psi} - \frac{\partial_r \tau \partial_r w}{1 - 2\Psi} - \frac{\partial_a \tau \partial^a w}{1 - 2\Psi} \right) \quad (4.2.22)$$

To first order the angular derivatives disappear, and we are left with

$$\begin{aligned} 1/Y^{(1)} &= a^{-2} \left(\frac{a}{1 + 2\Psi} + \partial_\eta \tau^{(1)} + a \partial_\eta w^{(1)} - \partial_r \tau^{(1)} \right) \\ &= a^{-1} \left(\partial_\eta w^{(1)} - \Psi - \partial_r P \right) = a^{-1} \left(\partial_+ w^{(1)} - \partial_r P \right) \end{aligned} \quad (4.2.23)$$

where I use $\partial_\eta w^{(1)} = \partial_+ w^{(1)} + \Psi$. To get U^a we look at the $\tau - a$ components of equation (4.2.12). These give to first order

$$\begin{aligned} U^a Y^{-1} &= a^{-2} \left(\partial_\eta \tau \partial_\eta \tilde{\theta}^a - \partial_r \tau \partial_r \tilde{\theta}^a - \partial_b \tau \partial^b \tilde{\theta}^a \right) = a^{-2} \left(\partial_\eta \tilde{\theta}^{(1)a} - \partial^a \tau^{(1)} \right) \\ \Rightarrow U^{(1)a} &= \partial_\eta \tilde{\theta}^a - \partial^a P \end{aligned} \quad (4.2.24)$$

Finally, we look at the $a - a$ part of equation (4.2.12). To first order both η and r derivatives drop out, which leaves us with

$$\gamma^{ab} = a^{-2} \frac{\partial_c \tilde{\theta}^a \partial^c \tilde{\theta}^b}{1 - 2\Psi} = a^{-2} \left(\frac{\gamma^{(0)ab}}{1 - 2\Psi} + \partial^b \tilde{\theta}^a + \partial^a \tilde{\theta}^b \right) \quad (4.2.25)$$

$$\Rightarrow \gamma^{(1)ab} = a^{-2} \left(2\Psi \gamma^{(0)ab} + \partial^{(a} \tilde{\theta}^{b)} \right) \quad (4.2.26)$$

where $X^{(\dots)}$ denotes symmetrization of the enclosed indices.

Having defined all the above functions we can begin translating the exact results in GLC gauge to approximate results in Poisson gauge. The redshift as given by equation (4.2.10) becomes, by inserting equation (4.2.23) and rewriting $\partial_+ w^{(1)} = \partial_\eta w^{(1)} - \Psi$,

$$1 + z_s \equiv \frac{a_0}{a_s} (1 + z^{(1)} + \dots) = \frac{a_0}{a_s} \left(1 - \partial_r P - 2 \int_{\eta_s}^{\eta_0} d\eta' \partial_\eta \Psi[\eta'] - \Psi \right) \quad (4.2.27)$$

Let us now find a more familiar form of the first term, $-\partial_r P$. Remember that the geodesic sources and observers have velocities $u_\mu = -\partial_\mu \tau$. By taking the spatial part of the scalar product of a unit vector along the line of photon propagation with the

source velocity, we get the velocity of the source parallel to the line of sight. The unit vector is $n_\mu = (0, -a\sqrt{1-2\Psi}, 0, 0)$ – note it is pointing inwards – and so the product is

$$v_{||} = \mathbf{v} \cdot \mathbf{n} = g_{PG}^{r\mu} a \sqrt{1-2\Psi} \partial_\mu \tau = \frac{1}{a\sqrt{1-2\Psi}} \partial_r \tau \quad (4.2.28)$$

$$v_{||}^{(1)} = \partial_r P \quad (4.2.29)$$

This shows that the first term of equation (4.2.27) is simply the recession velocity, ie. minus the speed towards us. This is the well known *Doppler shift*. Its effect is clear: when we observe a galaxy and infer its distance from us in terms of the redshift, the Doppler shift will change the two quantities. There is as such no direct translation from redshift to cosmic distance unless one knows the velocity of the galaxy.

4.2.2 Galaxy number count perturbation from GLC to Poisson gauge

Now to find the perturbation to Δ , we must find the perturbations of both parts of equation (4.2.4), ρ and V . The Newtonian calculation we did in section 3.2 gives us part of the answer, namely the simple expression of $\rho^{(n)}(z, \theta^a) = \bar{\rho} \delta_\rho^{(n)}$ for $n > 1$ in terms of $\rho^{(1)}$. However, we know that eg. the redshift has been perturbed, so we must also expand the first order contribution – and all higher orders – around the observed coordinates.

To do this, we first define a fiducial cosmology, in a sense the naively observed distances. This is simply identifying the redshift directly with the FRW conformal time and distance,

$$1 + z_s = a(\eta_o) / a(\eta_s^{(0)}), \quad w = w_o = \eta_o = \eta_s^{(0)} + r_s^{(0)} \quad (4.2.30)$$

We will then expand all observed quantities around these, and calculate the perturbations in GLC coordinates in powers of $\delta^{(1)}$. For these quantities, we need the following defining equations, which I equate with the definitions in equation (4.2.30)

$$\frac{a(\eta_o)}{a(\eta_s)} (1 + z^{(1)} + \dots) = \frac{a(\eta_o)}{a(\eta_s^{(0)})} \quad (4.2.31)$$

$$w^{(0)} + w^{(1)} + \dots = \eta_s^{(0)} + r_s^{(0)} \quad (4.2.32)$$

where I leave “...” in place of higher orders. Solving these equations for the higher order Poisson variables, as expanded around the fiducial value, $\eta_s = \eta_s^{(0)} + \eta_s^{(1)} + \dots$, $r_s = r_s^{(0)} + r_s^{(1)} + \dots$. The perturbative solutions for the first order is

$$\eta_s^{(1)} = z^{(1)} \mathcal{H}_s^{-1} \quad (4.2.33)$$

$$r_s^{(1)} = -\eta_s^{(1)} + 2 \int_{\eta_s^{(0)}}^{\eta_o} d\eta' \Psi[\eta'] \quad (4.2.34)$$

The first equation comes from expanding $a(\eta_s) / a(\eta_s^{(0)})$ taking $\eta_s = \eta_s^{(0)} + \dots$ in equation (4.2.31), which gives the factor $\mathcal{H}_s = a'(\eta_s^{(0)}) / a(\eta_s^{(0)})$, the conformal Hubble

parameter at the fiducial conformal time. The second equation is simply the collection of terms in equation (4.2.32), giving an expression for $r_s^{(n)}$ in terms of the GLC coordinates and $\eta_s^{(n)}$. We also need the angular changes. At first order, this is easy, since going from GLC to Poisson angles simply gives a sign change,

$$\theta^{(1)a} = -\tilde{\theta}^{(1)a} \quad (4.2.35)$$

With these perturbed Poisson coordinates, we may directly write down the perturbation of the observed density field,

$$\rho = \bar{\rho}(\eta_s^{(0)}) + \eta^{(1)}\partial_{\eta}\rho(\eta_s^{(0)}) + \delta\rho^{(1)}(\eta_s^{(0)}) + \dots \quad (4.2.36)$$

Since the zeroth order density field only depends on the conformal time, there is only the one correction at this order. At higher orders, we will find also coordinate perturbations of the perturbed density field. In terms of physical quantities, we may use the relation $d\bar{\rho}/dz = 3\bar{\rho}/(1+z)$ to write

$$\delta^{(1)} = \bar{\rho}^{-1}(\eta_s^{(1)}\partial_{\eta}\bar{\rho} + \delta\rho^{(1)}) = -3\delta z^{(1)} + \delta_{\rho}^{(1)} \quad (4.2.37)$$

where δ_{ρ} is the result of the Newtonian calculation.

We now also need the volume perturbation in order to get the full number count result. The 3 dimensional volume element as seen by an observer with velocity $u_{\mu} = -\partial_{\mu}\tau$ is

$$dV = \sqrt{-g}\epsilon_{\mu\nu\sigma\lambda}u^{\mu}dx^{\nu} \wedge dx^{\sigma} \wedge dx^{\lambda} \quad (4.2.38)$$

We may change coordinates to the observed redshift and angles, which defines a quantity v as follows

$$dV = \sqrt{-g}\epsilon_{\mu\nu\sigma\lambda}u^{\mu} \frac{\partial x^{\nu}}{\partial z} \frac{\partial x^{\sigma}}{\partial \theta_s} \frac{\partial x^{\lambda}}{\partial \phi_s} \left| \frac{\partial(\theta_s, \phi_s)}{\partial(\theta_o, \phi_o)} \right| dz d\theta_o d\phi_o \equiv v(z, \theta_o, \phi_o) dz d\theta_o d\phi_o \quad (4.2.39)$$

where the term in $|\dots|$ is simply a Jacobian. The volume perturbation we are trying to find is directly related to this v , since $\delta V/\bar{V} = (v - \bar{v})/\bar{v}$. As before, the result in GLC coordinates can be written down exactly. I remind that the geodesic null rays run along fixed GLC angles, so the Jacobian is trivial, and this fact also restricts the partial derivatives. Seeing as $g^{\tau\tau} = 0$ and $g^{\tau w} = Y^{-1}$ only one term in the sum ends up contributing. The determinant of the metric is easily found to be $\sqrt{-g} = \sqrt{|\gamma|}Y$, and so the result for the volume change is

$$dV = -\sqrt{-g}u^w \frac{\partial \tau}{\partial z} dz d\theta_o d\phi_o \Rightarrow v = -\sqrt{|\gamma|} \frac{d\tau}{dz} \quad (4.2.40)$$

I stress again that the expression in equation (4.2.40) is exact, and defines a very straight forward splitting of the volume change into redshift space distortion $-d\tau/dz$ and lensing effects, $\sqrt{|\gamma|}$. This splitting keeps its shape even after changing to Poisson variables, but is obvious in these coordinates. We will use this fact when calculating higher orders.

We now need to translate this expression into Poisson coordinates. To compute the first order contribution, as always, we can be a bit careless – things usually only get dirty at second order. We will use this to our advantage, as we can use the same trick to shorten the calculations for the following all-order result. I calculate first the determinant of γ divided by the zeroth order contribution, since we are calculating $\delta v/\bar{v}$. We can do this by taking the expression in equation (4.2.25) and do the explicit determinant to first order, which gives us the inverse determinant.

$$\sqrt{\gamma^{-1}}/\sqrt{(\gamma^{(0)})^{-1}} = \frac{1}{1-2\Psi} |\partial_b \tilde{\theta}^a| \quad (4.2.41)$$

To first order the last determinant here is simply $1 + \partial_a \tilde{\theta}^{(1)a}$. That means to first order we can invert this expression to get

$$\sqrt{\gamma}/\sqrt{\gamma^{(0)}} = 1 - 2\Psi - \partial_a \tilde{\theta}^{(1)a} \quad (4.2.42)$$

However, we are still missing a piece of the full first order expression, which is the change of the determinant due to the change in redshift. We have already in equations (4.2.33) and (4.2.34) calculated the changes in Poisson variables, so we simply need to add

$$\begin{aligned} & \partial_\eta \sqrt{\gamma^{(0)}} \eta_s^{(1)} + \partial_r \sqrt{\gamma^{(0)}} r_s^{(1)} + \partial_a \sqrt{\gamma^{(0)}} \theta^a \\ &= (2\mathcal{H}\eta^{(1)} + 2r^{-1}r^{(1)} + \cot(\theta)\theta) \sqrt{\gamma^{(0)}} \end{aligned} \quad (4.2.43)$$

where θ is only the first angle of the duo. The total first order change in the determinant of the Jacobian – what I call the lensing contribution – is then the sum of equations (4.2.42) and (4.2.43) minus 1,

$$\frac{\sqrt{|\gamma|}^{(1)}}{\sqrt{|\gamma|}^{(0)}} = -2\Psi - \partial_a \tilde{\theta}^a - \cot(\theta)\tilde{\theta} + 2\delta z^{(1)} + \frac{2}{r_s^{(0)}} \left(-\frac{z^{(1)}}{\mathcal{H}} + 2 \int_{\eta_s^{(0)}}^{\eta_0} d\eta' \Psi[\eta'] \right) \quad (4.2.44)$$

To make the comparison with Di Dio et al. (2014) explicit we rewrite the gradient of the angles. We calculated the angles in equation (4.2.21), and inserting and using equation (4.2.18) we get

$$\begin{aligned} \tilde{\theta}^{(1)a} &= \frac{1}{2} \int_{\eta_0}^{\eta^-} dx \partial^a w = 2 \int_{\eta_s}^{\eta_0} d\eta' \gamma_{PG}^{ab} \partial_b \int_{\eta'}^{\eta_0} d\eta'' \Psi[\eta''] \\ &= 2r^2 \partial^a \int_{\eta_s}^{\eta_0} d\eta' \frac{1}{(\eta_0 - \eta')^2} \int_{\eta'}^{\eta_0} d\eta'' \Psi[\eta''] \end{aligned} \quad (4.2.45)$$

To do one of these integrals, remember that the γ_{PG}^{ab} includes a factor r^{-2} , which we must include when integrating along the lightcone. We define the lensing potential ψ as follows,

$$\psi(z_s, \theta^a) = -2 \int_{\eta_s^{(0)}}^{\eta_0} d\eta' \frac{\eta' - \eta_s^{(0)}}{(\eta_0 - \eta_s^{(0)})(\eta_0 - \eta')} \Psi[\eta'] \quad (4.2.46)$$

You will notice this derivation does not use the expression for the luminosity distance, as it does in Di Dio et al. (2014). It is indeed nice to see that two different routes end up with the same result.

We can check that the angular derivative of the lensing potential is equal to the GLC angles. We first check the following derivative,

$$\frac{d}{d\eta}\psi = -2\frac{1}{(r_s^{(0)})^2}\int_{\eta_s^{(0)}}^{\eta_o} d\eta'\Psi[\eta'] \quad (4.2.47)$$

where I have identified $r_s^{(0)} = \eta_o - \eta_s^{(0)}$. It is clear when comparing this expression with equation (4.2.45) that we may write the angle as

$$\tilde{\theta}^{(1)a} = r^2\gamma_{PG}^{ab}\partial_a\psi \Rightarrow \partial_a\tilde{\theta}^a = r^2\partial_a\gamma_{PG}^{ab}\partial_b\psi \quad (4.2.48)$$

To this we add $\cot(\theta)\tilde{\theta}$, which gives us exactly the dimensionless Laplacian on the sphere, such that

$$-\partial_a\tilde{\theta}^a - \tilde{\theta}\cot\theta = \Delta_2\psi \quad \text{where} \quad (4.2.49)$$

$$\Delta_2 = \cot(\theta)\partial_\theta + \partial_\theta^2 + \sin\theta^{-2}\partial\phi^2 \quad (4.2.50)$$

That at last allows us to rewrite equation (4.2.44) to match the result of [Bonvin and Durrer \(2011\)](#); [Di Dio et al. \(2014\)](#),

$$\frac{\sqrt{|\gamma|}^{(1)}}{\sqrt{|\gamma|}^{(0)}} = -2\Psi + \Delta_2\psi + 2z^{(1)}\left(1 - (\mathcal{H}_s r_s^{(0)})^{-1}\right) + \frac{4}{r_s^{(0)}}\int_{\eta_s^{(0)}}^{\eta_o} d\eta'\Psi[\eta'] \quad (4.2.51)$$

We now have the lensing contribution to the volume change. We now need the contribution from redshift space distortion (RSD). This is, as we found, $-d\tau/dz$, and I remind we again need to divide out the zeroth order contribution. We again need to find the expansion around the fiducial cosmology, and then perform the differentiation. In terms of zeroth order coordinates, differentiation with respect to the redshift can be written as

$$-\frac{d\tau}{dz} = -\frac{d\eta_s^{(0)}}{dz}\frac{d\tau}{d\eta_s^{(0)}} = \frac{1}{(1+z_s)\mathcal{H}_s}\frac{d\tau}{d\eta_s^{(0)}} \quad (4.2.52)$$

Expanding τ around the fiducial cosmology, I denote by a subscript s that its arguments are now $(\eta_s^{(0)}, r_s^{(0)}, \theta_o^a)$. The zeroth and first orders are given by

$$\tau_s^{(0)} = \tau^{(0)} = \int^{\eta_s^{(0)}} d\eta' a(\eta') \quad (4.2.53)$$

$$\tau_s^{(1)} = \eta_s^{(1)}\partial_\eta\tau_s^{(0)} + \tau^{(1)} = a(\eta_s^{(0)})\eta_s^{(1)} + \int^{\eta_s^{(0)}} d\eta' a(\eta')\Psi(\eta', r_s^{(0)}, \theta_o^a) \quad (4.2.54)$$

The ratio of the first order to zeroth order of the RSD contribution is then

$$\frac{d\tau_s^{(1)}/dz}{d\tau_s^{(0)}/dz} = \frac{d\tau_s^{(1)}/d\eta_s^{(0)}}{d\tau_s^{(0)}/d\eta_s^{(0)}} \quad (4.2.55)$$

Remember here that $r_s^{(0)} = \eta_o - \eta_s^{(0)}$, and so we need to take this into consideration when differentiating with respect to $\eta_s^{(0)}$.

where we know $d\tau_s^{(0)}/d\eta_s^{(0)} = a$. Writing out the derivative of equation (4.2.54) we get

$$\frac{d}{d\eta_s^{(0)}}(a(\eta_s^{(0)})z^{(1)}\mathcal{H}^{-1}) = a\left(1 - \frac{\mathcal{H}'}{\mathcal{H}^2}\right)z^{(1)} + \frac{a}{\mathcal{H}}\frac{dz^{(1)}}{d\eta_s^{(0)}} \quad (4.2.56)$$

$$\frac{dz^{(1)}}{d\eta_s^{(0)}} = \mathcal{H}v_{||} + \partial_r v_{||} + \partial_\eta \Psi \quad (4.2.57)$$

$$\frac{d}{d\eta_s^{(0)}} \int^{\eta_s^{(0)}} d\eta' a(\eta') \Psi(\eta', r_s^{(0)}, \theta_o^a) = a(\eta) \Psi(\eta_s^{(0)}, r_s^{(0)}, \theta_o^a) - av_{||}^{(1)} \quad (4.2.58)$$

To get equation (4.2.57) I use the form $z^{(1)} = -v_{||} + \partial_+ w^{(1)}$ and write out the two terms as

$$\frac{dv_{||}^{(1)}}{d\eta_s^{(0)}} = \partial_r \psi - \mathcal{H}v_{||} - \partial_r v_{||}^{(1)} \quad (4.2.59)$$

$$\partial_+ \frac{dw^{(1)}}{d\eta_s^{(0)}} = \partial_+(2\Psi) = \partial_\eta \Psi + \partial_r \Psi \quad (4.2.60)$$

Summing it all up, we end with

$$\frac{d\tau_s^{(1)}/dz}{d\tau_s^{(0)}/dz} = \left(1 - \frac{\mathcal{H}'}{\mathcal{H}^2}\right)z^{(1)} + \mathcal{H}^{-1}(\partial_\eta \Psi + \partial_r v_{||}) + \Psi \quad (4.2.61)$$

We can finally write down the first order correction to the volume, and in turn the full first order correction to the galaxy number count.

$$\begin{aligned} \frac{v - \bar{v}}{\bar{v}} &= \frac{\sqrt{|\gamma|}^{(1)}}{\sqrt{|\gamma|}^{(0)}} + \frac{d\tau_s^{(1)}/dz}{d\tau_s^{(0)}/dz} \\ &= -\Psi + \Delta_2 \psi + z^{(1)} \left(3 - \frac{2}{\mathcal{H}r_s^{(0)}} - \frac{\mathcal{H}'}{\mathcal{H}^2}\right) + \frac{4}{r_s^{(0)}} \int_{\eta_s^{(0)}}^{\eta_o} d\eta' \Psi[\eta'] + \mathcal{H}^{-1}(\partial_\eta \Psi + \partial_r v_{||}^{(1)}) \end{aligned} \quad (4.2.62)$$

Adding the contributions of equations (4.2.37) and (4.2.62) we have the full first order result,

$$\begin{aligned} \Delta_{\text{full}}^{(1)} &= \delta_\rho^{(1)} - \Psi + \Delta_2 \psi + \left(v_{||}^{(1)} + \Psi + 2 \int_{\eta_s^{(0)}}^{\eta_o} d\eta' \Psi[\eta']\right) \left(\frac{2}{\mathcal{H}r_s^{(0)}} + \frac{\mathcal{H}'}{\mathcal{H}^2}\right) \\ &\quad + \frac{4}{r_s^{(0)}} \int_{\eta_s^{(0)}}^{\eta_o} d\eta' \Psi[\eta'] + \mathcal{H}^{-1}(\partial_\eta \Psi + \partial_r v_{||}^{(1)}) \end{aligned} \quad (4.2.63)$$

It is now interesting to study the approximate size of each of these terms. In particular I am interested in small scales at intermediate redshift – where one could imagine a galaxy survey. The terms I keep will be the ones that naively match the size of $\delta_\rho^{(1)}$. As we can see from eg. equation (3.2.6) the potential is

$$\Psi = -\frac{3}{2}\delta \frac{\mathcal{H}^2}{k^2} \quad (4.2.64)$$

It is suppressed by two factors of \mathcal{H}/k . Small scales have large k , and so this suppresses the potential. We also have from equation (3.2.16) that the gradient of the

Remember small scales on the full sky translate to our ability to approximate the result by a flat sky. Therefore the terms we find at small scales will have their computation greatly simplified.

velocity field times the conformal Hubble factor is of the same order as the density field. This means we have the following approximate result

$$\mathcal{H}^{-1}\partial_r v_{||}^{(1)} \approx \theta_1 = \delta_\rho^{(1)} \quad (4.2.65)$$

*Do not let the notation confuse.
This θ_1 is the perturbative expansion of the velocity potential – not an angle.*

Evidently, we need either angular or radial derivatives to pull out factors of k/\mathcal{H} , which enhance the terms. Terms like a bare potential are suppressed, and so we neglect them in the further analysis. The same goes for integrated potentials and velocities with no derivative. Going through all the terms in equation (4.2.63) it is clear that only three terms survive,

$$\Delta^{(1)} = \delta_\rho^{(1)} + \mathcal{H}^{-1}\partial_r v_{||}^{(1)} + \Delta_2\psi \quad (4.2.66)$$

The angular derivative of the potential gives a factor $\ell^2 \sim (k/\mathcal{H})^2$, which enhances the lensing term enough to be considered. In the notation of [Di Dio et al. \(2016\)](#) the middle term is written as $\mathcal{H}^{-1}\partial_r^2 v^{(1)}$ where v is the velocity potential.

It is in this limit that I want to derive the all-order result, for what we call the *dominant* terms. It should be clear that the dominating term of a particular order is not necessarily larger than subdominant terms of lower orders. However, both second and third order dominant terms are important for the bispectrum and for the first corrections to the power spectrum. The remaining higher orders will simply be a by-product of the general derivation. Should the full higher order perturbations ever be calculated, I hope this result can serve as a cross-check.

4.2.3 All-order result at small scales

Now I proceed to calculate the galaxy number count change at all orders, but only the dominant terms, as defined above. In doing this, I will at all times throw away subdominant terms immediately, to facilitate the process. This is the only reason the calculation is doable at all. As we have seen, even the first order result is somewhat long, and as I already mentioned, the second order result takes up many pages.

We start over from the beginning. That means we need the expressions for the GLC coordinates in terms of Poisson coordinates. Rewriting equation (4.2.14) and discarding subdominant terms we have

$$\partial_\eta \tau^{(N)} = a^{-1} \sum_{n=1}^{N-1} \partial_r \tau^{(n)} \partial_r \tau^{(N-n)} + \partial^a \tau^{(n)} \partial_a \tau^{(N-n)} \quad (4.2.67)$$

$$2\partial_- w^{(N)} = \sum_{n=1}^{N-1} \partial^a w^{(n)} \partial_a w^{(N-n)} \quad (4.2.68)$$

$$2\partial_- \tilde{\theta}^{(N)a} = \sum_{n=1}^N \partial^b w^{(n)} \partial_b \tilde{\theta}^{(N-n)a} \quad (4.2.69)$$

A clearly subdominant term is the potential. Unless it carries along angular derivatives, I discard a potential right away.

with the first order result

$$\partial_\eta \tau^{(1)} = a\Psi \quad \partial_- w^{(1)} = \Psi \quad 2\partial_- \theta^{(1)a} = \partial^a w^{(1)} \quad (4.2.70)$$

We may recursively generate all the higher orders of the coordinate transformation. We also need the two GLC functions Y and γ , which from equations (4.2.22) and (4.2.25) are simply

$$Y^{-1} = a^{-2} \partial_r \tau \quad (4.2.71)$$

$$\gamma^{ab} = a^{-2} \partial^c \bar{\theta}^a \partial_c \bar{\theta}^b \quad (4.2.72)$$

To get the redshift perturbation, we simply take the exact definition in GLC coordinates

$$1 + z_s = Y_o / Y_s \Rightarrow z^{(N)}(\eta_s, r_s, \theta_s^a) = a^{-1} \partial_r \tau^{(N)} = -v_{\parallel}^{(N)} = -\partial_r v^{(N)} \quad (4.2.73)$$

I have here identified the recession velocity with the radial velocity, as the difference is subdominant, and written it in terms of the velocity potential v . We now proceed to find the changes with respect to the fiducial cosmology, the naive expectation. Since all factors of w are subdominant, except for the first one, we simply have to solve

$$a(\eta_s^{(0)})^{-1} = a(\eta_s)^{-1} (1 + \sum z^{(N)}(\eta_s, r_s, \theta_s^a)) \quad \text{where} \quad \eta_s^{(N)} + r_s^{(N)} = 0 \quad (4.2.74)$$

$$\Rightarrow \eta_s^{(N)} = -r_s^{(N)} = \mathcal{H}^{-1}[z]^{(N)} \quad (4.2.75)$$

The bracket-notation is to signify *all* n -th order terms coming from the Taylor expansion around the fiducial model. Since the coordinates of z above are (η_s, r_s, θ^a) , the second order term will also include radial and angular derivatives. For instance, the second order redshift perturbation is

$$\begin{aligned} [z(\eta_s, r_s, \theta_s^a)]^{(2)} &= z^{(2)}(\eta_s^{(0)}, r_s^{(0)}, \theta_s^a) + r_s^{(1)} \partial_r z^{(1)}(\eta_s^{(0)}, r_s^{(0)}, \theta_s^a) \\ &\quad + \theta^{(1)a} \partial_a z^{(1)}(\eta_s^{(0)}, r_s^{(0)}, \theta_s^a) \end{aligned} \quad (4.2.76)$$

Note that since the second order redshift change is dependent on the first order redshift change, we need to do this procedure recursively.

Getting the angles right is somewhat tricky when starting from the GLC coordinates. Luckily, angular perturbations have been important since lensing in the CMB was found significant. That means we can lift the result from the old literature and mold them for our purposes. Here I take the results of [Pyne and Carroll \(1996\)](#). In particular, we will need to find the dominating terms in their $f^{(N)\mu}$, defined in their equations (3.3) and (3.4). These equations are simply the geodesic equation written in terms of an explicit expansion of coordinates and the connection,

$$\begin{aligned} \sum_{a=0}^{\infty} \left[\frac{d^2 x^{(a)\mu}}{d\lambda^2} + \left(\Gamma^{(a)\mu}{}_{\alpha\beta} + \sum_{b=1}^{\infty} \frac{1}{b!} \partial_{\sigma_1} \cdots \partial_{\sigma_b} \Gamma^{(a)\mu}{}_{\alpha\beta} (\sum_{c=1}^{\infty} x^{(c)\sigma_1}) \cdots (\sum_{d=1}^{\infty} x^{(d)\sigma_b}) \right) \right. \\ \left. \times (\sum_{e=1}^{\infty} k^{(e)\alpha}) (\sum_{f=1}^{\infty} k^{(f)\beta}) \right] = 0 \end{aligned} \quad (4.2.77)$$

Note here that I throw away the radial derivative of an integral on the lightcone. I also discard the term $\partial_a \tau \partial_a w$ – it has two derivatives, but also two factors of potential to suppress it, so it is one suppressive factor short of $\partial_r \tau$.

Here I only include the first derivative of a . It should be clear that higher derivatives will include products of higher order of $\eta_s^{(n)}$, which in turn are subdominant contributions

We now rewrite this equation order by order. This defines $f^{(N)\mu}$,

$$\frac{d^2 x^{(a)\mu}}{d\lambda^2} + 2\Gamma^{(0)\mu}{}_{\alpha\beta} k^{(0)\alpha} k^{(a)\beta} + \partial_\sigma \Gamma^{(0)\mu}{}_{\alpha\beta} k^{(0)\alpha} k^{(0)\beta} x^{(a)\sigma} = f^{(a)\mu} \quad (4.2.78)$$

An important feature of $f^{(a)\mu}$ is that the highest order of x or k appearing is $(a-1)$. Calculating this quantity will give us the angular perturbation when inserted into their equation (3.13), which in a flat universe reads

$$x_\perp^{(a)i} = \int_{\lambda_0}^{\lambda} (\lambda - \lambda') f_\perp^{(a)i}(\lambda') d\lambda' \quad (4.2.79)$$

The projection is defined as $x_\perp^i = (\delta_j^i - e^i e_j) x^j$ where e are unit vectors.

To find the dominating terms of f^μ it is easiest to first do a conformal transformation. Remember that all we are after is the angular changes, and conformal transformations leave angles unchanged. To first order in the gravitational potential, we can therefore change the metric to $\tilde{g}_{\mu\nu} = \text{diag}(-1 - 4\Psi, 1, 1, 1)$ and do the calculations here. The answer we get for the angles will then be conserved if we were to change coordinates back again. For this metric, the relevant terms in the connection are only

$$\Gamma_{i0}^{(1)0} = \Gamma_{00}^{(1)i} = 2\partial_i \Psi = 2\partial_i \sum_n \Psi^{(n)} \quad (4.2.80)$$

All other terms either contain time-derivatives or no derivatives at all, both of which are suppressed in the limit we are working with. It should also be clear, that all higher orders in the counting of [Pyne and Carroll \(1996\)](#) are similarly suppressed. So the only terms we need to include in f^μ are those containing $\Gamma^{(1)}$. In our counting, this will also contain higher order corrections of the gravitational potential coming from the evolution of large scale structure, ie. $\Psi^{(N)}$. We are further constrained to only look at the terms with the lowest order of k^α , since higher orders would simply lower the number of derivatives we have on the terms – fewer derivatives means the term is subdominant in our counting. Removing all these subdominant terms from their equation (3.3) it should be clear that the only terms we keep are

$$f^{(N)\mu} = -[\Gamma_{\alpha\beta}^{(1)\mu} k^{(0)\alpha} k^{(0)\beta}]^{(N)} = \begin{cases} -[2e^i \partial_i \Psi]^{(N)} & \text{when } \mu = 0 \\ -[2\partial_i \Psi]^{(N)} & \text{when } \mu = i \end{cases} \quad (4.2.81)$$

where again the brackets stand for the Taylor expansion of the expression, taken at order N . Now, to get the angular perturbations, we need to insert this expression in their equation (3.13). Specifically, we want the expression for the coordinates perpendicular to the line of sight, what I call the *screen space*, $x_\perp^{(n)i} \rightarrow r^{(0)} \theta^{(n)a}$. I remind that the derivatives in equation (4.2.81) are with respect to the screen space coordinates, not the angles, so another factor $r^{(0)}$ will appear when changing from these to angles. Inserting our answer for $f^{(N)\mu}$ in their expression for $x_\perp^{(N)i}$, we get

$$\frac{x_\perp^{(N)i}}{r_s^{(0)}} = -2 \int_0^{r_s^{(0)}} dr \frac{r_s^{(0)} - r}{r_s^{(0)} r} \left[\frac{r_s^{(0)} \partial \Psi}{\partial x_\perp^i} \right]^{(N)} \quad (4.2.82)$$

Changing the indices from screen space i to the angular a , we have immediately

$$\theta_s^{(N)a} = -2 \int_0^{r_s^{(0)}} dr \frac{r_s^{(0)} - r}{r_s^{(0)} r} [\partial^a \Psi]^{(N)} \quad (4.2.83)$$

As an example, the explicit form of the second order angular change is

$$\theta^{(2)a} = -2 \int_0^{r_s^{(0)}} dr \frac{r_s^{(0)} - r}{r_s^{(0)} r} \left[\partial^a \Psi^{(2)} + \theta^{(1)b} \partial_b \partial^a \Psi^{(1)} \right] \quad (4.2.84)$$

Note that the change in radial coordinates does not affect the angles. This would have entered in the limits of the integral, however inserting it, we see that it does not contribute with derivatives – the differentiation simply removes the integral, and we are a derivative short of being a dominant contribution. We therefore only need to expand the $\partial^a \Psi$ in angular coordinates inside the integral.

With all the fiducial coordinates determined, we are able to calculate the expansion of the density field around the fiducial coordinates and to calculate the change in the Jacobian. The expansion is rather simple, since we know all the coordinate changes. The derivatives with respect to conformal time are still subdominant, and are left out of the expansion,

$$\delta^{(N)}(\eta_s^{(0)}, r_s^{(0)}, \theta_o^a) = \left[\delta_\rho(\eta_s^{(0)}, r_s, \theta^a) \right]^{(N)} \quad (4.2.85)$$

As an example, the second and third orders are

$$\delta^{(2)} = \delta_\rho^{(2)} + (r_s^{(1)} \partial_r + \theta_s^{(1)a} \partial_a) \delta_\rho^{(1)} \quad (4.2.86)$$

$$\delta^{(3)} = \delta_\rho^{(3)} + (r_s^{(1)} \partial_r + \theta_s^{(1)a} \partial_a) \delta_\rho^{(2)} \quad (4.2.87)$$

$$\begin{aligned} &+ (r_s^{(2)} \partial_r + \theta_s^{(2)a} \partial_a) \delta_\rho^{(1)} \\ &+ \frac{1}{2} \left((r_s^{(1)})^2 \partial_r^2 + \theta_s^{(1)a} \theta_s^{(1)b} \partial_a \partial_b + 2r_s^{(1)} \theta^{(1)a} \partial_r \partial_a \right) \delta_\rho^{(1)} \end{aligned}$$

where all terms on the right-hand side are evaluated at the fiducial coordinates. What remains is the change in the perceived volume. We first look at the lensing part. From equation (4.2.72) we find the ratio to be

$$\frac{\sqrt{\gamma^{-1}}}{\sqrt{\gamma^{-1(0)}}} = \frac{\sqrt{|\gamma^{-1}|^{(0)} \times |\partial_a \tilde{\theta}^b|^2}}{\sqrt{\gamma^{-1(0)}}} = |\partial_a \tilde{\theta}^b| \quad (4.2.88)$$

$$\Rightarrow \frac{\sqrt{\gamma}}{\sqrt{\gamma^{(0)}}} = \left| \frac{\partial \theta_s^b}{\partial \theta_o^a} \right| \quad (4.2.89)$$

This is precisely the determinant of the lensing-map which takes observed angles to the actual source angles. We of course need this determinant at the fiducial coordinates. We therefore need to expand the terms in the determinant, like we did for the density field. We may write the following general expression for the determinant, where I define $\delta\theta^a = \theta^a - \theta_o^a = \sum_{n=1}^{\infty} \theta^{(n)a}$,

$$\left(\frac{v - \bar{v}}{\bar{v}} \right)^{(N)} = \left[\frac{\partial \theta_s^b}{\partial \theta_o^a} \right]^{(N)} = \left[1 + \partial_a \delta\theta^a + \frac{1}{2} \left((\partial_a \delta\theta^b)^2 - \partial_a \delta\theta^b \partial_b \delta\theta^a \right) \right]^{(N)} \quad (4.2.90)$$

The notation here is simply $[\dots]$ for the Taylor expansion and $|\dots|$ for the determinant. For the second and third order of the lensing contribution that gives

$$\left(\frac{v - \bar{v}}{\bar{v}}\right)^{(2)} = \partial_a \theta^{(2)a} + \frac{1}{2} (\partial_a \theta^{(1)a})^2 - \frac{1}{2} \partial_a \theta^{(1)b} \partial_b \theta^{(1)a} \quad (4.2.91)$$

$$\left(\frac{v - \bar{v}}{\bar{v}}\right)^{(3)} = \partial_a \theta^{(3)a} + \partial_a \theta^{(1)a} \partial_a \theta^{(2)a} - \partial_a \theta^{(2)b} \partial_b \theta^{(1)a} \quad (4.2.92)$$

Note again that all radial derivatives are gone, since the angles are all given by integrals along the lightcone.

To calculate the RSD term we need to find the dominating terms of $d\tau_s/dz$, where again τ has been expanded around the fiducial coordinates.

The only term in this expansion we get is the very first derivative of the zeroth order τ . That is, for all N we have $\tau_s^{(N)} = a(\eta_s^{(0)})\eta_s^{(N)} = a\mathcal{H}_s^{-1}z^{(N)}$. Note it is easy to check that this dominates all the expansions in $\tau^{(N)}$ – without the subscript s – since we see from equation (4.2.73) that $z^{(N)} = \partial_r \tau^{(N)}/a$ ie. it has a derivative, or a factor k , over the bare τ expansion in Poisson coordinates. Therefore, the dominating term does not include any of the terms from the expansion in equation (4.2.67). We also do not include higher derivatives of $\tau^{(0)}$ since these contribute with fewer derivatives. For example $r^{(1)}\partial_r \tau = a\mathcal{H}^{-1}(z^{(1)})^2$ is subdominant compared to eg. $z^{(2)}$.

The only contribution to the RSD term is therefore

$$\text{RSD}^{(N)} = \mathcal{H}^{-1} \frac{d(-z^{(N)})}{d\eta_s^{(0)}} = \mathcal{H}^{-1} \partial_r [z]^{(n)} \quad (4.2.93)$$

All in all we may write, in a somewhat concise notation

$$\Delta = (1 + \delta)(1 + \text{RSD}) |A_a^b| \quad (4.2.94)$$

where all terms are expanded around the fiducial coordinates. The matrix A is the lensing map, defined as $A_a^b = \partial \theta_s^b / \partial \theta_0^a$. The expansion can be found from equations (4.2.73), (4.2.75), (4.2.83), (4.2.90) and (4.2.93) We may immediately write out the second order perturbations, which are

$$\begin{aligned} \Delta^{(2)} &= \mathcal{H}^{-1} \delta^{(1)} \partial_r^2 v^{(1)} - 2\delta^{(1)} \kappa^{(1)} - 2\mathcal{H}^{-1} \partial_r^2 v^{(1)} \kappa^{(1)} \\ &+ \delta^{(2)} + \mathcal{H}^{-1} \partial_r v^{(1)} \partial_r \delta^{(1)} + \partial^a \psi^{(1)} \partial_a \delta^{(1)} \\ &+ \mathcal{H} \partial_r \left(\partial_r v^{(2)} + \mathcal{H} \partial_r v^{(1)} \partial_r^2 v^{(1)} + \partial^a \psi^{(1)} \partial_a \partial_r v^{(1)} \right) \\ &- 2\kappa^{(2)} + 2\kappa^{(1)2} - 2\partial_a \kappa^{(1)} \partial^a \psi^{(1)} \\ &- \frac{1}{2} \int_0^{r(z)} dr \frac{r(z) - r}{r(z)r} \Delta_2 \left(\partial^a \Psi_1^{(1)} \partial_a \Psi_1^{(1)} \right) - 2 \int_0^{r(z)} \frac{dr}{r} \partial^a \Psi_1^{(1)} \partial_a \kappa^{(1)} \end{aligned} \quad (4.2.95)$$

I have here introduced the *convergence* $\kappa^{(N)} = -\frac{1}{2} \partial_a \partial^a \psi^{(N)}$ and the shorthand for the logarithmic radial derivative of the lensing potential $\Psi_1^{(N)} = -rd\phi^{(N)}/dr$. The first line here are all the cross-products from the three terms, the next lines are the density

and RSD terms expanded, while the last two lines are the lensing term expanded and rewritten. This result matches exactly the result derived by Di Dio et al. (2016) from the full result of Di Dio et al. (2014). Since the calculation was done by Bertacca et al. (2014a) and Yoo and Zaldarriaga (2014) as well, let us delve into their calculations. They disagree on minor points. We shall see how they differ, and how they compare to the result of equations (4.2.67) to (4.2.94). The coming two sections follow Nielsen and Durrer (2017) closely.

4.2.4 Comparison with Bertacca et al. (2014b)

I start by relating the notation of one to the other. The main notational differences are:

- The second order metric perturbations are defined with a factor 2 difference.
- There is a factor (-1) between the definitions of the velocity potential.
- Projected derivatives are used, ie. $\partial_{\parallel} = \partial_r$ and $\partial_{\perp}^i = r^{-1}\partial^a$.

Identifying the leading terms in the expression for $\Delta^{(2)}$, and expanding the expression for $\Delta^{(1)}$, we find

$$\begin{aligned} \Delta^{(2)} = & \delta_g^{(2)} - \frac{1}{\mathcal{H}} \partial_{\parallel}^2 v^{(2)} - 2\kappa^{(2)} + 4\kappa^{(1)2} - 4\delta\kappa^{(1)} - 2\frac{\delta_g}{\mathcal{H}} \partial_{\parallel}^2 v \\ & + \frac{4\kappa^{(1)}}{\mathcal{H}} \partial_{\parallel}^2 v + \frac{2}{\mathcal{H}^2} \left(\partial_{\parallel}^2 v \right)^2 + \frac{2}{\mathcal{H}^2} \partial_{\parallel} v \partial_{\parallel}^3 v - \frac{2}{\mathcal{H}} \frac{d\delta_g}{d\tilde{\chi}} \Delta \ln a^{(1)} \\ & - 2 \left[\tilde{\chi} \partial_{\perp i} \delta_g - \frac{\tilde{\chi}}{\mathcal{H}} \partial_{\perp i} \partial_{\parallel}^2 v \right] \partial_{\perp}^i T^{(1)} + 4 \left[\tilde{\chi} \partial_{\perp i} \delta_g - \frac{\tilde{\chi}}{\mathcal{H}} \partial_{\perp i} \partial_{\parallel}^2 v \right] S_{\perp}^{i(1)} \\ & - 4 \left(\int_0^{\tilde{\chi}} d\tilde{\chi} \frac{\tilde{\chi}}{\tilde{\chi}} (\tilde{\chi} - \tilde{\chi}) \mathcal{P}_j^p \mathcal{P}^{iq} \tilde{\partial}_q \tilde{\partial}_p \Phi \right) \left(\int_0^{\tilde{\chi}} d\tilde{\chi} \frac{\tilde{\chi}}{\tilde{\chi}} (\tilde{\chi} - \tilde{\chi}) \mathcal{P}_i^n \mathcal{P}^{jm} \tilde{\partial}_m \tilde{\partial}_n \Phi \right). \end{aligned} \quad (4.2.96)$$

The translation of the majority of the terms is straight-forward. The term $a^{(1)}$ is the first order perturbation of the scale factor taken to be $1/(z+1)$. To leading order, we may substitute it by the redshift space distortion, $\Delta \ln a^{(1)} = -\partial_r v^{(1)}$. $\tilde{\chi}$ is the comoving distance which we call r and $d/d\tilde{\chi} = -d/d\lambda = \partial_r - \partial_t \simeq \partial_{\parallel}$, the difference ∂_t is subdominant. With this we can write the first two lines immediately in the more familiar form,

$$\begin{aligned} \delta^{(2)} + \frac{1}{\mathcal{H}} \partial_r^2 v^{(2)} - 2\kappa^{(2)} + 2 \left(2\kappa^{(1)2} - 2\delta\kappa^{(1)} + \frac{\delta^{(1)}}{\mathcal{H}} \partial_r^2 v^{(1)} \right. \\ \left. - \frac{2\kappa^{(1)}}{\mathcal{H}} \partial_r^2 v^{(1)} + \frac{1}{\mathcal{H}^2} \left(\partial_r^2 v^{(1)} \right)^2 + \frac{1}{\mathcal{H}^2} \partial_r v^{(1)} \partial_r^3 v^{(1)} + \frac{1}{\mathcal{H}} \partial_r \delta^{(1)} \partial_r v^{(1)} \right). \end{aligned} \quad (4.2.97)$$

Note that the index structure here enjoys a slight abuse of notation. However, the angular derivatives always appear contracted, and we do have the strict equality $\partial_{\perp}^i f \partial_{i\perp} g = r^{-2} \partial^a f \partial_a g$.

I will in these two sections keep the notation strictly as it is written in the relevant other paper. That means for example the derivatives are written as $d/d\lambda$ in one notation but as ∂_{\parallel} in another. This is done purposefully to keep the comparison across the literature explicit and simple.

The third line above requires the translation of $S_{\perp}^{i(1)}$ and $\partial_{\perp}^i T^{(1)}$. Denoting the transverse direction of a vector, v_{\perp}^i by v^a , these are

$$S_{\perp}^{i(1)} = -\partial^a \int_0^{r_s} dr \frac{1}{r} \Psi^{(1)}, \quad \partial_{\perp}^i T^{(1)} = -\partial^a \int_0^{r_s} dr \frac{2}{r_s} \Psi^{(1)}$$

so that $2S_{\perp}^{i(1)} - \partial_{\perp}^i T^{(1)} = \partial^a \psi^{(1)}$. (4.2.98)

This multiplies the term in brackets, hence this line is the angular Taylor expansion of $\delta + \mathcal{H}^{-1} \partial_r^2 v$, with the appropriate extra factor 2. In the last line of equation (4.2.96) we simply need to substitute the derivatives and notation of potentials to obtain

$$-\partial^a \partial^b \left(2 \int_0^{\tilde{\chi}} d\tilde{\chi} \frac{\tilde{\chi} - \tilde{\chi}}{\tilde{\chi} \tilde{\chi}} \Psi^{(1)} \right) \partial_a \partial_b \left(2 \int_0^{\tilde{\chi}} d\tilde{\chi} \frac{\tilde{\chi} - \tilde{\chi}}{\tilde{\chi} \tilde{\chi}} \Psi^{(1)} \right) = -2 \frac{1}{2} \partial^a \partial^b \psi^{(1)} \partial_a \partial_b \psi^{(1)}.$$

(4.2.99)

This is exactly twice the last term of equation (4.2.91), which cancels a term in $\partial_a [\theta^a]^{(2)}$, and therefore does not appear in the final result. The factor 2 comes from the definition of the second order perturbations.

This shows that the difference between the results of [Di Dio et al. \(2016\)](#) and [Bertacca et al. \(2014b\)](#) is simply the substitution of $\partial_a [\theta^a]^{(2)}$ with $\kappa^{(2)}$, which neglects the terms coming from the fact that in $\partial_a [\theta^a]^{(2)}$ there are the additional lensing terms, namely all terms coming from evaluating the first order lensing integral at the perturbed position, the so called ‘post-Born’ contributions.

The authors of Bertacca et al. (2014b) agree with this finding and they have corrected the error in v4 on the arXiv with which we fully agree.

4.2.5 Comparison with [Yoo and Zaldarriaga \(2014\)](#)

I now proceed to identify the leading terms of [Yoo and Zaldarriaga \(2014\)](#). Since the full final result is not written down in closed form, we perform the ‘stitching-together’ on the fly, working our way back through the paper. The main remarks about the notation here are:

- Latin indices go from 0 to 3, greek indices go from 1 to 3.
- The metric perturbations are called \mathcal{A} and $C_{\alpha\beta}$, where $C_{\alpha\beta} = -\Psi \delta_{\alpha\beta}$ in the gauge we are working, for purely scalar perturbations. They are however defined with no factor 2 at second order.
- All perturbation orders are left implicit. Here we keep them explicit.
- The angles (θ, ϕ) are written explicitly. This gives rise to some factors of $\sin \theta$ between expressions, which are implicit in our notation with θ^a and covariant derivatives.

The leading terms in the main result, their equation (94) are

$$\Sigma^{(2)} = \delta^{(2)} + \delta V^{(2)} + \delta^{(1)} \delta V^{(1)}. \quad (4.2.100)$$

The first order volume perturbation is given by

$$\delta V^{(1)} = -2\kappa^{(1)} + H_z \partial_z \delta r^{(1)} = -2\kappa^{(1)} + \mathcal{H}^{-1} \partial_r^2 v^{(1)}, \quad (4.2.101)$$

where we use $\partial_z = H_z^{-1} \partial_r$. The product of these terms with $\delta^{(1)}$ is readily identified in equation (4.2.95). Going on to the second order volume perturbation, we find

$$\delta V^{(2)} = \delta D^{(2)} + H_z \partial_z \delta r^{(2)} - 2H_z \kappa^{(1)} \partial_z \delta r^{(1)} + \Delta x^{(1)b} \partial_b \delta V^{(1)}, \quad (4.2.102)$$

where $\delta D^{(2)}$ is the equivalent of $[|A|]^{(2)} = [|\partial\theta_s/\partial\theta_o|]^{(2)}$, which we show now. The dominating terms are

$$\delta D^{(2)} = \frac{\partial}{\partial\theta} \delta\theta^{(2)} + \frac{\partial}{\partial\phi} \delta\phi^{(2)} + \frac{\partial}{\partial\theta} \delta\theta^{(1)} \frac{\partial}{\partial\phi} \delta\phi^{(1)} - \frac{\partial}{\partial\theta} \delta\phi^{(1)} \frac{\partial}{\partial\phi} \delta\theta^{(1)}. \quad (4.2.103)$$

Note the similarity to equation (2.20) of Di Dio et al. (2016). Now we need to make sure the terms above are correctly calculated. Concerning the angles, we will just look at θ and argue that with the appropriate factors $\sin\theta$ the calculations extend naturally to ϕ . Identifying $\mathcal{A} - C_{\alpha\beta} e^\alpha e^\beta = 2\Psi$, they are given by

$$\delta\theta^{(1)} = - \int_0^{\bar{r}_z} \left(\frac{\bar{r}_z - \bar{r}}{\bar{r}_z \bar{r}} \right) \partial_\theta \left(\mathcal{A} - C_{\alpha\beta} e^\alpha e^\beta \right) dr = \partial_\theta \psi^{(1)}, \quad (4.2.104)$$

just as expected. This shows that the last two terms of (4.2.103) are simply the last terms of equation (4.2.91). We want to show that the first two terms are equal to our $\partial_a[\theta^a]^{(2)}$. For the second order angles, the leading parts are

$$\delta\theta^{(2)} \bar{r}_z = - \int_0^{\bar{r}_z} (\bar{r}_z - \bar{r}) e_{\theta\alpha} \left(\delta\Gamma^{(2)\alpha} + \Delta x^{(1)b} \partial_b \delta\Gamma^\alpha \right) d\bar{r}. \quad (4.2.105)$$

Here $e_{\theta\alpha}$ is the α component of the unit vector in θ -direction. We expand the contracted Christoffel symbols, $\delta\Gamma$, and interpret the sum in $\Delta x^{(1)b} \partial_b \delta\Gamma^\alpha$ as a sum only over the two transversal directions. Substituting $\Delta x^{(1)b} \partial_b = \theta^{(1)a} \partial_a$, the correct expression becomes

$$\delta\theta^{(2)} = - \int_0^{\bar{r}_z} \left(\frac{\bar{r}_z - \bar{r}}{\bar{r}_z \bar{r}} \right) \left(\partial^\theta \Psi^{(2)} + \theta^{(1)a} \partial_a \partial^\theta \Psi^{(1)} \right) d\bar{r}. \quad (4.2.106)$$

This means the first two terms of equation (4.2.103) can be written as

$$\partial_a \theta^{(2)a} = \Delta_\Omega \phi^{(2)} - \int_0^{\bar{r}_z} \left(\frac{\bar{r}_z - \bar{r}}{\bar{r}_z \bar{r}} \right) \partial_b \left(\partial^a \phi^{(1)} \partial_a \partial^b \Psi^{(1)} \right) d\bar{r}. \quad (4.2.107)$$

This formula matches equation (4.2.84), showing that indeed $\delta D^{(2)} = [|A|]^{(2)}$, all pure lensing terms are included. For the remaining terms of equation (4.2.102), we find the leading order contributions to be $\delta r^{(2)} = \mathcal{H}^{-1} \partial_r v^{(2)} - \mathcal{H}^{-1} \Delta x^b \partial_b \delta z^{(1)}$. Writing out the terms, we obtain

$$\begin{aligned} & H_z \partial_z \delta r^{(2)} - 2H_z \kappa \partial_z \delta r^{(1)} = \\ & \mathcal{H}^{-1} \partial_r^2 v^{(2)} + \mathcal{H}^{-1} \partial^a \phi^{(1)} \partial_a \partial_r^2 v^{(1)} + \mathcal{H}^{-2} \partial_r [\partial_r v^{(1)} \partial_r^2 v^{(1)}] - 2\mathcal{H}^{-1} \kappa^{(1)} \partial_r^2 v^{(1)}, \end{aligned} \quad (4.2.108)$$

which directly matches the corresponding terms in equation (4.2.95). Since $\delta^{(2)}$ is left untouched here, we are missing terms relating to the Taylor expansion of $\delta^{(1)}$,

There is also a typo in their equations (51) and (52) where the angular derivative in the third line should only act on the metric components and not on Δx^b .

both radial and angular. Including these terms, we account for all leading order contributions, but are still left with the last term of equation (4.2.102), $\Delta x^{(1)b} \partial_b \delta V^{(1)}$. Expanding this expression gives

$$\Delta x^{(1)b} \partial_b \delta V^{(1)} = -2\partial^a \phi^{(1)} \partial_a \kappa^{(1)} + \mathcal{H}^{-1} \partial^a \phi^{(1)} \partial_a \partial_r^2 v^{(1)} + \mathcal{H}^{-2} \partial_r v^{(1)} \partial_r^3 v^{(1)}. \quad (4.2.109)$$

However all these terms are already accounted for above in $\delta D^{(2)}$ and in $H_z \partial_z \delta r^{(2)}$ respectively. The reason for this is clear. The three terms are the Taylor expansion of RSD and the lensing term which are contained in the expressions for $\delta r^{(2)}$ and $\delta \theta^{(2)}$ above. We argue that adding also $\Delta x^{(1)b} \partial_b \delta V^{(1)}$ is double-counting this effect. Discarding this last term entirely in (4.2.102), the results (4.2.100) and (4.2.95) agree.

Jaiyul Yoo agrees with this finding (private communications).

4.2.6 Explicit extension to higher perturbative orders

The procedure developed in section 4.2.3 is easily used to derive the expression for the dominant terms of higher perturbative orders in the number counts. Higher orders will in particular be important to calculate the 1-loop corrections to the power spectrum and bispectrum, where at least third order perturbative results are needed.

Following the recipe, this time to third order, we arrive at the following expression for the dominant third order terms,

$$\begin{aligned} \Delta^{(3)} = & [\delta]^{(3)} + [\text{RSD}]^{(3)} + [|A^a_b|]^{(3)} \\ & + \delta^{(1)} [\text{RSD}]^{(2)} + [\delta^{(2)}] \text{RSD}^{(1)} + \delta^{(1)} [|A^a_b|]^{(2)} + [\delta^{(2)}] |A^a_b|^{(1)} \\ & + \text{RSD}^{(1)} [|A^a_b|]^{(2)} + [\text{RSD}]^{(2)} |A^a_b|^{(1)} + \delta^{(1)} \text{RSD}^{(1)} |A^a_b|^{(1)}, \end{aligned} \quad (4.2.110)$$

where all first and second order terms have already been calculated. The brackets around the second and third order terms still serve as a reminder that these are not simply the corresponding order term at the unperturbed position but we also have to take into account the lower order terms $X^{(3-n)}$ with the deviation from the Born approximation at order n . Note also that the separation of second order terms is important, as it determines which cross terms appear at third order.

The third order leading contribution to the angles has already been calculated by [Fanizza et al. \(2015\)](#) and we check our simple prescription against their result. We obtain to third order, by including second order deviations of the photon path,

$$\begin{aligned}
[\theta^a]^{(3)} &= -2 \int_0^{r(z)} dr \frac{r(z) - r}{r(z)r} \left(\nabla^a \Psi^{(3)} + \nabla^b \phi^{(1)} \nabla_b \nabla^a \Psi^{(2)} + [\theta^b]^{(2)} \nabla_b \nabla^a \Psi^{(1)} \right. \\
&\quad \left. + \frac{1}{2} \nabla^b \phi^{(1)} \nabla^c \phi^{(1)} \nabla_b \nabla_c \nabla^a \Psi^{(1)} \right) \\
&= \nabla^a \phi^{(3)} - 2 \int_0^{r(z)} dr \frac{r(z) - r}{r(z)r} \left(\nabla^b \phi^{(1)} \nabla_b \nabla^a \Psi^{(2)} + \nabla^b \phi^{(2)} \nabla_b \nabla^a \Psi^{(1)} \right. \\
&\quad \left. - 2 \left[\int_0^r dr' \frac{r - r'}{r r'} \nabla^c \phi^{(1)} \nabla_c \nabla^b \Psi^{(1)} \right] \nabla_b \nabla^a \Psi^{(1)} + \frac{1}{2} \nabla^b \phi^{(1)} \nabla^c \phi^{(1)} \nabla_b \nabla_c \nabla^a \Psi^{(1)} \right).
\end{aligned} \tag{4.2.111}$$

The first two lines here match exactly the dominant contribution in the result of [Fanizza et al. \(2015\)](#), when taking into account factors $\frac{1}{2}$ and $\frac{1}{3!}$ in their definitions of second and third order metric perturbations.

4.2.7 Galaxy count power spectrum

We will now calculate the first order observed galaxy count power spectrum. To this end we need the result of equation (4.2.66). To find the power spectrum, we need to extend the procedure following equation (2.2.17) to account for the derivatives and integrals in our expression.

First, rewrite the result in terms of the velocity potential and convergence,

$$\Delta^{(1)} = \delta_\rho^{(1)} + \mathcal{H}^{-1} \partial_r^2 v^{(1)} - 2\kappa^{(1)} \tag{4.2.112}$$

where the convergence is $\kappa = -\Delta_2 \psi / 2$. In order of appearance the three spherical harmonic coefficients of this are

$$\begin{aligned}
a_{\ell m}^\delta &= (2\pi)^{-3} \int d^3 k \int d^2 n Y_{\ell m}^*(\mathbf{n}) \exp(-i\mathbf{k} \cdot \mathbf{n}r) \delta(\mathbf{k}, \eta_s) \\
&= \frac{1}{2\pi^2 i^\ell} \int d^3 k j_\ell(kr) Y_{\ell m}^*(\hat{\mathbf{k}}) \delta(\mathbf{k}, \eta_s)
\end{aligned} \tag{4.2.113}$$

$$\begin{aligned}
a_{\ell m}^{v'} &= (2\pi)^{-3} \frac{\partial_r^2}{\mathcal{H}} \int d^3 k \int d^2 n Y_{\ell m}^*(\mathbf{n}) \exp(-i\mathbf{k} \cdot \mathbf{n}r) v(\mathbf{k}, \eta_s) \\
&= \frac{1}{2\pi^2 i^\ell} \int d^3 k \frac{k^2}{\mathcal{H}} j_\ell''(kr) Y_{\ell m}^*(\hat{\mathbf{k}}) v(\mathbf{k}, \eta_s)
\end{aligned} \tag{4.2.114}$$

$$\begin{aligned}
a_{\ell m}^\kappa &= (2\pi)^{-3} (-2) \int_0^{r_s} dr \frac{r_s - r}{r_s r} \int d^3 k \int d^2 n Y_{\ell m}^*(\mathbf{n}) \Delta_2 \exp(-i\mathbf{k} \cdot \mathbf{n}r) \Psi(\mathbf{k}, \eta(r)) \\
&= \frac{2}{2\pi^2 i^\ell} \int d^3 k Y_{\ell m}^*(\hat{\mathbf{k}}) \ell(\ell + 1) \int_0^{r_s} dr \frac{r_s - r}{r_s r} j_\ell(kr) \Psi(\mathbf{k}, \eta(r))
\end{aligned} \tag{4.2.115}$$

In the last expression I use the fact that the spherical harmonic in the expansion of the exponential is an eigenfunction of the Laplacian. Using the separation of the

Note I define the velocity potential according to $v = -ikv$ – with a factor k different than eg. [Bonvin and Durrer \(2011\)](#). That is why I have $-k^2$ where they have k .

density, velocity and potential into transfer function times the primordial fluctuations Φ , we may write $a_{\ell m}$ for the contribution A as

$$a_{\ell m}^A(z) = \frac{1}{2\pi^2 i^\ell} \int d^3k Y_{\ell m}^*(\hat{\mathbf{k}}) \Phi(\mathbf{k}) \Delta_\ell^A(k, z) \quad (4.2.116)$$

where the factors Δ_ℓ can be read off equations (4.2.113) to (4.2.115) as

$$\Delta_\ell^\delta(k, z) = j_\ell(kr(z)) T_\delta(k, z) \quad (4.2.117)$$

$$\Delta_\ell^{v'}(k, z) = \mathcal{H}^{-1} j_\ell'(kr(z)) T_\theta(k, z) \quad (4.2.118)$$

$$\Delta_\ell^\kappa(k, z) = 2\ell(\ell+1) \int_0^{r(z)} dr \frac{r(z)-r}{r(z)r} j_\ell(kr) T_\Psi(k, r) \quad (4.2.119)$$

I have here used that $-k^2 T_v = T_\theta$ where $\theta = \partial^2 v$ is the divergence of the velocity field. Incidentally it is also the transfer function which is standard output of CLASS. With the notation $C_\ell^{AB}(z, z') = \langle a_{\ell m}^A(z) a_{\ell m}^{B*}(z') \rangle$, we can now write down the general result for the C_ℓ , which is

$$\begin{aligned} C_\ell^{AB}(z, z') &= \frac{1}{4\pi^4} \int d^3k d^3k' Y_{\ell m}(\mathbf{k}) Y_{\ell m}^*(\mathbf{k}') \langle \Phi(\mathbf{k}) \Phi(\mathbf{k}') \rangle \Delta_\ell^A(k, z) \Delta_\ell^B(k', z') \\ &= \frac{2}{\pi} \int dk k^2 P(k) \Delta_\ell^A(k, z) \Delta_\ell^B(k, z) \end{aligned} \quad (4.2.120)$$

Thus the power spectrum is, in total

$$\begin{aligned} C_\ell^\Delta(z, z') &= C_\ell^{\delta\delta}(z, z') + C_\ell^{v'v'}(z, z') + C_\ell^{\kappa\kappa}(z, z') + C_\ell^{v'\delta}(z, z') \\ &\quad + C_\ell^{\delta v'}(z, z') + C_\ell^{\delta\kappa}(z, z') + C_\ell^{\kappa\delta}(z, z') + C_\ell^{v'\kappa}(z, z') + C_\ell^{\kappa v'}(z, z') \end{aligned} \quad (4.2.121)$$

For exactly equal z , these functions are manageable, even numerically. However for slightly different redshift, we see that the arguments of the many different spherical bessel function differ just enough to make beats – which have very high frequencies. Numerically, this is very challenging. In the coming sections we will see how to simplify this result on the flat sky, and how the answer compares to the exact answer we have just found.

4.2.8 Galaxy count bispectrum

With the second order galaxy count perturbations calculated we may also find the bispectrum *solely induced by general relativistic effects*. This *will* pollute any attempt to find a primordial bispectrum, since we must determine the pollution to at least the precision we wish to look for primordial bispectra.

With the notation just developed on the $a_{\ell m}$ it is easy to extend the calculation to the 'product terms' of the second order number count. These are all the terms except

$\delta^{(2)}, \mathcal{H}^{-1}\partial_r^2 v^{(2)}, -2\kappa^{(2)}$. For such a real product term – the galaxy count is real after all – it is clear that we may write

$$\Delta^{(2)}(\mathbf{n}, z) \supset \Delta^A(\mathbf{n}, z)\Delta^B(\mathbf{n}, z) = \sum_{\ell m} Y_{\ell m}^*(\mathbf{n})(a_{\ell m}^A(z))^* \sum_{\ell' m'} Y_{\ell' m'}^*(\mathbf{n})(a_{\ell' m'}^B(z))^* \quad (4.2.122)$$

$$a_{\ell_1 m_1}^{AB}(z) = \int d^2 n Y_{\ell_1 m_1}^*(\mathbf{n}) \Delta^A(\mathbf{n}, z) \Delta^B(\mathbf{n}, z) = \sum_{\ell \ell' m m'} \mathcal{G}_{\ell_1 \ell \ell'}^{m_1 m m'} (a_{\ell m}^A(z))^* (a_{\ell' m'}^B(z))^* \quad (4.2.123)$$

It should then be clear, when forming correlators of the second order $a_{\ell m}$ and two first order $a_{\ell m}$ – which is the lowest order correction to the bispectrum – one encounters terms like

$$\begin{aligned} b^{(AB)CD} &= \left\langle a_{\ell_1 m_1}^{AB}(z_1) a_{\ell_2 m_2}^C(z_2) a_{\ell_3 m_3}^D(z_3) \right\rangle \left(\mathcal{G}_{\ell_1 \ell_2 \ell_3}^{m_1 m_2 m_3} \right)^{-1} \\ &= C_{\ell_2}^{AC}(z_1, z_2) C_{\ell_3}^{BD}(z_1, z_3) + C_{\ell_2}^{BC}(z_1, z_2) C_{\ell_3}^{AD}(z_1, z_3) \end{aligned} \quad (4.2.124)$$

Note that the first order contributions ‘decide’ the ℓ on the C_ℓ , however all the three ℓ s are intertwined in the selection rules of the Gaunt factor. The shorthand subscript notation b is simply $b \equiv b_{\ell_1 \ell_2 \ell_3}(z_1, z_2, z_3)$ – the arguments are usually not critical. The superscript letters tell which contribution is under consideration. The parenthesis denotes the second order contribution. To complete the notation we have to derive similar rules as equations (4.2.117) to (4.2.119) for the terms appearing in equation (4.2.95). For the terms with no angular derivatives it is straight forward. The terms we are missing can be calculated just as before, and they are

$$\partial_r \delta \rightarrow \Delta_\ell^{\delta'}(k, z) = T_\delta \frac{k}{\mathcal{H}} j'_\ell(kr) \quad (4.2.125)$$

$$\partial_r v \rightarrow \Delta_\ell^v(k, z) = T_\theta \frac{1}{k} j'_\ell(kr) \quad (4.2.126)$$

$$\mathcal{H}^{-2} \partial_r^3 v \rightarrow \Delta_\ell^{\partial^3 v}(k, z) = T_\theta \frac{k}{\mathcal{H}^2} j'''_\ell(kr) \quad (4.2.127)$$

$$\Psi_1 \rightarrow \Delta_\ell^{\Psi_1}(k, z) = \frac{2}{r} \int_0^{r(z)} dr j_\ell(kr) T_\Psi(k) \quad (4.2.128)$$

The term ψ is already given, since we have

$$\Delta_2 \psi = (-2\kappa) \Rightarrow \Delta_\ell^\psi(k, z) = -\frac{1}{\ell(\ell+1)} \Delta_\ell^\kappa(k, z) \quad (4.2.129)$$

We now only need to know how to treat the terms with angular derivatives. Using equations (2.2.29) and (2.3.8), we may write for the simple terms $\nabla_a A \nabla^a B$ the bispectra as

$$\begin{aligned} b^{(\nabla A \nabla B)CD} &= -A_{\ell_1 \ell_2 \ell_3} \sqrt{\ell_2(\ell_2+1)\ell_3(\ell_3+1)} \\ &\quad \left(C_{\ell_2}^{AC}(z_1, z_2) C_{\ell_3}^{BD}(z_1, z_3) + C_{\ell_2}^{BC}(z_1, z_2) C_{\ell_3}^{AD}(z_1, z_3) \right) \end{aligned} \quad (4.2.130)$$

The last term I want to detail is the four-derivative lensing term, $\Delta_2(\nabla \Psi_1 \nabla \Psi_1)$ which appears integrated over the lightcone. With the same identities as before, we may immediately write this term as

$$\Delta_2(\nabla_a \Psi_1 \nabla^a \Psi_1) = \Delta_2 \left(\sum_{\ell m} a_{\ell m}^{\nabla \Psi_1 \nabla \Psi_1} Y_{\ell m} \right) = - \sum_{\ell m} \ell(\ell+1) a_{\ell m}^{\nabla \Psi_1 \nabla \Psi_1} Y_{\ell m} \quad (4.2.131)$$

Remember the superscript κ here really stands for the contribution from -2κ to the number count.

This gives us the very simple expression for the associated bispectrum,

$$b^{\Delta_2(\nabla\Psi_1\nabla\Psi_1)^{CD}} = A_{\ell_1\ell_2\ell_3} \sqrt{\ell_2(\ell_2+1)\ell_3(\ell_3+1)\ell_1(\ell_1+1)} \quad (4.2.132)$$

$$\left(C_{\ell_2}^{\Psi_1^C}(z_1, z_2) C_{\ell_3}^{\Psi_1^D}(z_1, z_3) + C_{\ell_2}^{\Psi_1^C}(z_1, z_2) C_{\ell_3}^{\Psi_1^D}(z_1, z_3) \right)$$

Let me compare this to the expression found in [Di Dio et al. \(2016\)](#), where the term was split up into many pieces. In terms of the factors in front of the product of C_{ℓ_i} they calculate it as the sum of the following three terms

$$2(\nabla^a \Delta_2 \Psi_1) \nabla_a \Psi_1 \rightarrow A_{\ell_1\ell_2\ell_3}^{(1)} \sqrt{\ell_2(\ell_2+1)\ell_3(\ell_3+1)(\ell_2(\ell_2+1) + \ell_3(\ell_3+1))}$$

$$\bar{\partial}^2 \Psi_1 \bar{\partial}^2 \Psi \rightarrow A_{\ell_1\ell_2\ell_3}^{(2)} \sqrt{\frac{(\ell_2+2)!}{(\ell_2-2)!}} \sqrt{\frac{(\ell_3+2)!}{(\ell_3-2)!}}$$

$$(\Delta_2 \Psi_1)^2 \rightarrow \ell_2(\ell_2+1)\ell_3(\ell_3+1)$$

Looking to the results of section 2.3.1 we can rewrite $A^{(2)}$ in terms of $A^{(1)}$ and add the three terms. The dominating terms – the leading order in ℓ_i – match. equations (4.2.124), (4.2.130) and (4.2.132) describe all the simple terms of the bispectrum. We will in the flat sky calculation see what the physics of the different factors of $A^{(1)}$ are.

Let me now briefly mention the remaining terms $\delta^{(2)}, v'^{(2)}, \kappa^{(2)}$ and their associated problems. The bare density perturbation can be calculated nicely, as has been done in [Di Dio et al. \(2016\)](#) in terms of Legendre polynomials. Let us go through their calculation and later on do it in the flat sky for comparison. We already have the Newtonian result for the second order density perturbation in terms of the first order. According to equation (3.2.15) it is

$$\delta_\rho^{(2)}(\mathbf{n}, z) = (2\pi)^{-3} \int d^3q_1 d^3q_2 e^{-i(\mathbf{q}_1+\mathbf{q}_2)\cdot\mathbf{n}r} F_2(\mathbf{q}_1, \mathbf{q}_2) \delta_\rho^{(1)}(\mathbf{q}_1) \delta_\rho^{(1)}(\mathbf{q}_2) \quad (4.2.133)$$

In terms of Legendre polynomials P_ℓ we may write F_2 , defined in equation (3.2.19) as

$$F_2(\mathbf{q}_1, \mathbf{q}_2) = \frac{17}{21} + \frac{1}{2} \left(\frac{q_1}{q_2} + \frac{q_2}{q_1} \right) P_1(\hat{\mathbf{q}}_1 \cdot \hat{\mathbf{q}}_2) + \frac{4}{21} P_2(\hat{\mathbf{q}}_1 \cdot \hat{\mathbf{q}}_2)$$

$$= \sum_{\ell, m} f_\ell(q_1, q_2) \frac{4\pi}{2\ell+1} Y_{\ell m}(\hat{\mathbf{q}}_1) Y_{\ell m}^*(\hat{\mathbf{q}}_2) \quad (4.2.134)$$

and we can thereby split up the second order density perturbation in three terms, that we treat separately. For the first term with no angular dependence, the calculation is straight-forward. We have a completely separable term $\propto \delta_\rho^{(1)}(\mathbf{n}) \delta_\rho^{(1)}(\mathbf{n})$ which can be treated with equation (4.2.124). Let us however do all the terms in one go. Taking the coefficients of the spherical harmonics of equation (4.2.133) we get

$$a_{\ell_1 m_1}^{\delta^{(2)}} = \frac{(4\pi)^3}{(2\pi)^6} \int dk_1 k_1^2 dk_2 k_2^2 \sum_{\ell \ell' \ell'' m m' m''} i^{\ell'+\ell''} f_\ell(k_1, k_2) \Delta_{\ell'}^\delta(k_1 r) \Delta_{\ell''}^\delta(k_2 r) \mathcal{G}_{\ell_1 \ell' \ell''}^{m_1 m' m''}$$

$$\int d^2\hat{k}_1 d^2\hat{k}_2 Y_{\ell' m'}(\hat{\mathbf{k}}_1) Y_{\ell'' m''}(\hat{\mathbf{k}}_2) Y_{\ell m}(\hat{\mathbf{k}}_1) Y_{\ell m}^*(\hat{\mathbf{k}}_2) \Phi(\mathbf{k}_1) \Phi(\mathbf{k}_2) \quad (4.2.135)$$

where the sum over ℓ goes to 2 and ℓ', ℓ'' go to infinity. Taking a correlator with two first order $a_{\ell m}$ as defined in equation (4.2.116) we get

$$\begin{aligned} \langle a_{\ell_1 m_1}^{\delta(2)} a_{\ell_2 m_2}^C a_{\ell_2 m_2}^D \rangle &= \frac{16}{\pi^2} \sum_{\ell \ell' \ell'' m m' m''} \int dk_1 k_1^2 dk_2 k_2^2 P(k_1) P(k_2) f_\ell(k_1, k_2) \quad (4.2.136) \\ & i^{\ell' + \ell'' - \ell_2 - \ell_3} (-1)^{m + m' + m''} \Delta_{\ell'}^\delta(k_1) \Delta_{\ell''}^\delta(k_2) \mathcal{G}_{\ell_1 \ell' \ell''}^{-m_1 m' m''} (2\ell + 1)^{-1} \\ & \left(\Delta_{\ell_2}^C(k_1) \Delta_{\ell_3}^D(k_2) \mathcal{G}_{\ell_2 \ell' \ell}^{-m_2 - m' m} \mathcal{G}_{\ell_3 \ell'' \ell}^{m_3 m'' m} + \Delta_{\ell_2}^C(k_2) \Delta_{\ell_3}^D(k_1) \mathcal{G}_{\ell_2 \ell'' \ell}^{m_2 m'' m} \mathcal{G}_{\ell_3 \ell' \ell}^{-m_3 - m' m} \right) \end{aligned}$$

This form is unfortunately not very enlightening. The velocity and gravitational potential terms suffer even worse fates. Both of these have a factor k^{-2} that we cannot easily get rid of. The calculations are written in Di Dio et al. (2016) and I will not repeat it here. Suffice to say the calculation is long, and the numerical computation of the terms, even worse. As we shall see, however, this calculation *does* simplify on the flat sky. We will be able to reduce the number of integral drastically, to the point that the eg. the second order lensing contribution has just one integral.

Let me finally list explicitly how all the permutations come out. Remember, each ℓ_i in the bispectrum has both a first and second order contribution, which interact with the two others. Therefore, writing the first and second order number counts as sums of the individual contributions A and (BB') for first and second order respectively, we can write the bispectrum as a sum over all these,

$$\Delta = \sum_A \Delta^A + \sum_{(BB')} \Delta^{(BB')} \Rightarrow a_{\ell m} = \sum_A a_{\ell m}^A + \sum_{(BB')} a_{\ell m}^{(BB')} \quad (4.2.137)$$

$$b = \sum_{(AB), C, D} b^{(AB)CD} + b^{C(AB)D} + b^{CD(AB)} \quad (4.2.138)$$

where each of the terms b contain 2 products of C_{ℓ} s. With three first order terms and 12 simple second order contributions, this sum contains $12 \times 2 \times 2 \times 3 \times 2 = 288$ terms *for each* ℓ – and this is just the contaminating GR contribution. Seeing as integrals over spherical Bessel functions are hard enough as it is, it is imperative that we simplify the computations as much as possible. This can be done in the flat sky.

4.2.9 Computing the primordial bispectrum of the galaxy number count

We also need to know how a primordial bispectrum looks in the galaxy number counts. Due to the somewhat simpler nature of the galaxy counts, this will be computationally easier than the corresponding CMB calculation. In particular the transfer functions will not be integrals. I denote the primordial part with a tilde to

distinguish it from the GR part of the bispectrum. Inserting equation (4.2.116) and taking the correlator we get

$$\begin{aligned} \tilde{b}^{ABC} &= (\mathcal{G}_{\ell_1 \ell_2 \ell_3}^{m_1 m_2 m_3})^{-1} \langle a_{\ell_1 m_1}^A a_{\ell_2 m_2}^B a_{\ell_3 m_3}^C \rangle = \\ & \left(\frac{2}{\pi} \right)^3 \int dk_1 k_1^2 dk_2 k_2^2 dk_3 k_3^2 dx x^2 B(k_1, k_2, k_3) \\ & \times j_{\ell_1}(k_1 x) j_{\ell_2}(k_2 x) j_{\ell_3}(k_3 x) \Delta_{\ell_1}^A(k_1, z_1) \Delta_{\ell_2}^B(k_2, z_2) \Delta_{\ell_3}^C(k_3, z_3) \end{aligned} \quad (4.2.139)$$

I have here written out the delta function as the integral over an exponential function. The exponential is then expanded in spherical harmonics and spherical Bessel functions, and the angular part integrated out to give the Gaunt integral, as follows

$$\begin{aligned} \langle \Phi \Phi \Phi \rangle &= B(k_1, k_2, k_3) \int d^3 x \exp(ix \cdot (\mathbf{k}_1 + \mathbf{k}_2 + \mathbf{k}_3)) = \\ & 8B(k_1, k_2, k_3) \sum_{\ell_i, m_i} i^{\ell_1 + \ell_2 + \ell_3} \mathcal{G}_{\ell_1 \ell_2 \ell_3}^{m_1 m_2 m_3} Y_{\ell_1 m_1}(\hat{\mathbf{k}}_1) Y_{\ell_2 m_2}(\hat{\mathbf{k}}_2) Y_{\ell_3 m_3}(\hat{\mathbf{k}}_3) \\ & \times \int dx x^2 j_{\ell_1}(k_1 x) j_{\ell_2}(k_2 x) j_{\ell_3}(k_3 x) \end{aligned} \quad (4.2.140)$$

The spherical harmonics of the momenta are then integrated out and gets rid of the sum over ℓ_i, m_i .

While the integral in equation (4.2.139) is in principle the correct answer, it is not quite the right answer. The four integrals over what is effectively a delta function is simply not numerically feasible. What we need is again a flat sky calculation, which we finally get to next.

4.2.10 Computing the bispectrum of the galaxy number count on a flat sky

I now want to derive the flat sky approximation for the galaxy number counts. This consists of two steps. First we find all the flat sky $C_{\ell S}$, which give us a large part of the GR induced bispectrum. Second, we do a calculation similar to section 4.1.2 to find the primordial part of the galaxy count bispectrum.

Let us begin with the flat sky $C(\ell)$ calculations. Because the lensing terms have integrals in them already, we end up treating the two different ‘kinds’ of first order contributions slightly differently. Along with the calculation I will compare our calculations here with the full sky results, from which we will gain valuable insight into both physics and computational aspects. First look at the density term. I call the Fourier transform $a^A(\ell)$ as a reminder that it should end up corresponding to the full sky results. We have for the density term

$$a^\delta(\ell, z) = \int d^2 n e^{i\ell \cdot n} \delta(n, z) \approx \int d^2 n \int \frac{d^3 k}{(2\pi)^3} e^{i(\ell - \mathbf{k}_\perp r_s) \cdot n} e^{-ik_z r_s} T_\delta(k, \eta_s) \Phi(\mathbf{k}) \quad (4.2.141)$$

I here make the approximation that $\mathbf{k} \cdot \mathbf{x} \approx r_s k_\perp \cdot \mathbf{n} + k_z r_s$, meaning the \mathbf{n} only spans a small square on the flat sky, and I can split up the contributions. This also re-introduces the perpendicular, or *screen*, direction, denoted by \perp and the z -direction. Doing this approximation allows me to perform the d^2n integral, and I get

$$a^\delta(\ell, z) \approx (2\pi)^{-1} \int d^3k \delta(\ell - \mathbf{k}_\perp r_s) e^{-ik_z r_s} T(k, \eta_s) \Phi(\mathbf{k}) \quad (4.2.142)$$

To make further progress we need to calculate correlators to get rid of the initial perturbations. Doing so with two density contributions, we get

$$\langle a^\delta(\ell, z) a^\delta(\ell', z')^* \rangle = (2\pi) \int d^3k \delta^D(\ell - \mathbf{k}_\perp r_s) \delta^D(\ell' - \mathbf{k}_\perp r'_s) T(k, \eta_s) T(k, \eta'_s) P(k) e^{-ik_z r_s + ik_z r'_s} \quad (4.2.143)$$

To proceed, we do a Limber approximation, as described by [Bernardeau et al. \(2011\)](#): we realise that the exponential function kills the integral unless $r_s \approx r'_s$. That allows us to everywhere put $z \approx z' \Rightarrow r_s \approx r'_s$. So apparently, in the Limber approximation, only same- z correlators are important for the density contrast. This is well reflected in the full-sky computation. The two 2-dimensional delta functions in k_\perp now have the same argument only if $\ell = \ell'$, in which case we get a number of r_s out from the integral and a delta function in ℓ . Anticipating the form of the correlator, we therefore write

$$\langle a^\delta(\ell, z) a^\delta(\ell', z')^* \rangle = (2\pi)^2 \delta(\ell - \ell') (2\pi r_s r'_s)^{-1} \int dk_z T(k, \eta_s) T(k, \eta'_s) P(k) e^{-ik_z r_s + ik_z r'_s} \quad (4.2.144)$$

where $k_\perp = \ell/r_s \approx (\ell + 1/2)/r_s \approx \sqrt{\ell(\ell + 1)}/r_s$ and $k = \sqrt{k_\perp^2 + k_z^2}$. We notice that the integral for negative and positive k_z are complex conjugates, and therefore write

$$\langle a^\delta(\ell, z) a^\delta(\ell', z')^* \rangle \approx (2\pi)^2 \delta(\ell - \ell') \frac{1}{\pi r_s r'_s} \int_0^\infty dk_z T(k, \eta_s) T(k, \eta'_s) P(k) \cos(k_z(r_s - r'_s)) \quad (4.2.145)$$

from which we read off

$$C^{\delta\delta}(\ell) = \frac{1}{\pi r_s r'_s} \int_0^\infty dk_z T(k, \eta_s) T(k, \eta'_s) P(k) \cos(k_z(r_s - r'_s)) \quad (4.2.146)$$

Notice that the integral is over k_z , *not* k . This will be important in what follows – and for computational purposes. Let us immediately check how the result compares to the full answer. To do that, we need a fantastic approximation for the spherical Bessel functions, which is given by [Mukhanov \(2004\)](#),

$$j_\ell(x) \approx \begin{cases} 0 & x < \nu \\ x^{-1/2} (x^2 - \nu^2)^{-1/4} \cos(\sqrt{x^2 - \nu^2} - \nu \arccos(\nu/x) - \pi/4) & x > \nu \end{cases} \quad (4.2.147)$$

Note that this means we have little hope for this approximation when z_1 and z_2 are very different. As it turns out, we will get a reasonable order-of-magnitude, however the exact number cannot be trusted for redshift differing by more than about a half.

This approximation is his equation (60)

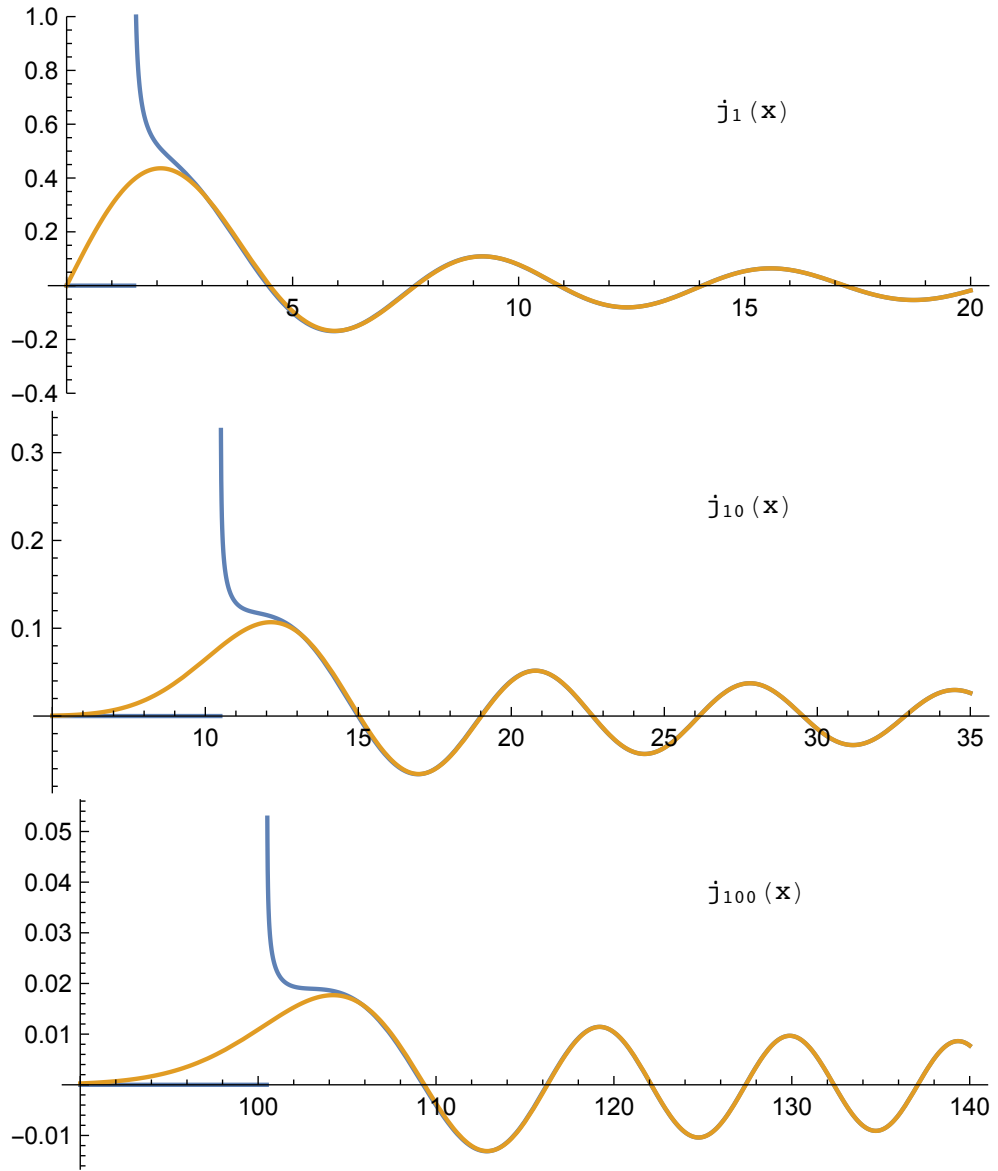


Figure 6: Illustration of the approximation of the spherical Bessel function by equation (4.2.147). We see astonishing agreement at values of x only slightly larger than ν . The divergence at $x = \nu$ does not cause any problems, as the further calculations show.

where $\nu = \ell + 1/2$. This approximation for $\ell = 1, 10, 100$ is illustrated in figure 6. We now use this approximation in the calculation of equation (4.2.120) with two density contributions

$$C_\ell^{\delta\delta}(z, z') = \frac{2}{\pi} \int dk k^2 P(k) T_\delta(k, \eta_s) T_\delta(k, \eta'_s) j_\ell(kr_s) j_\ell(kr'_s) \quad (4.2.148)$$

Separating off the two spherical Bessel functions and the factor k^2 , we have

$$j_\ell(kr_s) j_\ell(kr'_s) k^2 \approx \frac{k}{k_z r_s r'_s} \cos(k_z r_s - \nu \arccos(\nu/kr_s) - \pi/4) \cos(k_z r'_s - \nu \arccos(\nu/kr'_s) - \pi/4) \quad (4.2.149)$$

This product of cosines can be written as beats. For small differences $r_s - r'_s$, this leaves us with a low frequency, which we keep, and a high frequency we can disregard. Neglecting the difference in the arccos which decreases at large k , this simply leaves us with

$$\cos(k_z r_s - \pi/4) \cos(k_z r'_s - \pi/4) \approx \frac{1}{2} (\cos(k_z [r_s - r'_s]) + \text{high frequency}) \quad (4.2.150)$$

The prefactor k/k_z helps us change the measure, as we have $dk_z = k dk/k_z$. Inserting this in the original integral, we get

$$C_\ell \approx \frac{1}{\pi r_s r'_s} \int_0^\infty dk_z T(k, \eta_s) T(k, \eta'_s) P(k) (\cos(k_z (r_s - r'_s))), \quad (4.2.151)$$

Where the lower limit of the integral has changed due to the approximation of the spherical Bessel function. It is now clear that the lower of the beat frequencies gives us the flat sky approximation. The high frequency quite simply oscillates too quickly to pick out any features in the transfer functions or primordial power spectrum. This means that when we compute the C_ℓ in the flat-sky approximation, we can live with sampling the integral over k *much* less, since we do not need to resolve the high frequency at all.

Let us then see how the lensing term behaves. We start off as before with Fourier transforming the lensing term -2κ ,

$$\begin{aligned} a^\kappa(\ell, z) &= \int d^2n \int \frac{d^3k}{(2\pi)^3} e^{i\ell \cdot n} \int_0^{r_s} dr \frac{r_s - r}{r_s r} (-k_\perp^2 r^2) e^{-i\mathbf{k}_\perp \cdot n r} e^{-ik_z r} 2T_\Psi(k, \eta) \Phi(\mathbf{k}) \\ &= (2\pi)^{-1} \int d^3k \int_0^{r_s} dr \frac{r_s - r}{r_s r} (-k_\perp^2 r^2) \delta(\ell - \mathbf{k}_\perp r) e^{-ik_z r} 2T_\Psi(k, \eta) \Phi(\mathbf{k}) \end{aligned} \quad (4.2.152)$$

where I have differentiated the exponential twice to get the factor $(-k_\perp^2 r^2)$ down – this factor will turn out to be just $-\ell(\ell + 1)$, as we know it from the full sky calculation. Like before, we now take a lensing-lensing correlator,

$$\begin{aligned} \langle a^\kappa(\ell, z) a^\kappa(\ell', z')^* \rangle &= 2\pi \int d^3k \int_0^{r_s} dr \frac{r_s - r}{r_s r} \int_0^{r'_s} dr' \frac{r'_s - r'}{r'_s r'} \delta(\ell - \mathbf{k}_\perp r) \delta(\ell' - \mathbf{k}_\perp r') \\ &\quad \times 4T_\Psi(k, \eta) T_\Psi(k, \eta') P(k) (k_\perp^2 r r')^2 e^{-ik_z(r-r')} \end{aligned} \quad (4.2.153)$$

Now we do a Limber approximation, however slightly differently than before. Following [Bernardeau et al. \(2011\)](#) Equation (42), I simply exchange the integral over k_z to a delta function in $r - r'$ and a factor 2π , while simply setting $k_z = 0$. That allows me to do the r' integral – assuming $z' \geq z$ to make sure I ‘catch’ the delta function – and in turn do the k_\perp integral. I end up with

$$\langle a^\kappa(\ell, z) a^\kappa(\ell', z')^* \rangle = \delta(\ell - \ell') (2\pi)^2 \int_0^{r_s} dr r^{-2} \frac{r_s - r}{r_s r} \frac{r'_s - r}{r'_s r} 4 T_\Psi(k, \eta)^2 P(k) (\ell[\ell + 1])^2 \quad (4.2.154)$$

where $k \approx k_\perp \approx \sqrt{\ell(\ell + 1)}/r$. To make this result look more familiar, we change variables from r to k . Taking out just the $C(\ell)$ we get

$$C^{\kappa\kappa}(\ell) = 4 \int_{1/r_s}^{\infty} dk \frac{r_s - r}{r_s r} \frac{r'_s - r}{r'_s r} T_\Psi(k, \eta)^2 P(k) (\ell[\ell + 1])^{3/2} \quad (4.2.155)$$

where we have $r = \sqrt{\ell(\ell + 1)}/k$ and so $\eta = \eta_0 - \sqrt{\ell(\ell + 1)}/k$. To compare this with the full sky calculation, we need the following approximation,

$$\int_a^b d\chi F(\chi) j_\ell(\chi k) \approx \sqrt{\frac{\pi}{2}} F(\sqrt{\ell(\ell + 1)}/k) \frac{1}{k(\ell[\ell + 1])^{1/4}} \quad (4.2.156)$$

We can use this directly on equation (4.2.119) to get

$$\Delta_{\ell m}^\kappa(k, z) \approx \frac{\sqrt{2\pi}(\ell[\ell + 1])^{3/4}}{\sqrt{k}} \frac{r_s - r}{r_s r} T_\Psi(k, \eta) \quad (4.2.157)$$

where again $r = \sqrt{\ell(\ell + 1)}/k$ and $\eta = \eta_0 - \sqrt{\ell(\ell + 1)}/k$. From this we get the following power spectrum

$$C_\ell^{\kappa\kappa}(z, z') = 4 \int dk P(k) T_{\Phi+\Psi}(k, \eta)^2 (\ell[\ell + 1])^{3/2} \frac{r_s - r}{r_s r} \frac{r'_s - r}{r'_s r} \quad (4.2.158)$$

which is what we anticipated. It is indeed encouraging that two different ways of approximating the same thing agree. The only difference is the lower limit in the integral, which in the flat sky was determined by the lowest redshift conformal distance. As is evident, that small distinction is unimportant.

We have now seen that the two terms behave somewhat differently, and need different approximations. It is therefore interesting to see how they behave together in a mixed-term $C_\ell^{\delta\kappa}$. As it turns out, this will completely remove *all* the integrals. Taking the correlator of equations (4.2.142) and (4.2.152) we get

$$\begin{aligned} & \langle a^\delta(\ell, z) a^\kappa(\ell', z') \rangle \quad (4.2.159) \\ &= 2\pi \int d^3k \int dr \delta(\ell - \mathbf{k}_\perp r_s) \delta(\ell' - \mathbf{k}'_\perp r) 2 T_\delta(k) T_\Psi(k) P(k) \frac{r'_s - r}{r'_s r} \exp(ik_z(r_s - r)) \\ &\approx (2\pi)^2 \delta(\ell - \ell') 2 P(k) T_\delta(k, \eta_s) T_\Psi(k, \eta_s) \frac{r'_s - r_s}{r'_s r_s} \frac{\ell(\ell + 1)}{r_s^2} \end{aligned}$$

Where $k \approx \ell/r_s$, and r_s the distance to the density perturbation – which has to be in front ie. $z < z'$. What happens here is the integral over k_z is Limber approximated by

a delta function in $r_s - r$ and a factor 2π . Inserting this delta function we can do the r integral from the lensing term, which latches on to $r = r_s$. Evidently, the contribution to the mixed term depends only on the lensing at the location of the foreground galaxy. This makes sense, since we are correlating the lensing of the background with the density of the foreground. Conversely a galaxy in the background will hardly be lensed by the foreground.

The comparison with the full calculation requires two Limber approximations in the form of equation (4.2.156). First we again approximate the Δ_ℓ^κ which gives us

$$C_\ell^{\delta\kappa} = \frac{2}{\pi} \int dk P(k) j_\ell(kr_s) T_\delta(k, \eta_s) T_{\Phi+\Psi}(k, \eta_s) \sqrt{\frac{\pi}{2}} (\ell[\ell+1])^{3/4} k \frac{r'_s - r}{r'_s r} \quad (4.2.160)$$

When we again apply equation (4.2.156), we get exactly the desired result.

All these calculations speed up the C_ℓ computations we are going to need. The speed-up comes mainly from lower sampling rates – as we saw, eg. the high frequencies of the Bessel function beats are approximated away.

We are of course going to need to calculate all the terms required for the C_ℓ . However, let us first generalize what we just saw to make future calculations easier. I will split the terms into two groups, the density-like and lensing-like. The defining difference is the integral. The lensing-like terms are κ, Ψ_1, ψ , and all the remaining are density-like: $\delta, \delta', v, v', v''$. The two types of terms can be written in the following way,

$$\Delta^D(n) = f(n) \Rightarrow a^D(\ell) = (2\pi)^{-1} \int d^3k \delta(\ell - \mathbf{k}_\perp r_s) e^{-ik_z r_s} \Delta^D(k, \eta_s) \Phi(\mathbf{k}) \quad (4.2.161)$$

$$\Delta^L(n) = \int dr f(n) \Rightarrow a^L(\ell) = (2\pi)^{-1} \int d^3k \int dr \delta(\ell - \mathbf{k}_\perp r) e^{-ik_z r} \Delta^L(k, \eta) \Phi(\mathbf{k}) \quad (4.2.162)$$

where in each case $f(n) = (2\pi)^{-3} \int d^3k \Delta(k, \eta) \Phi(\mathbf{k}) \exp(-i\mathbf{k} \cdot \mathbf{n}r_s)$. This makes for three different combinations in the C_ℓ s, given by $\langle \Delta\Delta \rangle = (2\pi)^2 \delta(\ell - \ell') C_\ell$. Following the explicit derivations from before we have

$$C_\ell^{DD} = (\pi r_s r'_s)^{-1} \int dk_z \cos(k_z [r_s - r'_s]) \Delta_1^D(k, \eta_s) \Delta_2^D(k, \eta'_s) P(k) \quad (4.2.163)$$

$$C_\ell^{LL} = [\ell(\ell+1)]^{-1/2} \int dk \Delta_1^L(k, \eta) \Delta_2^L(k, \eta) P(k) \quad (4.2.164)$$

$$C_\ell^{DL} = r_s^{-2} \Delta^D(k, \eta_s) \Delta^L(k, \eta_s) P(k) \quad z_D < z_L \quad (4.2.165)$$

In these expressions, the different variables are given by eg. $\eta = \eta_0 - r$ and $r = \sqrt{\ell(\ell+1)}/k$. In the last one, we have $k = \sqrt{\ell(\ell+1)}/r_s$ and $k_z = 0$. I already

found the density and lensing transfer functions explicitly. All the relevant transfer functions are

$$\Delta_D^\delta = T_\delta(k, z) \quad (4.2.166)$$

$$\Delta_D^{\delta'} = (-i) \frac{k_z}{\mathcal{H}} T_\delta(k, z) \quad (4.2.167)$$

$$\Delta_D^v = i \frac{k_z}{k^2} T_\Theta(k, z) \quad (4.2.168)$$

$$\Delta_D^{v'} = \left(\frac{k_z}{k} \right)^2 \mathcal{H}^{-1} T_\Theta(k, z) \quad (4.2.169)$$

$$\Delta_D^{v''} = (-i) \frac{k_z^3}{k^2 \mathcal{H}^2} T_\Theta(k, z) \quad (4.2.170)$$

$$\Delta_L^k = 2 \frac{r_s - r}{r_s r} T_\Psi(k, z) \ell(\ell + 1) \quad (4.2.171)$$

$$\Delta_L^\psi = -2 \frac{r_s - r}{r_s r} T_\Psi(k, z) \quad (4.2.172)$$

$$\Delta_L^{\Psi_1} = 2r_s^{-1} T_\Psi(k, z) \quad (4.2.173)$$

Some of these transfer functions are apparently imaginary. However, a glance at equation (4.2.95) shows that any one of the imaginary functions is always multiplied by another imaginary transfer function. Specifically, we only encounter the products (v, v'') and (δ', v) . We see that for both products, the i 's cancel. We may therefore simply leave them out when computing the transfer functions numerically.

As an example of the radially differentiated contributions, let me explicitly derive the v' transfer function.

$$\Delta^{v'}(n, z) = \mathcal{H}^{-1} \partial_r^2 \int \frac{d^3 k}{(2\pi)^3} \exp(-i\mathbf{k} \cdot \mathbf{n} r_s) \frac{-T_\Theta(k, z)}{k^2} \Phi(\mathbf{k}) \quad (4.2.174)$$

where I use that $-k^2 T_v = T_\Theta$. The partial derivative now pulls out $-(\mathbf{k} \cdot \mathbf{n})^2 \approx -k_z^2$. We thus see immediately the claimed result

$$\Delta_D^{v'} = \left(\frac{k_z}{k} \right)^2 \mathcal{H}^{-1} T_\Theta(k, z) \quad (4.2.175)$$

It is again insightful to compare this with the full calculation. Equation (4.2.118) contains a differentiated spherical Bessel function. We may approximate that as follows,

$$j_\ell'' = \left(\frac{\ell(\ell + 1)}{x^2} - 1 \right) j_\ell - 2j_\ell'/x \approx \left(\frac{\ell(\ell + 1)}{x^2} - 1 \right) j_\ell \quad (4.2.176)$$

where I throw away the term suppressed by x . Inserting $x = kr_s$ and the approximation $k_\perp \approx \sqrt{\ell(\ell + 1)}/r_s$ we see that the parenthesis in front reduces to $(k_z/k)^2$. This means the full sky transfer function is approximated as

$$\Delta_\ell(z, k) = -\mathcal{H}^{-1} T_\Theta(k, z) j_\ell''(kr_s) \approx T_\Theta \mathcal{H}^{-1} \left(\frac{k_z}{k} \right)^2 j_\ell(kr_s) \quad (4.2.177)$$

Now calculating the C_ℓ we again use equation (4.2.147) and the calculation that follows to find the flat sky result. Note the similarity between equations (4.2.175) and (4.2.177), the only difference is the spherical Bessel function. This behavior mimics what happens for the density contribution. Unlike the density however, we see here, that on the flat sky, the correlation between the velocity field and the lensing is *strictly zero*, since the former contains a factor k_z . This approximate zero helps a

great deal to shorten our computations. This fact makes a lot of sense physically – the density or rather the gravitational potential, is doing the lensing, not the velocity of the galaxies. The effect of the velocity as such is not part of the dominating contribution to the power spectrum.

Figures 7 to 11 show how the flat sky calculations compare with the computations coming from the public code CLASS, written by Lesgourgues (2011). These computations are done for a standard Λ CDM universe, the parameters of which are immaterial. Do note the changing y-axes. From the last figure it should be clear why we need the lensing contribution, which is a purely general relativistic effect. For very different redshift, it and *especially* its correlation with the density field far outshines both the density and RSD contributions – although with different signs. So, if we hope to make use of the correlations between redshift bins, we absolutely must include lensing effects. For these very different redshifts, both computations even look like simple numerical artefacts – the density and RSD look alike in the two different computations, even though across the computations they look nothing alike. It is therefore nice that the lensing contribution dominates, so we can worry less about these problems. We are in a sense lucky that as the accuracy of the density computation degrades, its importance also fades.

We in principle only need to insert the flat sky C_ℓ expressions we just calculated in the expression for the bispectrum we already calculated on the full sky. It is however amusing to see how the angular derivatives behave on the flat sky, to see explicitly that the factors $A_\ell^{(1)}$ are just cosines of angles between ℓ -vectors. Let us therefore write down a generic expression with angular derivatives,

$$\nabla_a B \nabla^a C = (-i\mathbf{k}_B r_B) \cdot (-i\mathbf{k}_C r_C) BC \quad (4.2.178)$$

We thereby expand the expression BC by minus the dot product of what turn into the corresponding ℓ s. Both D and L -like transfer functions have delta functions surrounding them, meaning the dot product we get in front of BC is simply $-\ell_B \cdot \ell_C$. This should not be surprising at all. Looking at equation (2.3.13) this is exactly what we expect to get once all the expectation values have been taken, and the two initial ℓ s become ℓ_2, ℓ_3 . Remember that outside the flat sky bispectrum we have a delta function in $\sum \ell_i$ making sure the ℓ s form a triangle. This is reminiscent of what happened in the Δ^κ calculation, where the Δ_2 pulls down two factors kr , which turn into the known $\ell(\ell + 1)$.

The calculations so far have focused on the product-terms of the bispectrum. The terms coming from the Newtonian calculation are not quite as simple. The density term $\delta^{(2)}$, as it turns out, is manageable. We can write it in the same way as we have

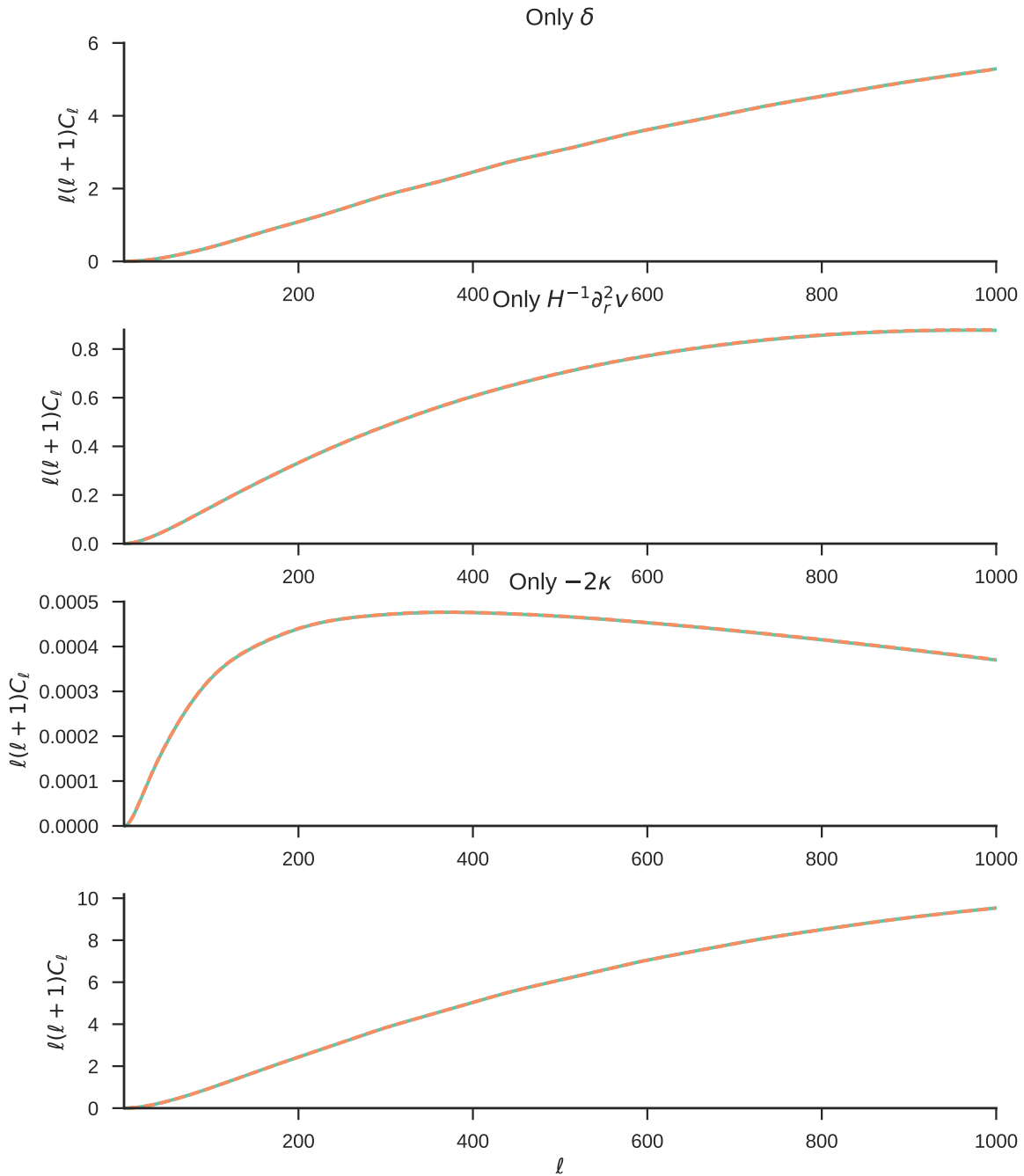


Figure 7: Galaxy count power spectrum computed by CLASS in cyan lines and by the flat sky approximation we calculated in orange dashed lines. The top three show the individual contributions from density, RSD, and lensing. The bottom plot includes the correlations as well. Here calculated for $z_1 = z_2 = 1$. For equal redshifts, evidently, it is an excellent approximation, including the fact that RSD and lensing do *not* correlate.

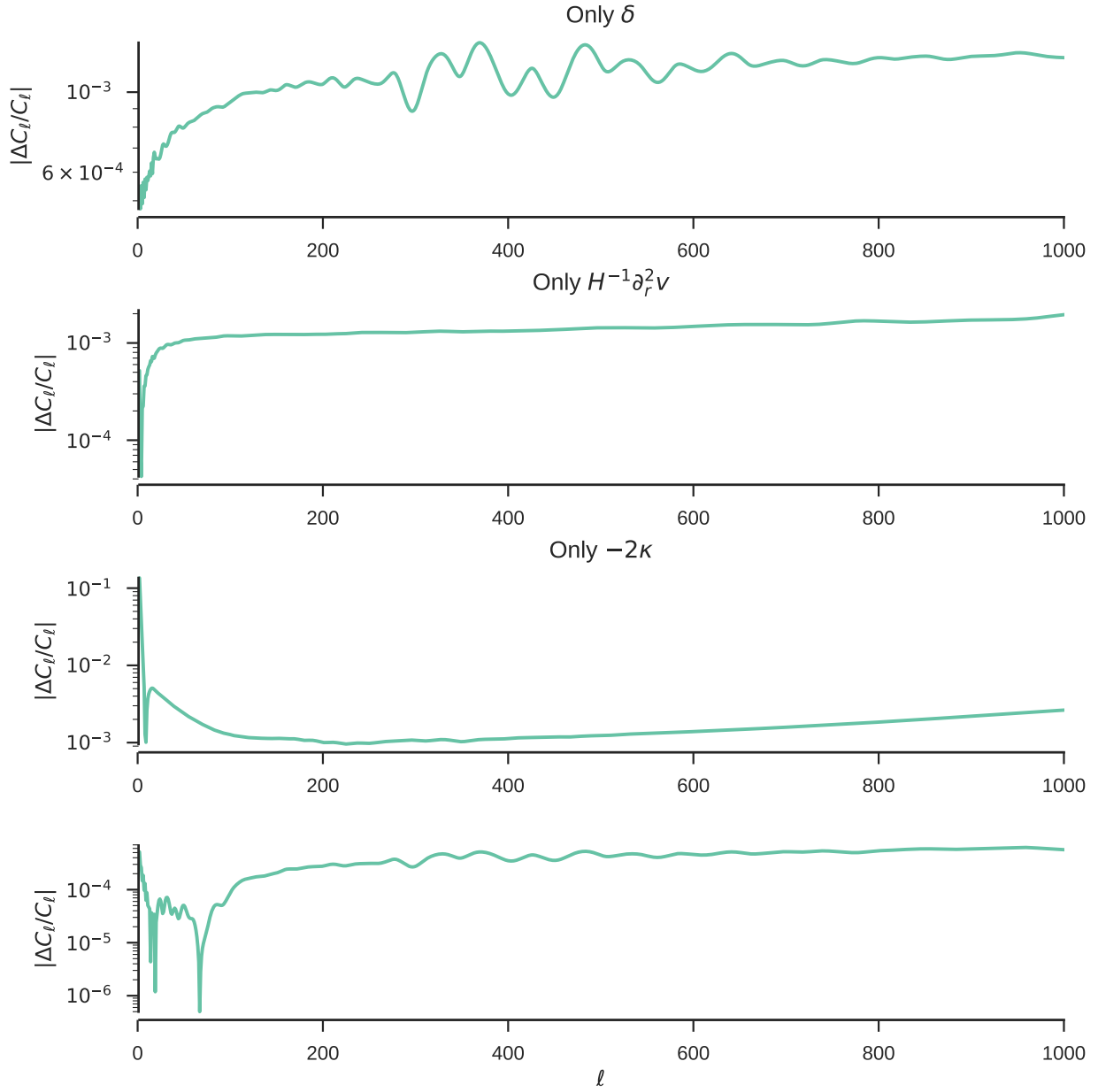


Figure 8: Normalized difference of the galaxy count power spectra computed by CLASS and by the flat sky approximation. Here calculated for $z_1 = z_2 = 1$. The difference for equal redshift is evidently kept at about permille level.

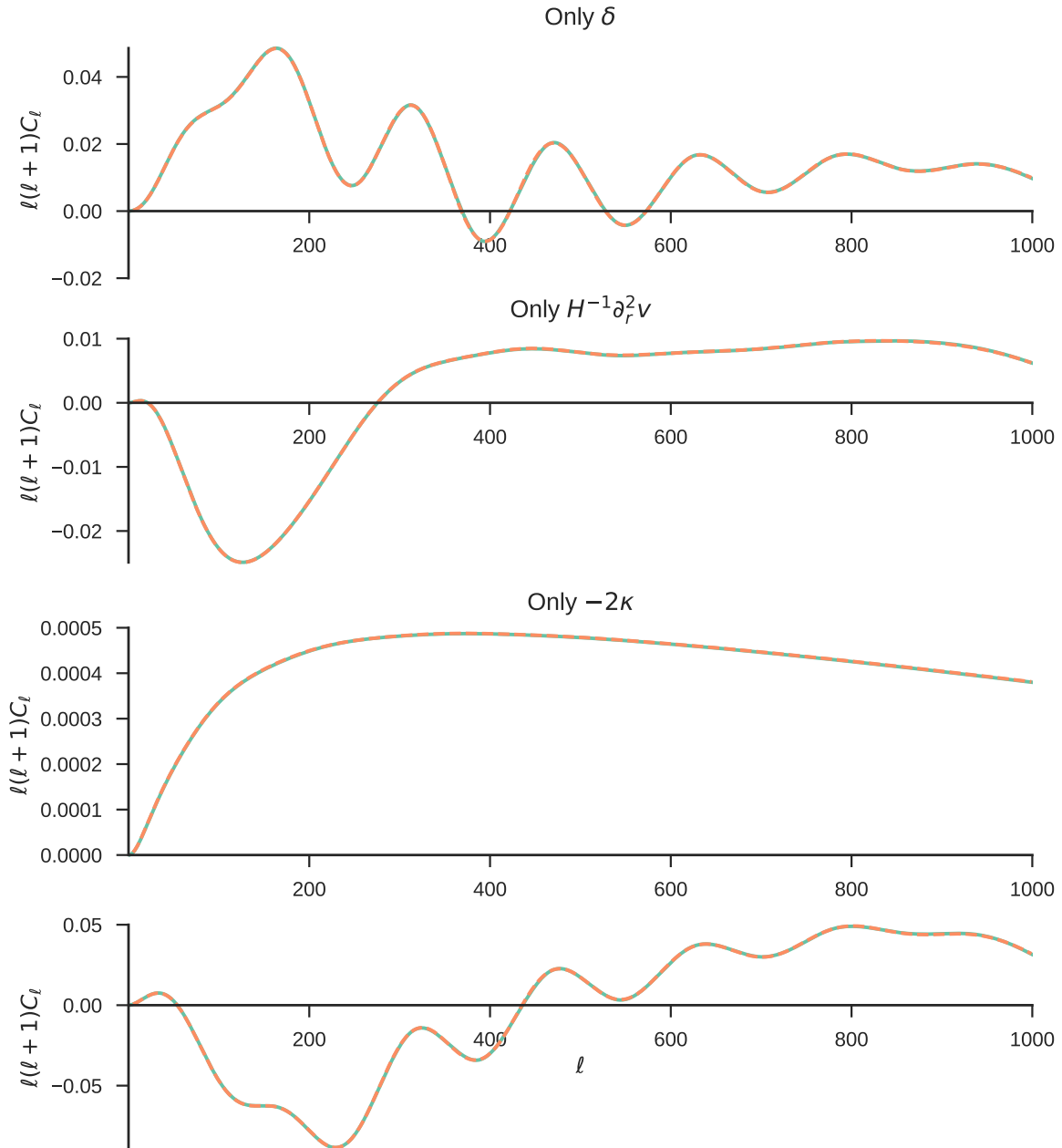


Figure 9: Galaxy count power spectrum computed by CLASS in cyan lines and by the flat sky approximation we calculated in orange dashed lines. Here calculated for $z_1 = 1, z_2 = 1.02$. Even for slightly different redshifts, it remains an excellent approximation.

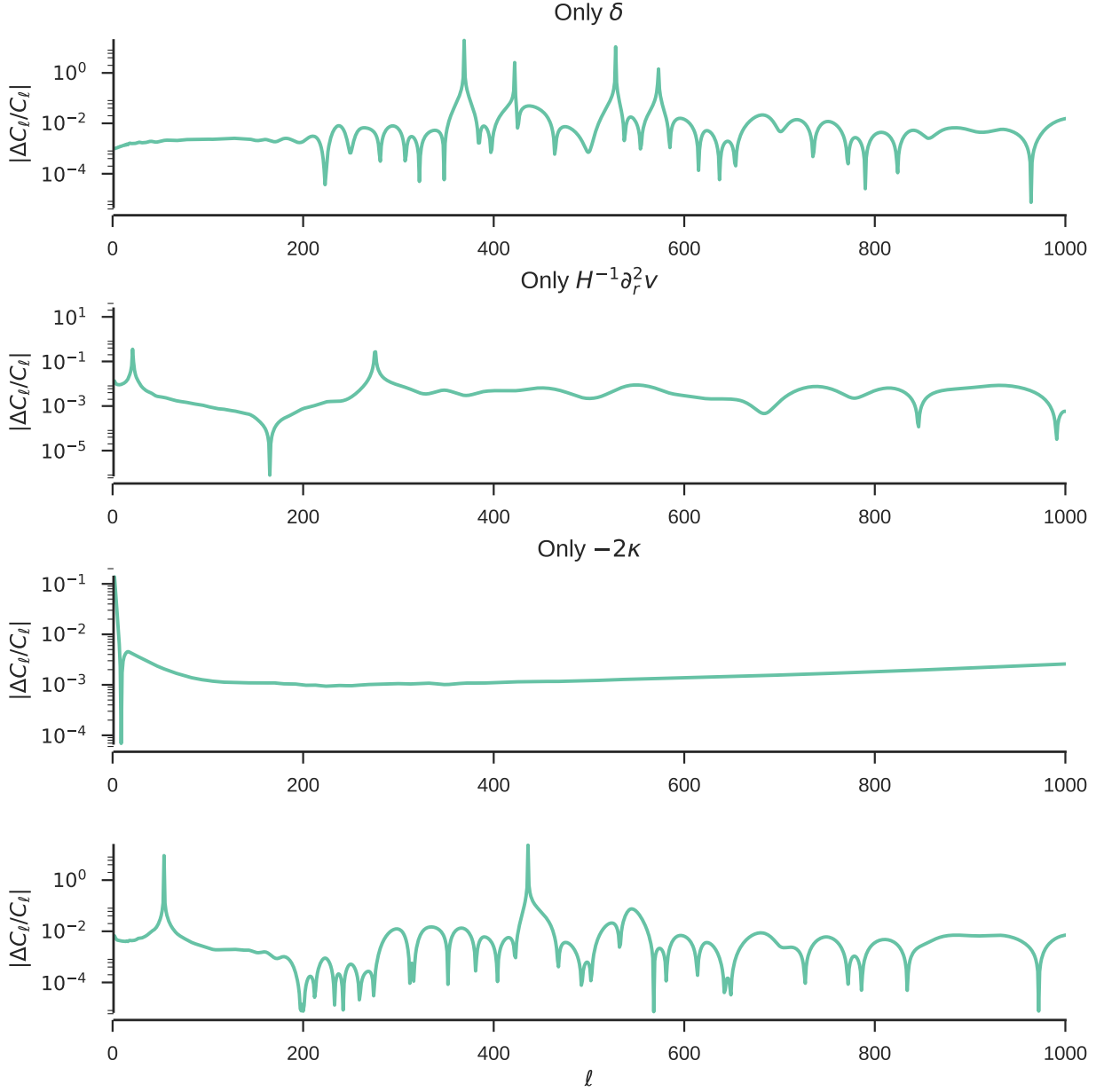


Figure 10: Normalized difference of the galaxy count power spectra computed by CLASS and by the flat sky approximation. Here calculated for $z_1 = 1$, $z_2 = 1.02$. The wiggles, to very high and very low differences line up with the zero-points and accidental intersections of the two computations. We see here, that the precision is still at the sub-percent level.

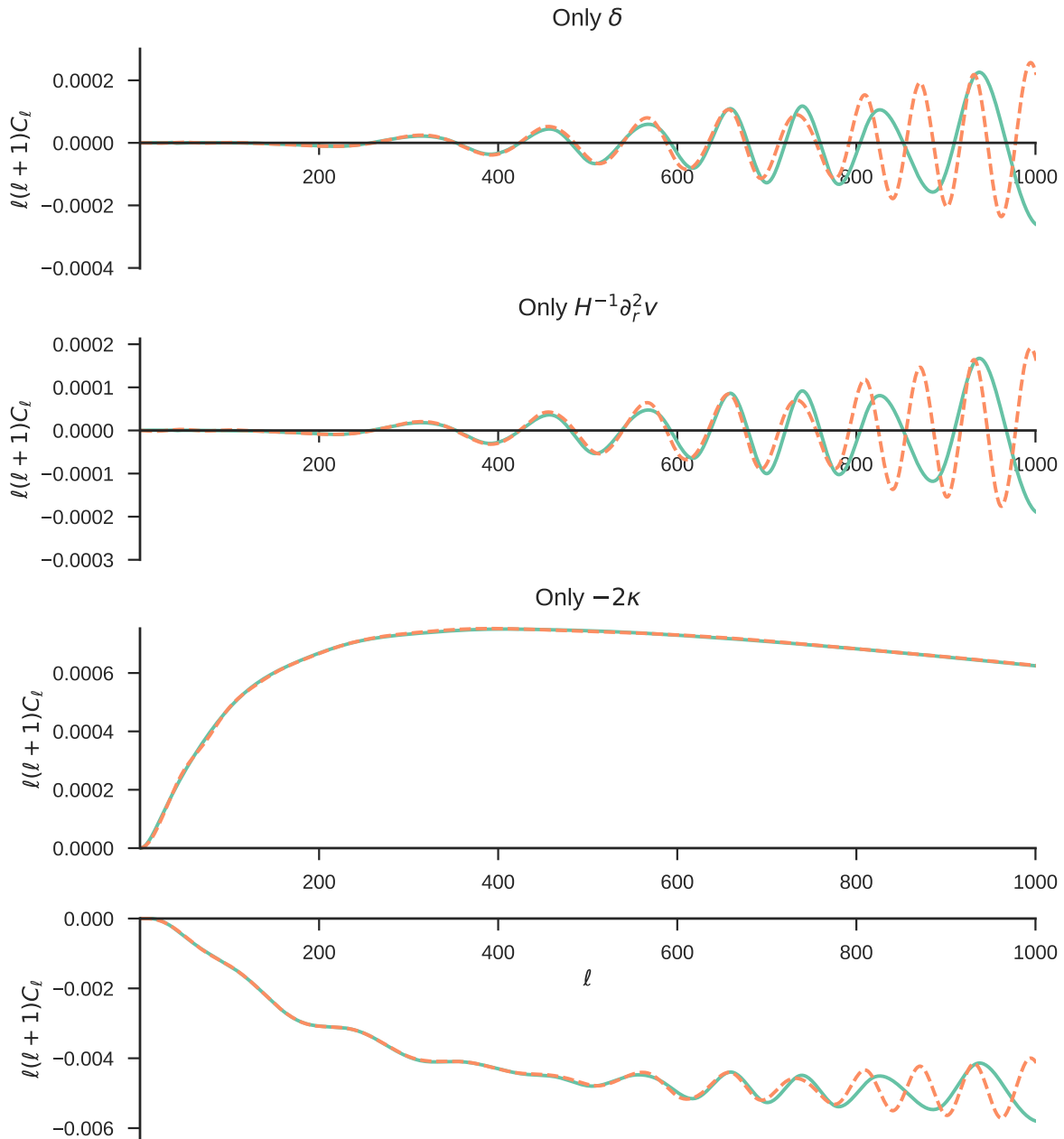


Figure 11: Galaxy count power spectrum computed by CLASS in cyan lines and by the flat sky approximation we calculated in orange dashed lines. Here calculated for $z_1 = 1, z_2 = 2$. For different redshifts, evidently, the D-like computation is not very accurate anymore. The lensing contribution continues to be well-approximated by the flat sky however, as does the cross-correlation between it and the density.

the previous terms, with only few modifications. First we write $F_2(\mathbf{p}, \mathbf{q})$ as a sum of separable terms,

$$F_2(\mathbf{p}, \mathbf{q}) = \frac{5}{7} + (p^2 q^2)^{-1} \left\{ \frac{1}{2} (\mathbf{p}_\perp \cdot \mathbf{q}_\perp + p_z q_z) (p^2 + q^2) + \frac{2}{7} (\mathbf{p}_\perp \cdot \mathbf{q}_\perp + p_z q_z)^2 \right\} \quad (4.2.179)$$

where the dot product of screen-momenta are written as $\mathbf{p}_\perp \cdot \mathbf{q}_\perp \rightarrow -A_{\ell_1 \ell_2 \ell_3} p_\perp q_\perp$. Since we are now multiplying on extra factors of k_z , we will need extra transfer functions, given by

$$\Delta^{(1)\delta} = k_z T_\delta(k, z) \quad (4.2.180)$$

$$\Delta^{(2)\delta} = k_z^2 T_\delta(k, z) \quad (4.2.181)$$

The extra factors of p, q need only be inserted once we calculate the power spectrum of these contributions. These are defined as follows,

$$C_{\ell, -2}^{\delta(i)D} = (\pi r_s r'_s)^{-1} \int dk_z \cos(k_z [r_s - r'_s]) \Delta^{(i)\delta}(k, \eta_s) \Delta^D(k, \eta'_s) P(k) k^{-2} \quad (4.2.182)$$

Given all these expressions, we are able to do a straight forward computation of the bispectrum induced by the second order Newtonian density perturbation, which I remind is

$$\delta^{(2)} = (2\pi)^{-6} \int d^3 p d^3 q F_2(\mathbf{p}, \mathbf{q}) \delta(\mathbf{p}) \delta(\mathbf{q}) \exp(i[\mathbf{p} + \mathbf{q}] \cdot \mathbf{nr}) \quad (4.2.183)$$

Correlating this contribution with either D - or L -like first order contributions lead to many different terms. The contributions to the bispectrum $b^{\delta(2)XX}$ are listed in tables 1 and 2, with the expression in F_2 on the left and the final bispectrum contribution from one such term on the right. As for the RSD contributions, we have here that all k_z are zero when a lensing contribution is involved. That means many of the terms can be thrown away to avoid wasting time. There are, however, still many new terms, and with them many new C_ℓ to calculate. However, we still see the factorization into the contributions of products of C_ℓ , which brings down the computing time. As already mentioned, this does not happen as easily for the second order Newtonian potential and RSD contributions. It is however possible to simplify the lensing computations on the flat sky.

The second order potential from the Newtonian evolution is

$$\Psi^{(n)}(\mathbf{k}, \eta) = -\frac{3\mathcal{H}^2 \Omega_m(\eta)}{2k^2} \delta^{(n)}(\mathbf{k}, \eta) \quad (4.2.184)$$

The lensing contribution is then $\ell(\ell + 1)$ times the weighted integral of minus twice this quantity over the past lightcone. We would now like to calculate the bispectrum contribution coming from this term and two first order terms. To that end, let us first write down the coefficient from the contribution $-2\kappa^{(2)}$,

$$a^{\kappa(2)}(\ell) = \frac{3\mathcal{H}^2 \Omega_m(\eta) \ell(\ell + 1)}{(2\pi)^4} \int_0^{r_s} dr \frac{r_s - r}{r_s r} \int d^3 k k^{-2} e^{-ik_z r_s} \delta(k_\perp r - \ell) \times \int d^3 p d^3 q \delta(\mathbf{k} - \mathbf{p} - \mathbf{q}) F_2(\mathbf{p}, \mathbf{q}) \delta^{(1)}(\mathbf{p}) \delta^{(1)}(\mathbf{q}) \quad (4.2.185)$$

| 5/7 | $5/7 C_{\ell_2}^{\delta D_2}(z_1, z_2) C_{\ell_3}^{\delta D_3}(z_1, z_3)$ |
|---|--|
| $\frac{1}{2} p^{-2} p_{\perp} \cdot q_{\perp}$ | $-A_{\ell_1 \ell_2 \ell_3} \ell_2 \ell_3 (2r_{1s}^2)^{-1} C_{\ell_2, -2}^{\delta D_2}(z_1, z_2) C_{\ell_3}^{\delta D_3}(z_1, z_3)$ |
| $\frac{1}{2} q^{-2} p_{\perp} \cdot q_{\perp}$ | $-A_{\ell_1 \ell_2 \ell_3} \ell_2 \ell_3 (2r_{1s}^2)^{-1} C_{\ell_2}^{\delta D_2}(z_1, z_2) C_{\ell_3, -2}^{\delta D_3}(z_1, z_3)$ |
| $\frac{1}{2} p^{-2} p_z q_z$ | $\frac{1}{2} C_{\ell_2, -2}^{\delta(1)D_2}(z_1, z_2) C_{\ell_3}^{\delta(1)D_3}(z_1, z_3)$ |
| $\frac{1}{2} q^{-2} p_z q_z$ | $\frac{1}{2} C_{\ell_2}^{\delta(1)D_2}(z_1, z_2) C_{\ell_3, -2}^{\delta(1)D_3}(z_1, z_3)$ |
| $\frac{2}{7} p^{-2} q^{-2} (p_{\perp} \cdot q_{\perp})^2$ | $2(A_{\ell_1 \ell_2 \ell_3})^2 \ell_2^2 \ell_3^2 (7r_{1s}^4)^{-1} C_{\ell_2, -2}^{\delta D_2}(z_1, z_2) C_{\ell_3, -2}^{\delta D_3}(z_1, z_3)$ |
| $\frac{4}{7} p^{-2} q^{-2} p_{\perp} \cdot q_{\perp} p_z q_z$ | $-4A_{\ell_1 \ell_2 \ell_3} \ell_2 \ell_3 (7r_{1s}^2)^{-1} C_{\ell_2, -2}^{\delta(1)D_2}(z_1, z_2) C_{\ell_3, -2}^{\delta(1)D_3}(z_1, z_3)$ |
| $\frac{2}{7} p^{-2} q^{-2} p_z^2 q_z^2$ | $\frac{2}{7} C_{\ell_2, -2}^{\delta(2)D_2}(z_1, z_2) C_{\ell_3, -2}^{\delta(2)D_3}(z_1, z_3)$ |

Table 1: Contributions to the bispectrum due to the second order Newtonian density perturbation and two D -like first order contributions. The term in F_2 on the left gives the bispectrum contribution on the right.

| 5/7 | $5/7 C_{\ell_2}^{\delta L_2}(z_1, z_2) C_{\ell_3}^{\delta X_3}(z_1, z_3)$ |
|---|---|
| $\frac{1}{2} p^{-2} p_{\perp} \cdot q_{\perp}$ | $-\frac{1}{2} A_{\ell_1 \ell_2 \ell_3} (\ell_2 / \ell_3) C_{\ell_2}^{\delta X_2}(z_1, z_2) C_{\ell_3}^{\delta L_3}(z_1, z_3)$ |
| $\frac{1}{2} q^{-2} p_{\perp} \cdot q_{\perp}$ | $-\frac{1}{2} A_{\ell_1 \ell_2 \ell_3} (\ell_3 / \ell_2) C_{\ell_2}^{\delta X_2}(z_1, z_2) C_{\ell_3}^{\delta L_3}(z_1, z_3)$ |
| $\frac{1}{2} p^{-2} p_z q_z$ | 0 |
| $\frac{1}{2} q^{-2} p_z q_z$ | 0 |
| $\frac{2}{7} p^{-2} q^{-2} (p_{\perp} \cdot q_{\perp})^2$ | $\frac{2}{7} (A_{\ell_1 \ell_2 \ell_3})^2 C_{\ell_2}^{\delta L_2}(z_1, z_2) C_{\ell_3}^{\delta X_3}(z_1, z_3)$ |
| $\frac{4}{7} p^{-2} q^{-2} p_{\perp} \cdot q_{\perp} p_z q_z$ | 0 |
| $\frac{2}{7} p^{-2} q^{-2} p_z^2 q_z^2$ | 0 |

Table 2: Contributions to the bispectrum due to the second order Newtonian density perturbation and either two L -like first order contributions, or one L - and one D -like contribution. I denote here either D or L by X . The term in F_2 on the left gives the bispectrum contribution on the right.

We would now like to calculate the correlators with both D - and L -like first order contributions, which behave slightly differently. First, I take two D -like contributions,

$$\begin{aligned}
\langle a_1^D a_2^D a_3^{\kappa(2)} \rangle &= 6\mathcal{H}^2 \ell_3 (\ell_3 + 1) \int_0^{r_{3s}} dr \frac{r_{3s} - r}{r_{3s} r} \int d^3 k_1 d^3 k_2 d^3 p d^3 q \\
&\quad \times (\mathbf{p} + \mathbf{q})^{-2} e^{-ik_{1z} r_{1s} - ik_{2z} r_{2s} - i(p_z + q_z)r} \\
&\quad \times \delta(\mathbf{k}_{1\perp} r_{1s} - \ell_1) \delta(\mathbf{k}_{2\perp} r_{2s} - \ell_2) \delta([\mathbf{p}_\perp + \mathbf{q}_\perp]r - \ell_3) \\
&\quad \times \Delta_1^D(k_1, \eta_1) \Delta_2^D(k_2, \eta_2) F_2(\mathbf{p}, \mathbf{q}) T_\delta(\mathbf{p}, \eta) T_\delta(\mathbf{q}, \eta) \\
&\quad \times \delta(\mathbf{p} + \mathbf{k}_1) \delta(\mathbf{q} + \mathbf{k}_2) P(k_1) P(k_2) \Omega_m(\eta) \\
&= 6\mathcal{H}^2 \ell_3 (\ell_3 + 1) \int_0^{r_{3s}} dr \frac{r_{3s} - r}{r_{3s} r} \int d^3 k_1 d^3 k_2 \\
&\quad \times (\mathbf{k}_1 + \mathbf{k}_2)^{-2} e^{-ik_{1z}(r_{1s} - r) - ik_{2z}(r_{2s} - r)} \\
&\quad \times \delta(\mathbf{k}_{1\perp} r_{1s} - \ell_1) \delta(\mathbf{k}_{2\perp} r_{2s} - \ell_2) \delta([\mathbf{k}_{1\perp} + \mathbf{k}_{2\perp}]r - \ell_3) \\
&\quad \times \Delta_1^D(k_1, \eta_1) \Delta_2^D(k_2, \eta_2) F_2(\mathbf{k}_1, \mathbf{k}_2) T_\delta(k_1, \eta) T_\delta(k_2, \eta) P(k_1) P(k_2) \Omega_m(\eta)
\end{aligned} \tag{4.2.186}$$

where a factor two appears from the two permutations of the expectation value combined with the symmetry $p \leftrightarrow q$ of the lensing contribution. We now wish to Limber approximate the exponentials. However, let us first rewrite the argument of the exponential, so the symmetry $1 \leftrightarrow 2$ is more apparent. We rewrite the argument as

$$k_{1z}(r_{1s} - r) + k_{2z}(r_{2s} - r) = \frac{k_{1z} + k_{2z}}{2} (r_{1s} + r_{2s} - 2r) + \frac{k_{1z} - k_{2z}}{2} (r_{1s} - r_{2s}) \tag{4.2.187}$$

Changing variables from k_{1z}, k_{2z} to $k_\pm = (k_{1z} \pm k_{2z})/2$ introduces a jacobian factor of 2 in the integral. We then Limber approximate the k_+ integral by setting $k_+ = 0$ and inserting $(2\pi)\delta(r_{1s} + r_{2s} - 2r)$. Integrating out the r using the delta function gives a factor $1/2$, which cancels with the jacobian. This naturally requires the lensing contribution to be in the background, $z_3 > z_1, z_2$. Having done these integrals, we may integrate out the screen- k , and approximate the last delta function as over the sum of the ℓ_i . Thus we end up with

$$\begin{aligned}
b^{DD\kappa(2)} &\approx - \frac{6\mathcal{H}^2 \Omega_m(\eta_1) \ell_3 (\ell_3 + 1)}{2\pi r_{1s}^2 r_{2s}^2} \frac{2r_{3s} - r_{1s} - r_{2s}}{r_{3s}(r_{1s} + r_{2s})} \int_{-\infty}^{\infty} dk_- e^{-ik_-(r_{1s} - r_{2s})} \\
&\quad \frac{r_{1s} + r_{2s}}{2\ell_3} \Delta_1^D(k_1, \eta_1) \Delta_2^D(k_2, \eta_2) F_2(\mathbf{k}_1, \mathbf{k}_2) T_3(k_1, \eta_1) T_3(k_2, \eta_2) P(k_1) P(k_2) \\
&= - \frac{6\mathcal{H}^2 \Omega_m(\eta_1) (\ell_3 + 1)}{2\pi r_{1s}^2 r_{2s}^2} \times \frac{2r_{3s} - r_{1s} - r_{2s}}{r_{3s}} \\
&\quad \int_0^\infty dk_z \cos(k_z[r_{1s} - r_{2s}]) \Delta_1^D(k_1, \eta_1) \Delta_2^D(k_2, \eta_2) F_2(\mathbf{k}_1, \mathbf{k}_2) T_\delta(k_1, \eta_1) T_\delta(k_2, \eta_2) P(k_1) P(k_2)
\end{aligned} \tag{4.2.188}$$

where in the last line I write $k_- = k_{1z} = -k_{2z} \equiv k_z$. We have thereby reduced the number of integrals for this contribution to the bispectrum to just *one*. The important thing happening for the lensing term is that the Limber approximation makes sure the sum of k_{iz} is zero. That means the problematic term k^{-2} , which on the full

Do note that this fact rests on the appearance of the integral.

For the corresponding RSD contribution, this does not happen for the $DDv^{(2)}$ contribution, which will have two integrals over a kernel G_2 .

sky completely hinders the computation of this term, now *does* reduce, and in fact is entirely unproblematic. For the last integral, one may simply insert the explicit expression from equation (4.2.179) and use the fact that the screen- k are given by ℓ_i/r_{is} . That means we can write the kernel F_2 as a function of just the k_z , given the ℓ_i ,

$$F_2(k_z) = \frac{5}{7} + (k_1^2 k_2^2)^{-1} \left\{ -\frac{1}{2} (A_{\ell_3 \ell_1 \ell_2} \ell_1 \ell_2 / (r_{1s} r_{2s}) + k_z^2) (k_1^2 + k_2^2) + \frac{2}{7} (A_{\ell_3 \ell_1 \ell_2} \ell_1 \ell_2 / (r_{1s} r_{2s}) + k_z^2)^2 \right\} \quad (4.2.189)$$

where the sizes are given by $k_i^2 = k_z^2 + \ell_i^2 / r_{is}^2$.

The generalisation of this result to the $DL\kappa^{(2)}$ and $LL\kappa^{(2)}$ cases is straight-forward. The only change is the integrals over r_2 and r_1 instead of fixed $r_i = r_{is}$. For the DL case, we therefore insert another integral over r_s in equation (4.2.186). This integral stays in place all the way to the result, where now we allow another Limber approximation. That means instead of writing the exponential as two times cosine, we now Limber approximate the k_z integral by setting $k_z = 0$ and inserting $2\pi\delta(r_{1s} - r_2)$. The integral over r_2 is then performed, provided $z_2 > z_1$, and we end with the result

$$b^{DL\kappa(2)} \approx -\frac{6\mathcal{H}^2 \Omega_m(\eta_1)(\ell_3 + 1)}{r_{1s}^4} \times \frac{r_{3s} - r_{1s}}{r_{3s}} \quad (4.2.190)$$

$$\Delta_1^D(k_1, \eta_1) \Delta_2^L(k_2, \eta_1) F_2(0) T_\delta(k_1, \eta_1) T_\delta(k_2, \eta_1) P(k_1) P(k_2)$$

This time with *no* integrals left. Note that in this case, the $k_z = 0$, and eg. RSD contribution vanish. The kernel is furthermore evaluated at zero, where it is given by the somewhat simpler expression

$$F_2(0) = \frac{5}{7} + \left\{ -\frac{1}{2} A_{\ell_3 \ell_1 \ell_2} \left(\frac{\ell_1}{\ell_2} + \frac{\ell_2}{\ell_1} \right) + \frac{2}{7} A_{\ell_3 \ell_1 \ell_2}^2 \right\} \quad (4.2.191)$$

Finally, setting all contributions to be lensing is to include yet another integral over r_1 . That means the answer this time is

$$b^{LL\kappa(2)} \approx -\int_0^{r_{1s}} dr \frac{6\mathcal{H}^2 \Omega_m(\eta)(\ell_3 + 1)}{r^4} \times \frac{r_{3s} - r}{r_{3s}} \quad (4.2.192)$$

$$\Delta_1^L(k_1, \eta) \Delta_2^L(k_2, \eta) F_2(0) T_\delta(k_1, \eta) T_\delta(k_2, \eta) P(k_1) P(k_2)$$

Having reduced the number of integrals from five to just one, this term is now easily computed along with the rest. The results are generally not separable in the ℓ_i as the product terms and the $\delta^{(2)}$ term are. That means the computations scale as ℓ_{\max}^3 instead of simply ℓ_{\max} . If one is to calculate this for a very large number of ℓ , it is possible to further write the expressions with the ℓ_3 factorized out. This can be done by writing out $A_{\ell_3 \ell_1 \ell_2}$ in F_2 and extracting the ℓ_3 term.

The splitting of the terms into results with different numbers of integrals is also exhibited in the calculation of the primordial contribution to the bispectrum, which we calculate next.

4.2.11 Computing the primordial galaxy bispectrum on a flat sky

Now let us look at the galaxy bispectrum coming from a primordial bispectrum on a flat sky. I remind that this computation is all but impossible on the full sky. It is therefore very important to calculate on the flat sky. We have already calculated the relevant $a(\ell)$, and now simply need to calculate the correlators given an initial bispectrum. Because of the classification into D - and L -like transfer functions, we will have four different bispectrum calculations – one for each combination of types of transfer functions. Like before, some will be simpler than others, as more integrals are taken off the calculation. I first do the DDD correlator,

$$\begin{aligned}
& \langle a_1^D(\ell_1) a_2^D(\ell_2) a_3^D(\ell_3) \rangle = & (4.2.193) \\
& (2\pi)^{-3} \int d^3k_1 d^3k_2 d^3k_3 \delta(\mathbf{k}_{1\perp} r_{1s} - \ell_1) \delta(\mathbf{k}_{2\perp} r_{2s} - \ell_2) \delta(\mathbf{k}_{3\perp} r_{3s} - \ell_3) \\
& \times \langle \Phi(\mathbf{k}_1) \Phi(\mathbf{k}_2) \Phi(\mathbf{k}_3) \rangle \Delta_1^D(k_1, \eta_{1s}) \Delta_2^D(k_2, \eta_{2s}) \Delta_3^D(k_3, \eta_{3s}) e^{-i(k_{1z} r_{1s} + k_{2z} r_{2s} + k_{3z} r_{3s})} \\
& = (2\pi)^2 \delta(\ell_1 + \ell_2 + \ell_3) \int_{-\infty}^{\infty} dk_{1z} dk_{2z} (2\pi r_{1s} r_{2s})^{-2} B(k_1, k_2, |\mathbf{k}_1 + \mathbf{k}_2|) \\
& \times \Delta_1^D(k_1, \eta_{1s}) \Delta_2^D(k_2, \eta_{2s}) \Delta_3^D(|\mathbf{k}_1 + \mathbf{k}_2|, \eta_{3s}) e^{-i(k_{1z}(r_{1s} - r_{3s}) + k_{2z}(r_{2s} - r_{3s}))}
\end{aligned}$$

Here I simply integrate out the delta functions and use $r_{1s} \approx r_{2s} \approx r_{3s}$, which is reasonable for the D -like contributions. Like we did for equation (4.1.25) we would like to have this result manifestly real. We may again use the trick that the negative part of the k_{2z} integral is simply the complex conjugate of the positive part. We may therefore write the result as

$$\begin{aligned}
b^{DDD} &= (2\pi r_{1s} r_{2s})^{-2} \int_{-\infty}^{\infty} dk_{1z} \int_0^{\infty} dk_{2z} B(k_1, k_2, |\mathbf{k}_1 + \mathbf{k}_2|) & (4.2.194) \\
& \times \Delta_1^D(k_1, \eta_{1s}) \Delta_2^D(k_2, \eta_{2s}) \Delta_3^D(|\mathbf{k}_1 + \mathbf{k}_2|, \eta_{3s}) \times 2 \cos[k_{1z}(r_{1s} - r_{3s}) + k_{2z}(r_{2s} - r_{3s})]
\end{aligned}$$

It is important to realise of course, that even though naively it seems we are favouring 1 and 2 over 3, we might as well have written this in terms of k_{1z} , k_{3z} or k_{2z} , k_{3z} with the same result. In an effort to make this even more transparent, one might consider using $(r_{1s} r_{2s} r_{3s})^{-4/3}$ in front of the integral as well.

Now we need the remaining three combinations. We begin with one L ,

$$\begin{aligned}
\langle a_1^D(\ell_1) a_2^D(\ell_2) a_3^L(\ell_3) \rangle &= \tag{4.2.195} \\
(2\pi)^{-3} \int d^3k_1 d^3k_2 d^3k_3 \int_0^{r_{3s}} dr_3 \delta(\mathbf{k}_{1\perp} r_{1s} - \ell_1) \delta(\mathbf{k}_{2\perp} r_{2s} - \ell_2) \delta(\mathbf{k}_{3\perp} r_3 - \ell_3) \\
&\times \langle \Phi(\mathbf{k}_1) \Phi(\mathbf{k}_2) \Phi(\mathbf{k}_3) \rangle \Delta_1^D(k_1, \eta_{1s}) \Delta_2^D(k_2, \eta_{2s}) \Delta_3^L(k_3, \eta_3) e^{-i(k_{1z} r_{1s} + k_{2z} r_{2s} + k_{3z} r_3)} \\
&= \int d^3k_1 d^3k_3 \int_0^{r_{3s}} dr_3 \delta(\mathbf{k}_{1\perp} r_{1s} - \ell_1) \delta((\mathbf{k}_{1\perp} + \mathbf{k}_{3\perp}) r_{2s} + \ell_2) \delta(\mathbf{k}_{3\perp} r_3 - \ell_3) \\
&\times B(k_1, |\mathbf{k}_1 + \mathbf{k}_3|, k_3) \Delta_1^D(k_1, \eta_{1s}) \Delta_2^D(|\mathbf{k}_1 + \mathbf{k}_3|, \eta_{2s}) \Delta_3^L(k_3, \eta_3) e^{-i(k_{1z}(r_{1s} - r_{2s}) + k_{3z}(r_3 - r_{2s}))} \\
&= (2\pi)^2 \delta(\ell_1 + \ell_2 + \ell_3) \int_{-\infty}^{\infty} dk_{1z} (2\pi)^{-1} (r_{1s} r_{2s})^{-2} B(k_1, k_2, |k_1 + k_2|) \\
&\times \Delta_1^D(k_1, \eta_{1s}) \Delta_2^D(k_2, \eta_{2s}) \Delta_3^L(|k_1 + k_2|, \eta_{1s}) e^{-ik_{1z}(r_{1s} - r_{2s})}
\end{aligned}$$

The first equality here is simply integrating out k_2 using the delta function. Then I Limber approximate the k_{3z} integral and replace the exponential by $2\pi\delta(\dots)$ while setting $k_{3z} = 0$. This delta function is integrated out, given $z_3 > z_2$ - ie. we again need the lensing to be behind the density contributions. This integration also fixes the conformal time at which to evaluate the lensing transfer function. The delta function on $\Sigma \ell$ is then written using $r_{1s} \approx r_{2s}$. The last integral here can again be written as a cosine. Let me call $k_{1z} = k_z$, to explicitly show how neither 1 nor 2 is 'preferred', even though I integrated out k_2 first above. With this, the bispectrum is

$$\begin{aligned}
b^{DDL} &= \frac{1}{\pi(r_{1s} r_{2s})^2} \int_0^{\infty} dk_z B(k_1, k_2, |k_1 + k_2|) \tag{4.2.196} \\
&\times \Delta_1^D(k_1, \eta_{1s}) \Delta_2^D(k_2, \eta_{2s}) \Delta_3^L(|k_1 + k_2|, \eta_{1s}) \cos(k_z(r_{1s} - r_{2s}))
\end{aligned}$$

It is not obvious from this expression how all the momenta are set. From the initial delta function we know however that $k_{2z} = k_{1z}$ since $k_{3z} = 0$. We also have for all the momenta $k_{i\perp} = \ell_i / r_{1s} \approx \ell_i / r_{2s}$. This also means we have at all values of k_z a fixed expression for $k_3 = |\mathbf{k}_1 + \mathbf{k}_2| = k_{3\perp} = \ell_3 / r_{1s}$. To our great joy, we have one less integral to perform in this case.

Next up is two L-like contributions.

$$\begin{aligned}
\langle a_1^D(\ell_1) a_2^L(\ell_2) a_3^L(\ell_3) \rangle &= \tag{4.2.197} \\
(2\pi)^{-3} \int d^3k_1 d^3k_2 d^3k_3 \int_0^{r_{2s}} dr_2 \int_0^{r_{3s}} dr_3 \delta(\mathbf{k}_{1\perp} r_{1s} - \ell_1) \delta(\mathbf{k}_{2\perp} r_2 - \ell_2) \delta(\mathbf{k}_{3\perp} r_3 - \ell_3) \\
&\times \langle \Phi(\mathbf{k}_1) \Phi(\mathbf{k}_2) \Phi(\mathbf{k}_3) \rangle \Delta_1^D(k_1, \eta_{1s}) \Delta_2^L(k_2, \eta_2) \Delta_3^L(k_3, \eta_3) e^{-i(k_{1z} r_{1s} + k_{2z} r_2 + k_{3z} r_3)} \\
&= \int d^3k_2 d^3k_3 \int_0^{r_{2s}} dr_2 \int_0^{r_{3s}} dr_3 \delta((\mathbf{k}_{2\perp} + \mathbf{k}_{3\perp}) r_{1s} + \ell_1) \delta(\mathbf{k}_{2\perp} r_2 - \ell_2) \delta(\mathbf{k}_{3\perp} r_3 - \ell_3) \\
&\times B(|\mathbf{k}_2 + \mathbf{k}_3|, k_2, k_3) \Delta_1^D(|\mathbf{k}_2 + \mathbf{k}_3|, \eta_{1s}) \Delta_2^L(k_2, \eta_2) \Delta_3^L(k_3, \eta_3) e^{-i(k_{2z}(r_2 - r_{1s}) + k_{3z}(r_3 - r_{1s}))} \\
&= (2\pi)^2 \delta(\ell_1 + \ell_2 + \ell_3) r_{1s}^{-4} B(k_1, k_2, k_3) \Delta_1^D(k_1, \eta_{1s}) \Delta_2^L(k_2, \eta_{1s}) \Delta_3^L(k_3, \eta_{1s})
\end{aligned}$$

Here we use the same trick as before, only this time, twice. The k_1 takes the initial delta function for the first equality. Then k_{2z}, k_{3z} are Limber approximated and the

delta functions integrated out, given $z_1 < z_2, z_3$, and all conformal times in the transfer functions are set to η_{1s} . Finally the screen-space momenta are integrated out and inserted in the delta function in $\Sigma \ell$. We get rid of *all* integrals, and the bispectrum is

$$b^{DLL} = r_{1s}^{-4} B(k_1, k_2, k_3) \Delta_1^D(k_1, \eta_{1s}) \Delta_2^L(k_2, \eta_{1s}) \Delta_3^L(k_3, \eta_{1s}) \quad (4.2.198)$$

where all momenta are given by $k_i = k_{i\perp} = \ell_i / r_{1s}$.

The final term has only L-like contributions.

$$\begin{aligned} \langle a_1^L(\ell_1) a_2^L(\ell_2) a_3^L(\ell_3) \rangle &= \quad (4.2.199) \\ (2\pi)^{-3} \int d^3 k_1 d^3 k_2 d^3 k_3 \int_0^{r_{1s}} dr_1 \int_0^{r_{2s}} dr_2 \int_0^{r_{3s}} dr_3 &\delta(\mathbf{k}_{1\perp} r_1 - \ell_1) \delta(\mathbf{k}_{2\perp} r_2 - \ell_2) \delta(\mathbf{k}_{3\perp} r_3 - \ell_3) \\ \times \langle \Phi(\mathbf{k}_1) \Phi(\mathbf{k}_2) \Phi(\mathbf{k}_3) \rangle \Delta_1^L(k_1, \eta_1) \Delta_2^L(k_2, \eta_2) \Delta_3^L(k_3, \eta_3) &e^{-i(k_{1z} r_1 + k_{2z} r_2 + k_{3z} r_3)} \\ = \int d^3 k_2 d^3 k_3 \int_0^{r_{1s}} dr_1 \int_0^{r_{2s}} dr_2 \int_0^{r_{3s}} dr_3 &\delta((\mathbf{k}_{2\perp} + \mathbf{k}_{3\perp}) r_1 + \ell_1) \delta(\mathbf{k}_{2\perp} r_2 - \ell_2) \delta(\mathbf{k}_{3\perp} r_3 - \ell_3) \\ \times B(|\mathbf{k}_2 + \mathbf{k}_3|, k_2, k_3) \Delta_1^L(|\mathbf{k}_2 + \mathbf{k}_3|, \eta_1) \Delta_2^L(k_2, \eta_2) \Delta_3^L(k_3, \eta_3) &e^{-i(k_{2z}(r_2 - r_1) + k_{3z}(r_3 - r_1))} \\ = (2\pi)^2 \delta(\ell_1 + \ell_2 + \ell_3) \int_0^{\min(r_{is})} \frac{dr}{r^4} \Delta_1^L(k_1, \eta) \Delta_2^L(k_2, \eta) \Delta_3^L(k_3, \eta) &B(k_1, k_2, k_3) \end{aligned}$$

Here I first integrate out k_1 . We then Limber approximate the remaining two k_{iz} integrals. The resulting delta functions are integrated out with r_2, r_3 , which are set equal to $r_1 \equiv r$, provided $z_1 < z_2, z_3$. After all this, the screen-space momenta are integrated out and give four factors of r and a delta function in $\Sigma \ell$. The momenta are given by $k_i = \ell_i / r$, as it was for the C_ℓ^{LL} . This gives us

$$b^{LLL} = \int_0^{\min(r_{is})} \frac{dr}{r^4} \Delta_1^L(k_1, \eta) \Delta_2^L(k_2, \eta) \Delta_3^L(k_3, \eta) B(k_1, k_2, k_3) \quad (4.2.200)$$

This last bispectrum of only lensing contributions has already been investigated to some extent in relation to weak lensing surveys by eg. [Bernardeau et al. \(2003\)](#); [Munshi et al. \(2008\)](#)

The four equations (4.2.194), (4.2.196), (4.2.198) and (4.2.200) are our result for the primordial bispectrum as observed in galaxy correlations on a flat sky. Considering the expressions have maximum two integrals, these are *much more* tractable than the full sky calculation of equation (4.2.139). This will allow us to compute the observed bispectrum for many redshifts and ℓ -combinations. When computing the bispectra, it is useful to remember that the velocity and lensing never correlate, since we have $k_z = 0$ due to the Limber approximation, which kills the velocity term. This fact cuts down the number of terms dramatically.

It is also wise to make sure we remember when the approximations are expected to be good. We see that both DDD and DDL rely on the radial distances to the D-like contributions being similar. The remaining two, DLL and LLL are however not relying on this. As we learned from figures 7, 9 and 11 it may not be wise to trust the computations of DDD and DDL for very large separations of the D-like contributions. The lensing contribution simply has to be in the background.

So why, in the end, are we calculating the GR induced bispectra? The answer is simple – this ‘fake’ bispectrum will bias any attempt at extracting a primordial bispectrum from any data we might get. In other words, if we simply try to extract directly the primordial bispectrum from the galaxy bispectrum, we *will* see something, namely the projection of the GR bispectrum onto the shape of the primordial bispectrum. Considering just these contributions, we may easily check how much one contaminates the determination of the other. We imagine an experiment measuring the galaxy count bispectrum b_ℓ , but forgetting to include the GR bispectrum in the fit for the f_{NL} . This results in a χ^2 of the following schematic form, similar to equation (4.1.14)

$$\chi^2 = \sum_{\ell=\{\ell_1, \ell_2, \ell_3\}} \frac{(n_\ell + h_\ell [b_\ell^{GR} - f_{NL} b_\ell^{infl}])^2}{C_{\ell_1} C_{\ell_2} C_{\ell_3}}, \quad (4.2.201)$$

where n_ℓ is the noise for the particular set ℓ of multipoles, b^{GR} is the bispectrum from general relativistic effects, and b^{infl} is the sought-for primordial bispectrum coming from inflation. The noise is drawn from a gaussian with variance $C_{\ell_1} C_{\ell_2} C_{\ell_3}$, since the cosmic variance is the only noise I include. This function is minimized to find the best fit f_{NL} . Normally, ie. with b_ℓ^{GR} set to zero, the best fit would be

$$\hat{f}_{NL} = \sum_{\ell} \frac{n_\ell h_\ell b_\ell^{infl}}{C_{\ell_1} C_{\ell_2} C_{\ell_3}} \bigg/ \sum_{\ell} \frac{(b_\ell^{infl} h_\ell)^2}{C_{\ell_1} C_{\ell_2} C_{\ell_3}} \quad (4.2.202)$$

However, with the non-zero GR contribution, this best fit is changed to

$$\hat{f}_{NL}^{contaminated} = \sum_{\ell} \frac{(n_\ell + h_\ell b_\ell^{GR}) h_\ell b_\ell^{infl}}{C_{\ell_1} C_{\ell_2} C_{\ell_3}} \bigg/ \sum_{\ell} \frac{(b_\ell^{infl} h_\ell)^2}{C_{\ell_1} C_{\ell_2} C_{\ell_3}}, \quad (4.2.203)$$

and so, the expected contamination in terms of a bias of the f_{NL} estimator is

$$bias(\hat{f}_{NL}) = \sum_{\ell} \frac{h_\ell^2 b_\ell^{GR} b_\ell^{infl}}{C_{\ell_1} C_{\ell_2} C_{\ell_3}} \bigg/ \sum_{\ell} \frac{(b_\ell^{infl} h_\ell)^2}{C_{\ell_1} C_{\ell_2} C_{\ell_3}} \quad (4.2.204)$$

We can think of this as a systematic effect of the experiment. We simply need to exactly remove the late-time bispectrum before trying to extract the primordial one. If we do not, we see here how much our result is affected.

Directly observing the bispectrum is the most obvious way of proving its existence. There exists other indirect observables however. A popular one is to find scale-dependent bias in the observed power spectrum, as suggested by Dalal et al. (2008). They calculate the corrections to the matter power spectrum from *local* primordial non-gaussianity. The detection of such a scale-dependent bias, while not direct evidence for a particular primordial bispectrum, would be evidence for *something more*. However, the observation of this power spectrum and its correction are still subject to the pollution we calculate. We cannot *a priori* disentangle primordial bispectrum from GR corrections in the observed matter distribution. As such, *all*

non-gaussianities in the observed galaxy number count must be accounted for when calculating this corrected power spectrum. It is not entirely clear how the bias we calculate in equation (4.2.204) translates to corrections of the power spectrum, which is usually calculated in k space, but one must expect corrections even after subtracting the Newtonian bispectrum.

4.2.12 Redshift binning and shot noise

The quantities we have calculated for LSS so far have been only theoretical quantities. They are, as the CMB calculation, the observed density field at *one* point in time. For realistic surveys however, we will need to bin the observed galaxies across redshift in order to get a reliable estimate of the density field. This has several effects. The variance of both power spectrum and bispectrum will, in addition to the cosmic variance, include shot-noise since we have a finite number of galaxies. Furthermore, any sharp features in the spectra tend to wash out when integrating over z . We are therefore fighting two contrasting limitations against one another: we need wide enough bins that the shot-noise becomes small, but we need tight enough bins that we retain the features we are looking for. The practical answer to this battle of terms depends on a number of things: the bispectra we look for, and which features it has; the expected number of observed galaxies in a particular survey; and the cosmological parameters determining the underlying physics.

We have already seen what the variance of the power spectrum and bispectrum are for a single redshift, ie. the infinitely thin bin. Let us now see how the calculation of equations (4.1.12) and (4.1.17) generalizes to finite redshift bins and so a finite sample. The observables are as always the $a_{\ell m}$. The calculation so far has focused on $a_{\ell m}(z)$, which we now generalize to a binned version,

$$a_{\ell m}^i = 1/V_z \int_{\text{bin } i} dz a_{\ell m}(z), \quad (4.2.205)$$

where V_z is the width of the bin. The remaining calculation simply substitutes this in the place of the theoretical $a_{\ell m}(z)$. That means we will have the binned power spectrum and bispectrum

$$C_\ell^{ij} = \langle a_{\ell m}^i (a_{\ell m}^j)^* \rangle = V_z^{-2} \int_{\text{bin } i} dz \int_{\text{bin } j} dz' C_\ell(z, z') \quad (4.2.206)$$

$$b_{\ell_1 \ell_2 \ell_3}^{ijk} = \langle a_{\ell_1 m_1}^i a_{\ell_2 m_2}^j a_{\ell_3 m_3}^k \rangle = V_z^{-3} \int_{\text{bin } i} dz \int_{\text{bin } j} dz' \int_{\text{bin } k} dz'' b_{\ell_1 \ell_2 \ell_3}(z, z', z'') \quad (4.2.207)$$

Note that the binned bispectrum coming from second order perturbations is *not* simply a product of binned C_ℓ like one might have expected. It is rather the 'double binning' of the two power spectra, which we may schematically write $\int dz dz' dz'' C_{\ell_2}(z, z') C_{\ell_3}(z, z'')$.

I here use only tophat bins. This may be generalized to any window function $W(z)$ – eg. a gaussian – and any redshift distribution dN/dz by taking the integral over $\frac{dN}{dz} W(z) a_{\ell m}(z)$, while still dividing out the bin-width, ie. normalizing $W(z)dN/dz$.

The interesting quantity now is the noise in $a_{\ell m}$, *not only* due to cosmic variance, but simply due to the finite number of observed galaxies in the redshift bin.

Given N observed galaxies in one redshift bin, we wish to estimate the distribution from which they came, and in particular its spherical harmonic coefficients. If we could simply see the field, as is the case for CMB, this is a simple integral over the field and a spherical harmonic. For a finite sample of galaxies, we will perform what looks like a *monte carlo* integral using *importance sampling*, as described by Kroese et al. (2013). Since we already have a sample from the distribution – the galaxies themselves – we can evaluate the integral as follows,

$$a_{\ell m} = \int d^2n \frac{\rho(n)}{\bar{\rho}} Y_{\ell m}^*(n) \approx \frac{4\pi}{N} \sum_{n_i} Y_{\ell m}^*(n_i) \quad (4.2.208)$$

where the n_i are positions on the sky drawn from a distribution proportional to the galaxy density field itself,

$$n_i \sim p(n) = 1 + \delta\rho(n) = \rho(n)/\bar{\rho} \quad (4.2.209)$$

The shot noise of the $a_{\ell m}$ observation is simply the variance of this monte carlo integral, which itself is estimating the random coefficient. The total variance of the observed galaxy distribution is then

$$\langle |\hat{a}_{\ell m}|^2 \rangle = \left(\frac{4\pi}{N} \right)^2 \sum_{n_i, n_j} \langle Y_{\ell m}^*(n_i) Y_{\ell m}(n_j) \rangle_p = N^{-2} \sum_{ij} (\langle |a_{\ell m}|^2 \rangle + \delta_{ij}(4\pi)) = C_\ell + 4\pi/N \quad (4.2.210)$$

where the subscript p denotes the expectation value under the distribution $p(n)$. The expectation values here furthermore are taken over both the random sampling of the $a_{\ell m}$ and the random sampling of galaxies over the resulting density field. The important factor is the simple $4\pi/N$ shot noise – as we know it from the Poisson distribution. This is simply the number of galaxies per steradian in the sky. In the case of two different redshift bins, the expectation value does *not* get biased from the shot noise. We may write this as

$$\langle \hat{a}_{\ell m}^i \hat{a}_{\ell m}^j \rangle = C_\ell^{ij} + \delta_{ij} 4\pi/N_i \quad (4.2.211)$$

The variance of the $a_{\ell m}$ first of all biases the naive estimator of C_ℓ for coincidental redshift bins. This however, is salvageable, since we know what the extra variance should be, and may simply subtract it when computing the estimate of C_ℓ , ie. we construct a new estimator

$$\hat{C}_\ell = \left((2\ell + 1)^{-1} \sum_m |a_{\ell m}|^2 \right) - 4\pi/N \quad (4.2.212)$$

It furthermore increases the variance of the spectra. We may, as we calculated it for the CMB, calculate the expected variance for our C_ℓ estimate, including both cosmic variance and shot noise

$$\text{Var}(\hat{C}_\ell) = \frac{2}{2\ell + 1} (C_\ell + 4\pi/N)^2 \quad (4.2.213)$$

While it is possible for this estimator to be negative, the physical power spectrum is of course always positive.

For different redshift bins this changes to a covariance. The structure is only slightly more complicated,

$$\begin{aligned} \text{Cov}(\hat{C}_\ell^{ij}, \hat{C}_\ell^{km}) &= (2\ell + 1)^{-1} \left((C_\ell^{ik} + \delta_{ik}4\pi/N_i)(C_\ell^{jm} + \delta_{jm}4\pi/N_j) \right. \\ &\quad \left. + (C_\ell^{im} + \delta_{im}4\pi/N_i)(C_\ell^{jk} + \delta_{jk}4\pi/N_j) \right) \end{aligned} \quad (4.2.214)$$

The Kronecker deltas here make sure that the extra variance only appears if two of the bins coincide. Note this means the variance of the power spectrum in different redshift bins is

$$\text{Var}(C_\ell^{ij}) = (2\ell + 1)^{-1} \left((C_\ell^{ii} + 4\pi/N_i)(C_\ell^{jj} + 4\pi/N_j) + (C_\ell^{ij})^2 \right). \quad (4.2.215)$$

That means the power spectrum across bins has cosmic variance determined by same- z power spectra.

We now need equivalent results for the bispectrum. In the case of no shot noise in a gaussian universe, the estimator and its variance are given by equations (4.1.11) and (4.1.12). With shot noise included, this expression changes to

$$\begin{aligned} \langle \hat{a}_{\ell_1 m_1} \hat{a}_{\ell_2 m_2} \hat{a}_{\ell_3 m_3} \rangle_p &= \left(\frac{4\pi}{N} \right)^3 \sum_{n_i, n_j, n_k} \langle Y_{\ell_1 m_1}^*(n_i) Y_{\ell_2 m_2}^*(n_j) Y_{\ell_3 m_3}^*(n_k) \rangle_p \\ &= N^{-3} \sum_{ijk} \langle a_{\ell_1 m_1} a_{\ell_2 m_2} a_{\ell_3 m_3} \rangle + (4\pi)^2 \delta_{ij} \delta_{jk} \mathcal{G}_{\ell_1 \ell_2 \ell_3}^{m_1 m_2 m_3} \\ &= \mathcal{G}_{\ell_1 \ell_2 \ell_3}^{m_1 m_2 m_3} \left(b_{\ell_1 \ell_2 \ell_3} + (4\pi/N)^2 \right) \end{aligned} \quad (4.2.216)$$

Evidently this estimator is biased as well, but again by a simple constant, which we may subtract. The variance, we may write by simply changing $C_\ell \rightarrow C_\ell + 4\pi/N$ like for the new shot noise limited C_ℓ estimator,

$$\text{Var}(B_{\ell_1 \ell_2 \ell_3}^{ijk}) \approx h_{\ell_1 \ell_2 \ell_3}^2 \left(C_{\ell_1}^{ii} + \frac{4\pi}{N_i} \right) \left(C_{\ell_2}^{jj} + \frac{4\pi}{N_j} \right) \left(C_{\ell_3}^{kk} + \frac{4\pi}{N_k} \right) \cdot [\ell_i = \ell_j] \quad (4.2.217)$$

where the superscript i, j, k denote the redshift bin. Note that this also goes on the number of galaxies N , which may well change between bins. Remember we had a factor $g_{\ell_1 \ell_2 \ell_3}$ in this expression in the case of CMB. I tentatively put a bracket here in its place. For the galaxy correlations, we have the extra dimension in the problem, the redshift. The C_{ℓ_i} above are all evaluated at their respective z_i . However, if two ℓ_i are equal, then we get expressions like $(C_{\ell_1}^{ij})^2 C_{\ell_3}^{kk}$ for $\ell_1 = \ell_2$. It is important here that the variance of the bispectrum ends up depending on the same- z power spectrum. As we have already seen in figures 7 and 9, the same- z δ, v' correlators completely dominate this signal. For bispectra at three different z this means the signal, which is now lowered due to the difference in z , is polluted by noise from the enormous same- z power spectrum. On the other hand, this may be a good sign for lensing surveys. Since for the small lensing contributions, the same- z power spectrum is usually very small, the cosmic variance of only lensing to a bispectrum with very different z could be relatively small.

The end result of our shot noise calculation is a guidance of how wide to pick our redshift-bins. We see that the important quantity to look at is simply $4\pi NC_\ell$. We want to keep this number well above one. That means the shot noise will be dominated by the physics, for both power spectrum and bispectrum. So in the next section when we will do the actual computations, we have to keep in mind that our redshift bins must be wide enough to accomodate enough galaxies. Another problem here is of course the precision with which the redshift is determined. For spectroscopic redshift determinations this is no problem, as it is rather well determined. For photometric surveys however, the redshift uncertainty must be reflected in the binning procedure. The *Dark Energy Survey*, which is currently under way, as an example aims at collecting photometric redshifts of some 300 million galaxies in a ≈ 5000 square degree footprint, (Abbott et al., 2016b). Whatever the number of galaxies are found like this, the redshift uncertainty is around 0.1 (Asorey et al., 2016). *Euclid* aims at having spectroscopic redshift of some 65 million galaxies on a ≈ 15000 square degree footprint between redshifts 0.7 and 2, (Majerotto et al., 2012). These numbers are for us only guiding, and the exact number will not be crucial.

4.2.13 Next-to-leading order corrections

I now briefly discuss the effect of higher order perturbations on the correlation function and the power spectrum, i.e. the C_ℓ s. This part follows Nielsen and Durrer (2017). The 1-loop correction to the correlation function is

$$\begin{aligned}\zeta^{(2)}(\mathbf{n} \cdot \mathbf{n}', z, z') &= \langle \Sigma^{(2)}(\mathbf{n}, z) \Sigma^{(2)}(\mathbf{n}', z') \rangle - \langle \Sigma^{(2)}(\mathbf{n}, z) \rangle \langle \Sigma^{(2)}(\mathbf{n}', z') \rangle \\ &+ \langle \Sigma^{(1)}(\mathbf{n}, z) \Sigma^{(3)}(\mathbf{n}', z') \rangle + \langle \Sigma^{(3)}(\mathbf{n}, z) \Sigma^{(1)}(\mathbf{n}', z') \rangle \\ &\equiv \frac{1}{4\pi} \sum_{\ell} (2\ell + 1) C_\ell^{(2)}(z, z') P_\ell(\mathbf{n} \cdot \mathbf{n}')\end{aligned}\quad (4.2.218)$$

Here we just derive the formal expressions for the simplest terms in the 1-loop power spectrum in ℓ -space. First we show how second order quantities from squared first order terms contribute. Denoting the different first order terms by $\Delta^A, \Delta^B, \Delta^C, \Delta^D$ (eg. $\delta^{(1)}, \partial_r^2 v^{(1)}$ etc.), we consider the following second order contributions (which is *not* completely general),

$$\Delta^{AB}(\mathbf{n}, z) \equiv (\Delta^A \cdot \Delta^B)(\mathbf{n}, z). \quad (4.2.219)$$

The contribution from such product terms to the 1-loop correlation function is

$$\begin{aligned}\zeta^{AB|CD}(\mathbf{n} \cdot \mathbf{n}', z, z') &\equiv \langle \Delta^{AB}(\mathbf{n}, z) \Delta^{CD}(\mathbf{n}', z') \rangle - \langle \Delta^{AB}(\mathbf{n}, z) \rangle \langle \Delta^{CD}(\mathbf{n}', z') \rangle \\ &= \langle \Delta^A(\mathbf{n}, z) \Delta^C(\mathbf{n}', z') \rangle \langle \Delta^B(\mathbf{n}, z) \Delta^D(\mathbf{n}', z') \rangle + \langle \Delta^A(\mathbf{n}, z) \Delta^D(\mathbf{n}', z') \rangle \langle \Delta^B(\mathbf{n}, z) \Delta^C(\mathbf{n}', z') \rangle \\ &= \zeta^{AC}(\mathbf{n} \cdot \mathbf{n}', z, z') \zeta^{BD}(\mathbf{n} \cdot \mathbf{n}', z, z') + \zeta^{AD}(\mathbf{n} \cdot \mathbf{n}', z, z') \zeta^{BC}(\mathbf{n} \cdot \mathbf{n}', z, z').\end{aligned}\quad (4.2.220)$$

These are simply products of first order correlation functions of the factors. We can use this to compute the corresponding contribution to the power spectrum. We first write out the first order correlation functions in terms of the $C_\ell(z, z')$,

$$\begin{aligned}\tilde{\xi}^{AB} &= \frac{1}{4\pi} \sum_{\ell} (2\ell + 1) C_\ell^{AB}(z, z') P_\ell(\mathbf{n} \cdot \mathbf{n}') \Rightarrow \\ \tilde{\xi}^{AB|CD}(\mathbf{n} \cdot \mathbf{n}', z, z') &= \frac{1}{(4\pi)^2} \sum_{\ell, \ell'} (2\ell + 1)(2\ell' + 1) \\ &\times [C_\ell^{AC}(z, z') C_{\ell'}^{BD}(z, z') + C_\ell^{AD}(z, z') C_{\ell'}^{BC}(z, z')] P_\ell(\mathbf{n} \cdot \mathbf{n}') P_{\ell'}(\mathbf{n} \cdot \mathbf{n}'),\end{aligned}\quad (4.2.221)$$

where P_ℓ denotes the Legendre polynomial of order ℓ . We would now like this in the form of equation (4.2.218). To do this, we use the following expansion of products of Legendre polynomials,

$$P_\ell(x) P_{\ell'}(x) = \sum_{L=|\ell-\ell'|}^{\ell+\ell'} \begin{pmatrix} \ell & \ell' & L \\ 0 & 0 & 0 \end{pmatrix}^2 (2L+1) P_L(x), \quad (4.2.222)$$

which is a special case of the expansion of a product of spherical harmonics. The squared Wigner 3j symbols are given by equations (2.3.6) and (2.3.7). This means the contribution from these terms to the 1-loop power spectrum is

$$\begin{aligned}C_\ell^{AB|CD}(z, z') &= \sum_{\ell_1 \ell_2} \frac{(2\ell_1 + 1)(2\ell_2 + 1)}{4\pi} \begin{pmatrix} \ell & \ell_1 & \ell_2 \\ 0 & 0 & 0 \end{pmatrix}^2 \\ &\times \left(C_{\ell_1}^{AC}(z, z') C_{\ell_2}^{BD}(z, z') + C_{\ell_1}^{AD}(z, z') C_{\ell_2}^{BC}(z, z') \right).\end{aligned}\quad (4.2.223)$$

Pure product contributions from third order are structurally even simpler. We set $\Delta^{ABD} = \Delta^A \Delta^B \Delta^C$. Since three of the four factors are evaluated at the same position and redshift, we get

$$\begin{aligned}\tilde{\xi}^{ABC|D}(\mathbf{n} \cdot \mathbf{n}', z, z') &\equiv \langle \Delta^{ABC}(\mathbf{n}, z) \Delta^D(\mathbf{n}', z') \rangle \\ &= \tilde{\xi}^{BC}(1, z, z) \tilde{\xi}^{AD}(\mathbf{n} \cdot \mathbf{n}', z, z') \\ &+ \tilde{\xi}^{AC}(1, z, z) \tilde{\xi}^{BD}(\mathbf{n} \cdot \mathbf{n}', z, z') \\ &+ \tilde{\xi}^{AB}(1, z, z) \tilde{\xi}^{CD}(\mathbf{n} \cdot \mathbf{n}', z, z'),\end{aligned}\quad (4.2.224)$$

where half of the functions are evaluated at $\mathbf{n} \cdot \mathbf{n} = 1$. Since $P_\ell(1) = 1$, these are simply given by

$$\tilde{\xi}^{AB}(1, z, z) = \frac{1}{4\pi} \sum_{\ell} (2\ell + 1) C_\ell^{AB}(z), \quad (4.2.225)$$

and we can write this contribution to the 1-loop power spectrum as

$$\begin{aligned}C_\ell^{ABC|D}(z, z') &= \frac{1}{4\pi} \sum_{\ell'} (2\ell' + 1) \\ &\times \left\{ C_{\ell'}^{BC}(z) C_\ell^{AD}(z, z') + C_{\ell'}^{AC}(z) C_\ell^{BD}(z, z') + C_{\ell'}^{AB}(z) C_\ell^{CD}(z, z') \right\}.\end{aligned}\quad (4.2.226)$$

One may also wonder about the next order contributions to the bispectrum. These terms will now involve 6, instead of 4, factors of the primordial perturbations. While their observation, even full calculation, is doubtful, it is interesting to see at least schematically, their effect. These corrections also come in two forms: one with three second order contributions and another with a first, a second and a third order contribution.

For the three second-orders contribution, we may write the correlator simply as

$$\zeta^{AB|CD|EF} = \langle \Delta^{AB}(\mathbf{n}, z) \Delta^{CD}(\mathbf{n}', z') \Delta^{EF}(\mathbf{n}'', z'') \rangle_c \quad (4.2.227)$$

from which one of the many terms – which behave alike – is the contraction $(AD)(BE)(CF)$, whose contribution is

$$\zeta^{AD}(\mathbf{n} \cdot \mathbf{n}') \zeta^{BE}(\mathbf{n} \cdot \mathbf{n}'') \zeta^{CF}(\mathbf{n}' \cdot \mathbf{n}'') \quad (4.2.228)$$

Now using equation (2.2.9) and the following equations to compute the bispectrum – note how this correlator exactly factorizes as is necessary – we see that

$$C_{\ell_1 \ell_2 \ell_3} = \frac{1}{(2\pi)^3} C_{\ell_1}^{AD} C_{\ell_2}^{BE} C_{\ell_3}^{CF} \quad (4.2.229)$$

with the bispectrum given by equation (2.2.16). This term is illustrated in the first picture of figure 12. For the correction from third order, we define

$$\zeta^{ABC|DE|F} = \langle \Delta^{ABC}(\mathbf{n}, z) \Delta^{DE}(\mathbf{n}', z') \Delta^F(\mathbf{n}'', z'') \rangle_c \quad (4.2.230)$$

The terms in this correlator come in two forms, one has the third order contribution interact with itself, illustrated in the middle of figure 12, and for the other, it does not, as illustrated in the last picture of figure 12. Examples of the terms of the resulting three-point correlators are therefore

$$\begin{aligned} \zeta^{ABC|DE|F} \supset & \zeta^{AB}(1, z, z) \zeta^{CD}(\mathbf{n} \cdot \mathbf{n}', z, z') \zeta^{EF}(\mathbf{n}' \cdot \mathbf{n}'', z', z'') \\ & + \zeta^{AD}(\mathbf{n} \cdot \mathbf{n}', z, z') \zeta^{BE}(\mathbf{n} \cdot \mathbf{n}'', z, z') \zeta^{CF}(\mathbf{n} \cdot \mathbf{n}'', z, z'') \end{aligned} \quad (4.2.231)$$

The first line here resembles the last correction we calculated for the power spectrum. Calculating the $C_{\ell \ell' \ell''}$ of equation (2.2.10) this first term gives the following correction,

$$C_{\ell \ell' \ell''} \supset \frac{\delta_{\ell 0}}{(2\pi)^3} C_{\ell'}^{CD}(z, z') C_{\ell''}^{EF}(z', z'') \sum_{\ell_s} (2\ell_s + 1) C_{\ell_s}^{AB}(z) \quad (4.2.232)$$

The last correction resembles the first correction to the power spectrum. We again have two correlators with the same argument, $\mathbf{n} \cdot \mathbf{n}'$, which we combine to one, like in equation (4.2.223). With this expression for $C_{\ell}^{AB|CD}$ we can again calculate the coefficient of equation (2.2.10), which is

$$C_{\ell \ell' \ell''} \supset \frac{\delta_{\ell 0}}{2\pi^2} C_{\ell'}^{AD|BE}(z, z') C_{\ell''}^{CF}(z, z'') \quad (4.2.233)$$

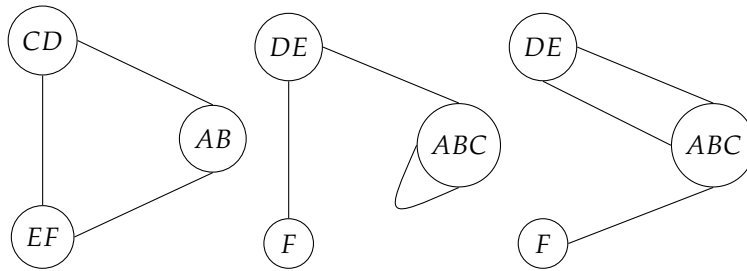


Figure 12: Illustration of the three higher order corrections to the bispectrum. Each picture stands for many different terms, which share the calculational details, but with the indices interchanged.

Note this is a very condensed version of the corrections. I have not included all permutations, by a long shot. Furthermore, the Kronecker deltas forcing one of the multipoles to be zero in the $C_{\ell\ell'\ell''}$ do *not* mean the multipoles are zero in the bispectrum. Remember from equation (2.2.16) that the reduced bispectrum is given by a large sum over the multipoles of the coefficients.

Of course these corrections to the power spectrum and bispectrum are mainly relevant in the weakly non-linear regime and perturbation theory is not expected to converge in the fully non-linear regime. Nevertheless, perturbation theory remains computationally much less heavy than N-body simulation and it is therefore interesting to translate the many promising results obtained in Fourier space [Pajer and Zaldarriaga \(2013\)](#); [Senatore and Zaldarriaga \(2014\)](#) into the more directly observable ℓ -space.

We now have all the calculations ready. Bispectra and power spectra are quickly computed due to the flat sky approximations we have developed. In the following chapter I do the actual computations of these numbers, which will hopefully give us a hint as to the nature of the perturbations we may hope to observe.

A THEORETICIAN'S EXPERIMENT

So far we have been setting the stage. Obviously I think it is an important stage to set – it is the main part of this work! – nonetheless there has been no attempt at numbers and real-world observations yet. We have models describing the universe from start to end, and we have the necessary statistical tools to analyse the potential observations. It is now my intention to briefly investigate a particular model of inflation. My main take-aways from the model are the primordial power spectrum and bispectrum. These will turn into observables in the CMB and the galaxy distributions.

The experiment I propose is as follows. We make the minimal change to the power spectrum we must, in order to make the CMB observations match the predictions of a universe, with only matter and radiation – no dark energy. While this model may be considered ruled out by other observations, it will be our starting point. The exercise will be to see what the CMB tells us, and what we tell ourselves, and whether higher order observables will help us. I will in a similar vein look at the bispectrum of the LSS and see if observations here will bring more information. The two analyses will be very similar. The decomposition into spherical harmonics of both CMB and LSS means we will use identical statistical tools to judge the two. The LSS naturally has the advantage of *depth* – there is only one CMB sky, while there are *many* LSS skies – or rather, redshift bins.

A similar analysis has been done by [Di Dio et al. \(2017\)](#), who calculate the contamination from the general relativistic correction on a series of simple bispectra. They look at large scales, and therefore include other terms than I do here. They take not the dominating terms, but look at the subdominating terms, which become important at larger scales. The last section can be seen as a continuation of this work, with some technical differences. I keep strictly to the dominating terms, and keep to higher multipoles, ie. smaller scales. This reduces the number of terms, but increases the number of multipoles to compute, both for power- and bispectrum. I circumvent this difficulty by using the flat sky expressions for both computations. This allows me to further extend the work by considering not just single redshifts, but to integrate over redshifts to get a more realistic picture of the spectra. Recall that we must perform some redshift binning in order to drive down the shot noise, and due to simple uncertainty in the redshift.

I will first assume a generic model of inflation, described by [Achúcarro et al. \(2011a,b\)](#); [Achúcarro et al. \(2013\)](#) and their related work. The idea is an *effective field theory*

By simple I think of separable primordial bispectra. These can be obtained from very generic, simple inflationary models, and simplify the following calculations.

of inflation. What was briefly described in chapter 3 was inflation with a single inflaton field. The eager theorist may, however, dream of more fields in the very early universe. Some of these fields surely will be heavier than the others. In the simplest case, all except one degree of freedom will be very heavy. That allows one to *integrate out* the heavy fields, in exchange for operators suppressed by the ratio of mass scales. That leaves us with the *effective* theory of just the one light field – an effective field theory. Such a theory can for example accommodate features in the power spectrum quite nicely. I will explore in the CMB and LSS with direct observations what we should and should *not* expect to observe.

Finally I also hope to more directly extend the work of [Di Dio et al. \(2017\)](#) and look for the GR pollution in higher multipoles of the usual, more manageable bispectra from very simple theories of inflation. This explores how much especially the lensing effects are expected to bias our attempts of finding primordial non-gaussianities.

5.1 THE MODEL

The *model* here refers to the model of inflation. For computations of transfer functions etc. we will stay within the comforting confines of perturbative FRW – for the time being, not quite Λ CDM, but rather a model with both hot and cold dark matter and a very low Hubble constant, dubbed HCDM. We will change the model of inflation, which changes the primordial statistics – the power spectrum and bispectrum. Changing these spectra will naturally change the observed CMB spectra. However, these depend also on the content of the universe – radiation, matter and cosmological constant – and so we can in a sense *undo* the change of the power spectrum by changing the intervening conditions. I am here going to explore the observable differences between Λ CDM with a featureless power spectrum and HCDM with a featureful power spectrum – and hence a bispectrum.

[Hunt and Sarkar \(2007\)](#) did an analysis of, amongst other things, the *WMAP* data ([Spergel et al., 2003](#)), showing that one can have excellent agreement with CMB data with a very different model than the current concordance Λ CDM parameters. The change was adding hot dark matter and a primordial power spectrum with a ‘bump’. The model we employ will follow the same spirit. We add hot dark matter and alter the power spectrum in order to get agreement with the CMB power spectrum. I then continue to see if, in the effective theory of inflation, this power spectrum will induce an observable bispectrum. The exact parameters of hot and cold dark matter densities and other cosmological parameters will not be of great importance. The main test I will do is to see if the changes in the power spectrum – which are *not* subtle – will induce remarkable changes in the bispectrum.

The important parameters are

$$h = 0.44, \omega_b = 0.018, \\ \omega_{\text{CDM}} = 0.16, \omega_v = 0.017.$$

For the galaxy counts however, we *know* there will be a bispectrum, no matter what primordial spectrum we put in. We shall see to which degree the bispectrum coming solely from relativistic non-linear effects will contaminate the signal we are looking for. This will guide us to determine how well we need to know and compute the relativistic effects in order to be able to observe the expected signal from primordial spectra. We must obviously remove the contaminating signal with *at least* the precision to which we wish to measure the primordial signal.

We will investigate the observability of the bispectrum of primordial perturbations as calculated in an effective field theory of inflation. Following [Achúcarro et al. \(2013\)](#), the model of inflation will generate features in the primordial spectra as a consequence of a changing speed of sound – the speed of the adiabatic fluctuations. Any small feature in the power spectrum is interpreted as the inflaton slowly rolling through a ‘wiggly’ potential. Keeping the notation from their work, we call the unperturbed power spectrum $\mathcal{P}_{\mathcal{R}}$ and the change to it $\Delta\mathcal{P}_{\mathcal{R}}$. The prediction for the change in the bispectrum is then

$$\Delta B_{\mathcal{R}}(k_1, k_2, k_3) = \frac{(2\pi)^4 \mathcal{P}_{\mathcal{R}}^2}{(k_1 k_2 k_3)^2} \times \quad (5.1.1)$$

$$\left\{ -\frac{3}{2} \frac{k_1 k_2}{k_3} \left[\frac{1}{2k} \left(1 + \frac{k_3}{2k} \right) \frac{\Delta\mathcal{P}_{\mathcal{R}}}{\mathcal{P}_{\mathcal{R}}}(k) - \frac{k_3}{4k^2} \frac{d}{d \log k} \left(\frac{\Delta\mathcal{P}_{\mathcal{R}}}{\mathcal{P}_{\mathcal{R}}} \right) \right] + 2 \text{ perm} \right.$$

$$+ \frac{1}{4} \frac{k_1^2 + k_2^2 + k_3^2}{k_1 k_2 k_3} \left[\frac{1}{2k} \left(4k^2 - k_1 k_2 - k_2 k_3 - k_3 k_1 - \frac{k_1 k_2 k_3}{2k} \right) \frac{\Delta\mathcal{P}_{\mathcal{R}}}{\mathcal{P}_{\mathcal{R}}}(k) \right.$$

$$\left. \left. - \frac{k_1 k_2 + k_2 k_3 + k_3 k_1}{2k} \frac{d}{d \log k} \left(\frac{\Delta\mathcal{P}_{\mathcal{R}}}{\mathcal{P}_{\mathcal{R}}} \right) + \frac{k_1 k_2 k_3}{4k^2} \frac{d^2}{d \log k^2} \left(\frac{\Delta\mathcal{P}_{\mathcal{R}}}{\mathcal{P}_{\mathcal{R}}} \right) \right] \right\} \Big|_{k=(k_1+k_2+k_3)/2}$$

While this long expression is slightly menacing, one feature sticks out. The changes of the power spectrum at wavenumber k carry over directly to features in the bispectrum at $\frac{k_1+k_2+k_3}{2} = k$. It is this feature we will need to see. It is not only enough that there is a bispectrum – if we are to discern the different predictions, we must not just observe them, but observe their individual features. The power spectrum we use is shown in figure 13 along with the bispectrum in various configurations.

5.2 COMPUTATIONAL OBSERVATIONS

We now go directly to the in observations of bispectra. All computations are performed in *Python*, using transfer functions computed using either `CAMB` or `CLASS`. The transfer functions have been subjected to the calculations of chapter 4 in order to compute the power spectra and bispectra in the CMB and the LSS. All computations are done on a local machine. All integrals over k and r for both power spectra and bispectra have been done using the simple *Simpson’s rule*, with manually adapted grids. The flat-sky expressions have in general very simple integrands, and as such there is no need for eg. monte carlo integrators.

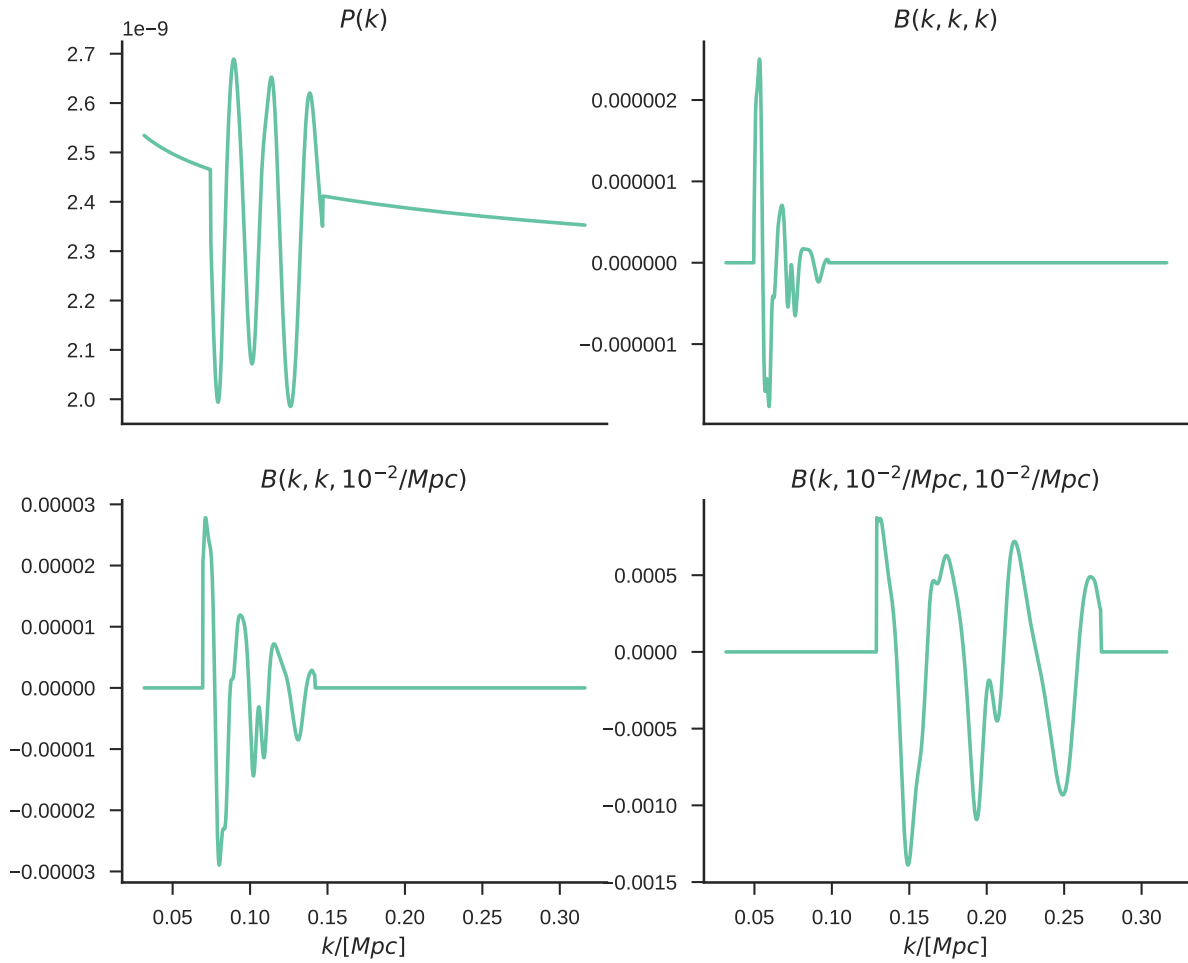


Figure 13: Plots of the power spectrum with large, but localised oscillations around $0.1/Mpc$. This induces the bispectrum shown in three different configurations in the three plots, as described above each one. We see here exactly how the oscillations in the power spectrum translate to features in the bispectrum at $\sum k_i = k/2$. All x-axes are shared, while all y-axes are individual.

We will explore the observable quantities of a bispectrum coming from reasonable, but still rather large changes in the power spectrum. The power spectrum we use is a very simple one. It has a couple of oscillations around $0.1/Mpc$ to help the gas physics make the acoustic peaks we see in the CMB. Without these oscillations, the model alone would not quite fit the Planck data. The first peak is here not taken into account when changing the power spectrum.

The missing first peak combined with the flat sky approximation means when checking the bispectrum, I do not include the very low multipoles. I will however include as many multipoles upwards as computationally feasible. For the bispectrum I work with, I found that reasonable accuracy is obtained when calculating every 30th multipole from $\ell = 300$ to 1200, and doing a 3rd degree three dimensional spline between these points to *all* relevant multipoles in between. Increasing the frequency to every 10th multipole hardly changes the result. The range is chosen to include as much of the input primordial bispectrum while respecting the missing first peak. Including all multipole triplets in the allowed region (there are 51,952,750 of them), I find that the signal to noise, as defined by equation (4.1.17) is $S/N \approx 1/26$. This number is, unfortunately, fantastically small – I remind that I do not even consider foregrounds, which are by far the greatest threat to any bispectrum observation in the CMB. Including lower multipoles naturally raises this number. Going down to $\ell = 100$ and for a moment ignoring the missing first acoustic peak, gives $S/N \approx 1/20$ for a total of 69,552,850 multipole triplets observed. I reiterate that observing a bispectrum is much different from discriminating between two. The check I do here is to see if one might hope to see a particular bispectrum with large oscillations, I am *not* checking whether *any* bispectrum at all will be visible.

Figure 14 shows the angular power spectrum in the relevant range and the bispectrum in various configurations.

As the discriminatory power of the CMB temperature is lacking, one might instead hope to be able to observe the signal in galaxy surveys which have an extra dimension, and as such offer more *modes* to observe. Polarization in the CMB also helps, but I will not investigate that.

As we have seen these extra modes are for some experiments obscured by poor redshift determination. Assuming in any case very sharp spectroscopic redshift observations, we may hope to observe many thin redshift bins. It should still be clear though, that most direct galaxy-galaxy correlation will be seen in same- z bins, as discussed in section 4.2.12. One might be able to leverage lensing effects alone, which would make observations across redshift more feasible. For such an observation, only the lensing contributions in the cosmic variance will come into play and so the small lensing bispectrum would stand out more clearly. This means again we have to be strict when splitting up the higher order terms to determine exactly which

The relevant multipoles are the ones allowed by the triangle inequalities of the Gaunt integral, the symmetry constraints, and the resolution of our experiment, both upwards and downwards.

Lower multipoles in this regard will usually carry a larger signal. However, the features from the power spectrum will only show at higher multipoles, and so even if there is a potential signal at low multipoles, it will not help us extract the features of the bispectrum.

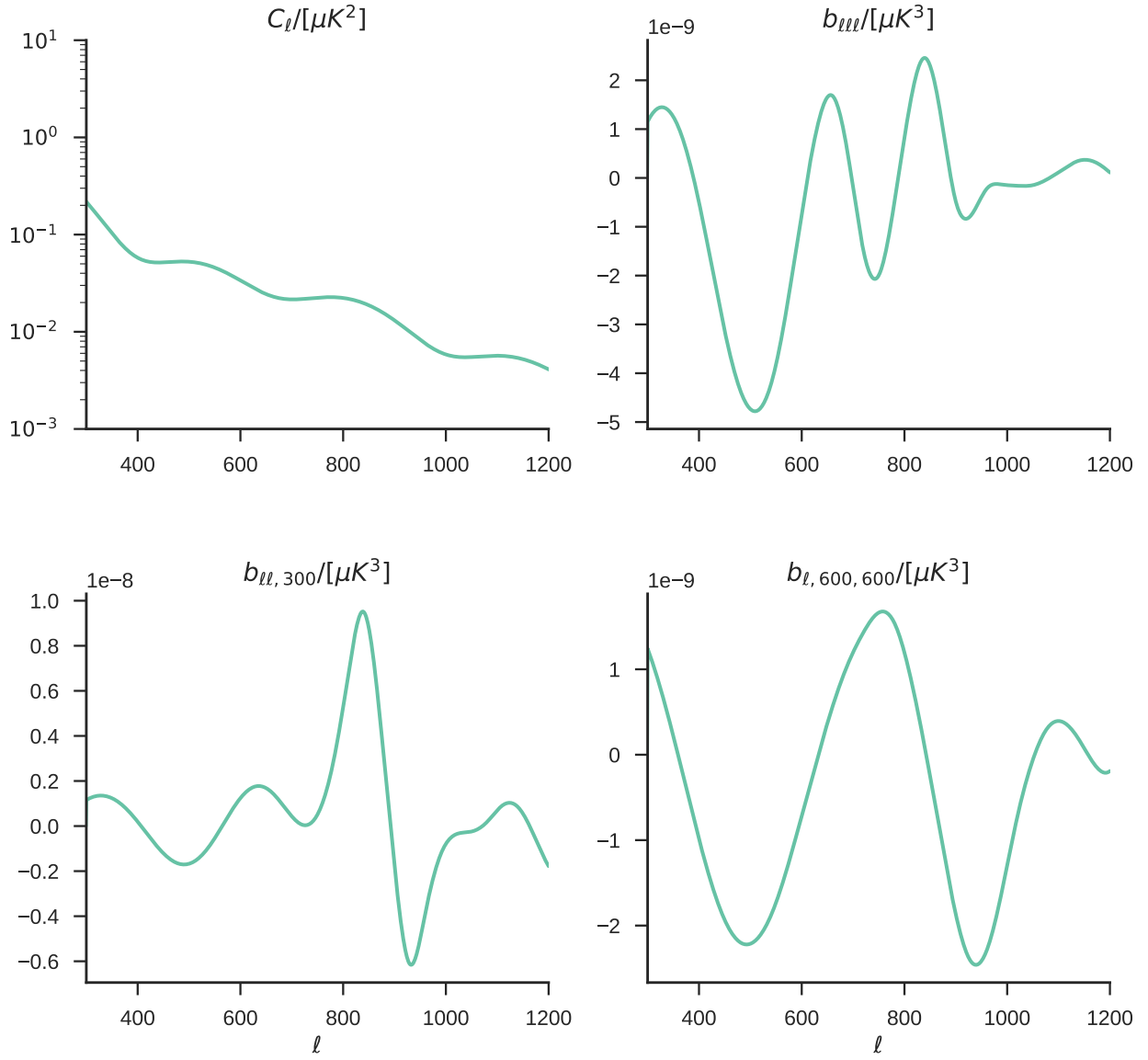


Figure 14: Plots of the CMB angular power spectrum and bispectrum in the EFT description, with the power spectrum from figure 13. The bispectrum is shown in various configurations, as described above the respective plots.

ones affect lensing and which ones do not – luckily, with the all-order calculation, this distinction is trivial.

Let us do the same comparison in the LSS as we just did for CMB. This will simply be computing the bispectrum predicted by the EFT and comparing it with the cosmic variance. Doing the redshift binning here is really what ramps up the computation time – *for every bin* we have to perform a triple integral over the redshifts. I do the redshift bins as simple top-hats, and the integrals over redshifts simply as the sum of many small top-hat sub-bins. Furthermore, we must do this for every redshift bin we have. For just the auto-correlations this is doable, but if we hope to see correlations across bins as well, that increases computing time dramatically.

Let us simply compute the expected signal to noise in small bins and estimate what we might hope to see. The signal to noise computed in a single bin of width 0.01 at redshift 1, with multipoles between 30 and 500 is

$$S/N(z = 1) \approx 1/16 \qquad S/N \underset{\text{not binned}}{(z = 1)} \approx 1/72 \qquad (5.2.1)$$

It is clear that binning help enormously to lower the cosmic variance. The numbers also tell us that we must use what the full 3d universe gives us, not just a single bin. Very roughly, the auto-correlation of 16 bins would seem to be sufficient to give a 1σ result. Using cross-correlations as well may help, but I remind that the cosmic variance on bispectra in different bins is relatively larger according to the result of equation (4.2.217). The dependence of these numbers on the redshift is very small, and is depicted in figure 15.

While this study is not quite representative of current experiments, it is at least heart-warming to see that the predicted bispectrum from the EFT is in principle observable. There is a long way from the observation of *something*, ie. seeing $f_{NL} \neq 0$ for a particular template, to saying one template fits better than another. In other words, even if one sees non-gaussianities in the LSS, it is hard to know exactly what the underlying bispectrum is. Given the infinite possibilities of the EFT of inflation only makes matters worse. Studies searching for features in the power spectrum, as done eg. by [Hunt and Sarkar \(2015\)](#), already show a large scatter in the possible reconstructed power spectra. It is not clear that the constraints from bispectrum observations will be enough to constrain such an arbitrary parametrisation, and it is very clear that the computational time needed will be *very* limiting. Although experimental systematics and non-linear physics are still in play and must be under control, LSS looks to be a valuable resource if the full potential of the 3d distribution can be harnessed.

The shape of the bin, when it is as small as this, does not matter much. The major defining factor of the bins is their width. However, I remind that the variance of a top-hat bin with full width w is $\sigma^2 = w^2/12$. Therefore, this tophat bin corresponds roughly to a gaussian with width $\sigma = w/\sqrt{12}$, not just w .

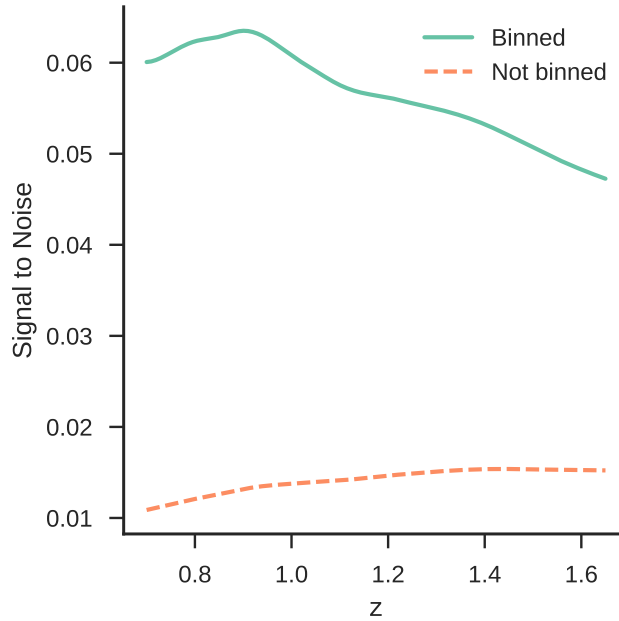


Figure 15: Redshift dependence on the signal-to-noise of the galaxy number count bispectrum in the HCDM model. For bins of width $\Delta z = 0.01$ this quantity is brought up by about a factor 6.

5.3 GENERAL RELATIVISTIC POLLUTION OF SIMPLE GALAXY BISPECTRA

I finish by calculating the pollution from *all* dominating lensing effects into the more usual templates of non-gaussianity on a standard Λ CDM background, with *Planck* best-fit parameters (Ade et al., 2016). I focus here on the *local* template, which is the primordial bispectrum given by

$$B_{\text{local}}(k_1, k_2, k_3) = \frac{6f_{NL}}{5} [P(k_1)P(k_2) + P(k_1)P(k_3) + P(k_2)P(k_3)] \quad (5.3.1)$$

This shape of bispectrum comes from non-gaussianity that only acts *locally*, in the following sense,

$$\Phi_{\text{local}}(\mathbf{x}) = \Phi_G(\mathbf{x}) + \frac{3}{5}f_{NL}(\Phi_G(\mathbf{x})^2 - \langle \Phi_G^2 \rangle) \quad (5.3.2)$$

where the prefactor is historical and the mean of the squared gaussian field Φ_G is subtracted to keep $\langle \Phi \rangle = \langle \Phi_G \rangle = 0$. The primordial power spectrum is in this case taken to be featureless and *almost* scale-invariant as is usually assumed for Λ CDM.

The reason this simple bispectrum is interesting is the chance to observe the f_{NL} and circumventing the cosmic variance of the spectra – as we just saw, the direct observation is very difficult. If one is not directly interested in the power spectrum,

but rather a constant in front, to put it roughly, then the cosmic variance can be circumvented by comparing two different *tracers* of the underlying field, as proposed by McDonald and Seljak (2009). However to extract eg. f_{NL} , the method relies on the assumption that the particular template one uses is a good representation of the primordial non-gaussianity. Dalal et al. (2008) calculate a scale-dependent bias of matter as a function of f_{NL} for local non-gaussianity in k -space, which is

$$\Delta b_{NL} \propto \frac{f_{NL}(b-1)}{k^2} \quad (5.3.3)$$

It is clear that for different populations of tracers, with different biases b , this number will be different, and one may subject it to the multi-tracer technique to extract f_{NL} . However, simply observing a scale-dependent bias is far from observing primordial non-gaussianities. As we have seen, relativistic and non-linear effects *will* systematically bias the spectra, and we must compute the bias of the local f_{NL} before making claims about observations of anything more. Using these techniques it is not possible to observe directly the bispectrum ie. the exact shape and features of it.

This analysis is similar to what is done in Di Dio et al. (2017). I here explore how redshift binning affects the result. It is naturally expected to reduce the power in both signal and noise, and I aim to see which of the two shrinks most quickly. I furthermore include additional lensing terms, in particular the corrections coming from first order lensing correlated with second order density contributions. I do *not* include the subdominant terms. Since we are only showing the effects of lensing, I exclude, as they do, terms which contain only density-like terms. The terms included here are both the second order lensing terms they include, *and* first order lensing terms correlated with second order density terms.

For very thin top-hat bins of width 0.01, the resulting GR pollution of the primordial, local bispectrum, according to equation (4.2.204) is

$$\text{bias}(f_{NL})(z=1) \approx -1.96 \quad \text{bias}(f_{NL})(z=1) \approx -3.28 \quad (5.3.4)$$

not binned

I calculate this number for the redshift range from 0.7 to 1.65, which is plotted in figure 16. These numbers are computed using multipoles between 30 and 500. It is not clear *a priori* whether these numbers will go up or down when properly including galaxy-biasing. Since the largest results generally are cross-correlations between density and lensing, the GR terms of the form $\langle \delta\delta\delta\kappa \rangle$ will naïvely receive the same bias-enhancement as the density contribution to the primordial bispectrum $\langle \delta\delta\delta \rangle$.

Figure 17 shows the shape of the GR and primordial bispectra in various multipole configurations. A clear trend is for the primordial signal to fade as we go to higher redshift, while the GR contribution rises, just as we saw in figure 16. This has a natural interpretation, as the GR signal we are looking at is lensing, which is expected

The tracers here can be for example different kinds of galaxies which are known to have different biases. Alonso and Ferreira (2015) as an example use red and blue galaxies in their forecasts.

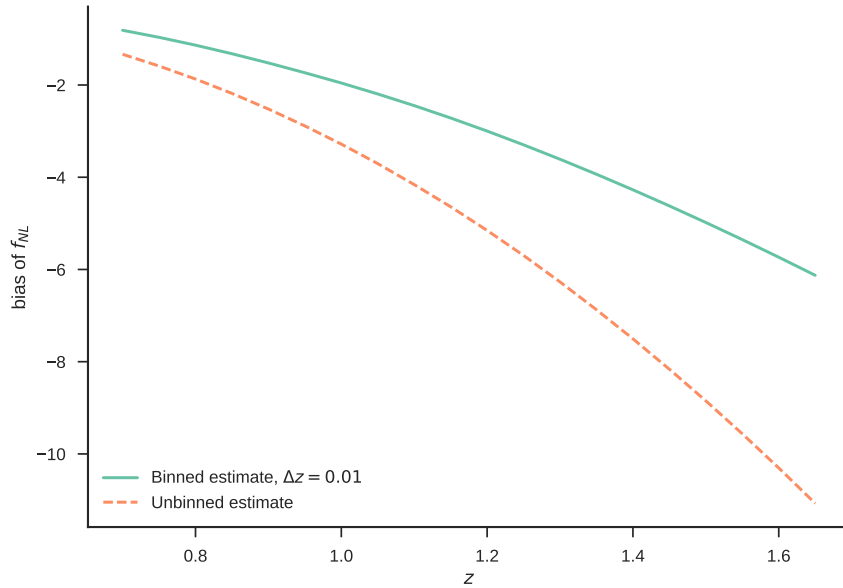


Figure 16: Plot of the contamination from lensing effects on the local f_{NL} parameter from binned and unbinned estimates. Evidently, binning does reduce the pollution from lensing effects, but only by roughly a factor 2.

to rise as we look further out in the universe, in particular at small scales. The all-density contribution, which is the major part of the primordial signal, however, is expected to reduce as we look at the younger universe. It therefore comes as no surprise that the size of the bias of f_{NL} grows as we go to higher redshift. Moreover, we see that for local primordial non-gaussianity, the signals expected from GR corrections look almost exactly like the primordial signal. This cements the need for precise theoretical calculations, as there is no obvious way to distinguish the signals experimentally. One must therefore rely on the theory to do proper subtraction of the unwanted signal.

Whether it be cosmic variance limited surveys or more indirect observations of the non-gaussianities, it is clear that precise computations of the GR contribution beyond RSD to the observed density field is needed. The calculation of these effects in the very physical coordinates we have performed here facilitates the inclusion of lensing. As the estimates in this last chapter shows, it is absolutely necessary to have fast and precise ways of doing these computations. The flat-sky computations are one way of obtaining this. Without the simplifications they result in, the computations in this chapter would not have been possible to obtain in any reasonable time.

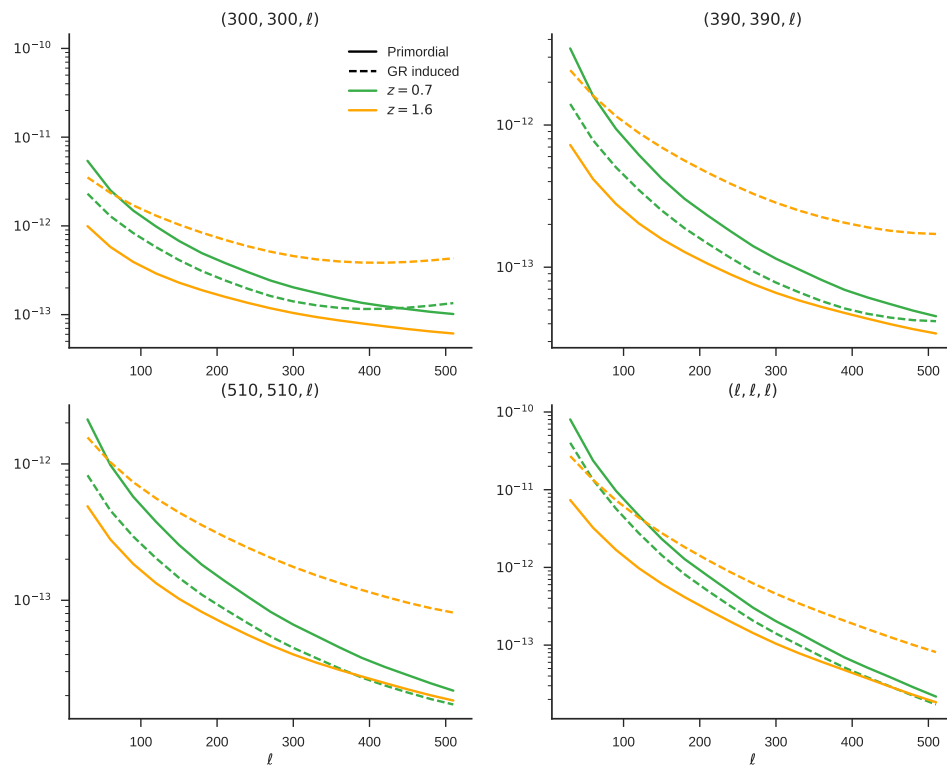


Figure 17: Plot of the absolute value of the bispectrum from a local primordial non-gaussianity and from general relativity. The signals are calculated in top-hat bins of width 0.01. The ℓ configurations are as described above each plot. The same legend describes all the plots.

FINAL REMARKS

To date, every cosmological experiment seems to be in agreement with the predictions of the simple concordance model. At the same time, every corner of the model is entirely mysterious to theorists. Inflation at its core relies on the energy density of the vacuum expectation value of a scalar field to make the inflationary scenario happen – a thing which is *not* happening for the Higgs field, the only scalar field we know exists today. In essence, the mechanism one uses is – if not falsified – completely unverified. The same logic applies to the dark energy of the Λ CDM model. The tiny amount of dark energy, in terms of fundamental physics, has no obvious explanation. The cosmological constant – the most obvious answer – would be the most fine-tuned physical constant ever observed. Even dark matter, as much evidence as there seems to be for it, has never been observed directly. All evidence we have, whether it be from CMB, LSS, galaxy cluster collisions, lensing, etc. are indirect and circumstantial. We always see its gravitational effects on something else, *never* any particle-like effect. All direct searches through colliders, or fixed-target experiments have so far *failed*.

For all these reasons, it is important to hold a theory to its predictions. A theory which can be tailored to fit anything, does not predict anything. However, all coming predictions are *de facto* small effects, since all data so far seem to fit the concordance model so well. This puts stress on precision calculations, not just of the new theory, but as much on the old theory. My work has focussed on the latter – precision predictions of general relativity.

In this thesis I have focused on the calculation of the bispectrum of galaxy number count correlations from gravitational effects. At small scales, one may separate the effects of general relativity into the dominating terms, and the remaining terms, which are suppressed by at least k/\mathcal{H} . In this small-scale limit, I have calculated the perturbative effects to all orders by combining the calculations in the geodesic lightcurve coordinates with results from lensing calculations. This has allowed me to check and verify the calculations in recent literature. The results have since been propagated to the relevant publications, which have been corrected.

As one needs more and more precise computations and observations, clearly the computational complexity rises. I have therefore developed the flat-sky approximation for galaxy number counts, which greatly decreases the computing time for both the power spectrum and the bispectrum. This approximation is *very* good, even at relatively large scales. The approximation relies on manually removing

beat-like effect in the integrands, and on the Limber approximation for contributions integrated over the past light-cone.

The computations I do show that when looking for the faint signatures of inflationary theories, it is of utmost importance to include – or rather subtract – lensing effects in the analysis. If this is not done properly, purely general relativistic effects may look like signs of inflation. This is in good agreement with earlier publications from this year. I have extended these computations, as is only possible thanks to the flat-sky approximation.

The effects I calculate are naturally part of a bigger picture. Beyond the Newtonian calculation, I have not included the non-linear evolution of galaxy clustering, and I have made a number of simplifying assumptions. I assume a full sky, and I do not include any systematic effects of experiments. However, all the calculations done here are easily extended to accommodate such effects. For example, the transfer functions may take into account non-linear evolution, and this does not change the following calculations.

The calculations I have done will allow experiments to really test the tiny effects of inflation. For all its virtues, it does not seem that theorists agree whether inflation works, and we have so far seen *no* direct evidence for it. I have therefore focussed on the possibility of directly observing an inflationary bispectrum. While it seems possible in the idealised setting I have provided, it will take a fantastic effort on the part of experiments to do both observations and data-reduction to the precision needed.

LIST OF FIGURES

| | | |
|-----------|---|----|
| Figure 1 | Illustration of the different terms of the <i>connected</i> three-point correlator. | 7 |
| Figure 2 | $A_\ell^{(m)}$ approximations. | 18 |
| Figure 3 | Illustration of last scattering by the NASA/WMAP Science Team. | 28 |
| Figure 4 | 2015 Planck temperature power spectrum | 32 |
| Figure 5 | Comparison of flat sky computation with CLASS result. | 35 |
| Figure 6 | Illustration of the approximation of the spherical Bessel function by equation (4.2.147) | 62 |
| Figure 7 | Galaxy count power spectrum for equal redshift | 68 |
| Figure 8 | Galaxy count power spectrum difference for equal redshift | 69 |
| Figure 9 | Galaxy count power spectrum for similar redshift | 70 |
| Figure 10 | Galaxy count power spectrum difference for similar redshift | 71 |
| Figure 11 | Galaxy count power spectrum for very different redshift | 72 |
| Figure 12 | Illustration of the three higher order corrections to the bispectrum | 87 |
| Figure 13 | Power spectrum and bispectrum in the EFT | 92 |
| Figure 14 | Angular CMB power spectrum and bispectrum in the EFT | 94 |
| Figure 15 | Redshift dependence on the signal-to-noise of the galaxy number count bispectrum in the Λ CDM model | 96 |
| Figure 16 | Plot of the contamination from lensing effects on the local f_{NL} parameter | 98 |
| Figure 17 | Plot of the absolute value of the bispectrum | 99 |

PUBLICATIONS

This thesis is based in part on the following publications:

JEPPE TRØST NIELSEN AND RUTH DURRER, 2017

Higher order relativistic galaxy number counts: dominating terms

The major catalyst for this thesis. We checked the existing literature for inconsistencies in the dominating terms in the galaxy number counts. This made sure all the existing calculations agreed as far as the dominating terms.

LAURE BERTHIER AND JEPPE TRØST NIELSEN, 2016

Statistics of predictions with missing higher order corrections

This paper describes a new statistical method for fitting of parameters in incomplete series expansions. This was used to fit electroweak data to the standard model effective field theory. The major, very simple result of the work is that as long as one has no evidence of the theory – as is the case for the standard model effective field theory – one should simply *do nothing*. When checking if the original ‘unperturbed’ theory – for example the standard model – is a good fit, including *any extra error at all is wrong*.

JEPPE TRØST NIELSEN, 2015

Supernovae as cosmological probes

My master’s thesis explaining in great detail the results of the supernova analysis we did. It includes an introduction to probability theory, macroscopic cosmological evolution, and supernova studies.

JEPPE TRØST NIELSEN, ALBERTO GUFFANTI, AND SUBIR SARKAR, 2016

Marginal evidence for cosmic acceleration from Type Ia supernovae

The main driver of my master’s work, an analysis of supernova observations, including the distributions of correction parameters explicitly in the analysis.

BIBLIOGRAPHY

- ABBOTT, B. P. ET AL. 2016a. GW150914: First results from the search for binary black hole coalescence with Advanced LIGO. *Phys. Rev.* **D93**, 12, 122003; [arXiv:\[1602.03839\]](#).
- ABBOTT, T. ET AL. 2016b. The Dark Energy Survey: more than dark energy – an overview. *Mon. Not. Roy. Astron. Soc.* **460**, 2, 1270–1299; [arXiv:\[1601.00329\]](#).
- ACHUCARRO, A., GONG, J.-O., HARDEMAN, S., PALMA, G. A., AND PATIL, S. P. 2011a. Features of heavy physics in the CMB power spectrum. *JCAP* **1101**, 030; [arXiv:\[1010.3693\]](#).
- ACHUCARRO, A., GONG, J.-O., HARDEMAN, S., PALMA, G. A., AND PATIL, S. P. 2011b. Mass hierarchies and non-decoupling in multi-scalar field dynamics. *Phys. Rev.* **D84**, 043502; [arXiv:\[1005.3848\]](#).
- ACHÚCARRO, A., GONG, J.-O., PALMA, G. A., AND PATIL, S. P. 2013. Correlating features in the primordial spectra. *Phys. Rev.* **D87**, 12, 121301; [arXiv:\[1211.5619\]](#).
- ADE, P. A. R. ET AL. 2016. Planck 2015 results. XIII. Cosmological parameters. *Astron. Astrophys.* **594**, A13; [arXiv:\[1502.01589\]](#).
- ADE, P. A. R. ET AL. 2015. Joint Analysis of BICEP2/KeckArray and Planck Data. *Phys. Rev. Lett.* **114**, 101301; [arXiv:\[1502.00612\]](#).
- ADE, P. A. R. ET AL. 2014b. Planck 2013 Results. XXIV. Constraints on primordial non-Gaussianity. *Astron. Astrophys.* **571**, A24; [arXiv:\[1303.5084\]](#).
- ADE, P. A. R. ET AL. 2014a. Detection of *B*-Mode Polarization at Degree Angular Scales by BICEP2. *Phys. Rev. Lett.* **112**, 24, 241101; [arXiv:\[1403.3985\]](#).
- AGHANIM, N. ET AL. 2016. Planck 2015 results. XI. CMB power spectra, likelihoods, and robustness of parameters. *Astron. Astrophys.* **594**, A11; [arXiv:\[1507.02704\]](#).
- ALONSO, D. AND FERREIRA, P. G. 2015. Constraining ultralarge-scale cosmology with multiple tracers in optical and radio surveys. *Phys. Rev.* **D92**, 6, 063525; [arXiv:\[1507.03550\]](#).
- ASOREY, J., CARRASCO KIND, M., SEVILLA-NOARBE, I., BRUNNER, R. J., AND THALER, J. 2016. Galaxy clustering with photometric surveys using PDF redshift information. *Mon. Not. Roy. Astron. Soc.* **459**, 2, 1293–1309; [arXiv:\[1601.00357\]](#).
- BABICH, D., CREMINELLI, P., AND ZALDARRIAGA, M. 2004. The Shape of non-Gaussianities. *JCAP* **0408**, 009; [arXiv:\[astro-ph/0405356\]](#).

- BAUMANN, D. 2011. Inflation. In *Physics of the large and the small, TASI 09, proceedings of the Theoretical Advanced Study Institute in Elementary Particle Physics, Boulder, Colorado, USA, 1-26 June 2009*. 523–686.
- BENNETT, C. L. ET AL. 2003. First year Wilkinson Microwave Anisotropy Probe (WMAP) observations: Preliminary maps and basic results. *Astrophys. J. Suppl.* **148**, 1–27; [arXiv:\[astro-ph/0302207\]](#).
- BERNARDEAU, F., COLOMBI, S., GAZTANAGA, E., AND SCOCCIMARRO, R. 2002. Large scale structure of the universe and cosmological perturbation theory. *Phys.Rept.* **367**, 1–248; [arXiv:\[astro-ph/0112551\]](#).
- BERNARDEAU, F., PITROU, C., AND UZAN, J.-P. 2011. CMB spectra and bispectra calculations: making the flat-sky approximation rigorous. *JCAP* **1102**, 015; [arXiv:\[1012.2652\]](#).
- BERNARDEAU, F., WAERBEKE, L. V., AND MELLIER, Y. 2003. Patterns in the weak shear 3-point correlation function. *Astron. Astrophys.* **397**, 405–414; [arXiv:\[astro-ph/0201029\]](#).
- BERTACCA, D. 2015. Observed galaxy number counts on the lightcone up to second order: III. Magnification Bias. *Class. Quant. Grav.* **32**, 195011; [arXiv:\[1409.2024\]](#).
- BERTACCA, D., MAARTENS, R., AND CLARKSON, C. 2014b. Observed galaxy number counts on the lightcone up to second order: II. Derivation. *JCAP* **1411**, 013; [arXiv:\[1406.0319\]](#).
- BERTACCA, D., MAARTENS, R., AND CLARKSON, C. 2014a. Observed galaxy number counts on the lightcone up to second order: I. Main result. *JCAP* **1409**, 037; [arXiv:\[1405.4403\]](#).
- BERTHIER, L. AND NIELSEN, J. T. 2016. Statistics of predictions with missing higher order corrections; [arXiv:\[1610.01783\]](#).
- BLAS, D., LESGOURGUES, J., AND TRAM, T. 2011. The Cosmic Linear Anisotropy Solving System (CLASS) II: Approximation schemes. *JCAP* **1107**, 034; [arXiv:\[1104.2933\]](#).
- BOLEJKO, K. AND KORZYŃSKI, M. 2016. Inhomogeneous cosmology and backreaction: current status and future prospects; [arXiv:\[1612.08222\]](#).
- BONVIN, C. AND DURRER, R. 2011. What galaxy surveys really measure. *Phys.Rev.* **D84**, 063505; [arXiv:\[1105.5280\]](#).
- BOYLE, M. 2016. How should spin-weighted spherical functions be defined? *J. Math. Phys.* **57**, 9, 092504; [arXiv:\[1604.08140\]](#).
- CHLUBA, J., HAMANN, J., AND PATIL, S. P. 2015. Features and New Physical Scales in Primordial Observables: Theory and Observation. *Int. J. Mod. Phys.* **D24**, 10, 1530023; [arXiv:\[1505.01834\]](#).

- CREMINELLI, P., NICOLIS, A., SENATORE, L., TEGMARK, M., AND ZALDARRIAGA, M. 2006. Limits on non-gaussianities from wmap data. *JCAP* **0605**, 004; [arXiv:\[astro-ph/0509029\]](#).
- CRESWELL, J., VON HAUSEGGER, S., JACKSON, A. D., LIU, H., AND NASELSKY, P. 2017. On the time lags of the LIGO signals; [arXiv:\[1706.04191\]](#).
- DALAL, N., DORE, O., HUTERER, D., AND SHIROKOV, A. 2008. The imprints of primordial non-gaussianities on large-scale structure: scale dependent bias and abundance of virialized objects. *Phys. Rev.* **D77**, 123514; [arXiv:\[0710.4560\]](#).
- DI DIO, E., DURRER, R., MAROZZI, G., AND MONTANARI, F. 2014. Galaxy number counts to second order and their bispectrum. *JCAP* **1412**, 017; [arXiv:\[1407.0376\]](#). [Erratum: *JCAP* **1506**, E01 (2015)].
- DI DIO, E., DURRER, R., MAROZZI, G., AND MONTANARI, F. 2016. The bispectrum of relativistic galaxy number counts. *JCAP* **1601**, 016; [arXiv:\[1510.04202\]](#).
- DI DIO, E., PERRIER, H., DURRER, R., MAROZZI, G., DIZGAH, A. M., NOREÑA, J., AND RIOTTO, A. 2017. Non-Gaussianities due to Relativistic Corrections to the Observed Galaxy Bispectrum. *JCAP* **1703**, 03, 006; [arXiv:\[1611.03720\]](#).
- DODELSON, S. 2003. *Modern cosmology*. Academic press.
- DURRER, R. 2008. *The Cosmic Microwave Background*. Cambridge University Press.
- ELLIS, G., NEL, S., MAARTENS, R., STOEGER, W., AND WHITMAN, A. 1985. Ideal observational cosmology. *Physics Reports* **124**, 5, 315 – 417.
- FANIZZA, G., GASPERINI, M., MAROZZI, G., AND VENEZIANO, G. 2013. An exact Jacobi map in the geodesic light-cone gauge. *JCAP* **1311**, 019; [arXiv:\[1308.4935\]](#).
- FANIZZA, G., GASPERINI, M., MAROZZI, G., AND VENEZIANO, G. 2015. A new approach to the propagation of light-like signals in perturbed cosmological backgrounds. *JCAP* **1508**, 020; [arXiv:\[1506.02003\]](#).
- FERGUSON, J. AND SHELLARD, E. 2008. [The shape of primordial non-gaussianity and the cmb bispectrum](#); [arXiv:\[0812.3413\]](#).
- FIXSEN, D. J. 2009. The Temperature of the Cosmic Microwave Background. *Astrophys. J.* **707**, 916–920; [arXiv:\[0911.1955\]](#).
- GANGUI, A. AND MARTIN, J. 2000. Best unbiased estimators for the three point correlators of the cosmic microwave background radiation. *Phys. Rev.* **D62**, 103004; [arXiv:\[astro-ph/0001361\]](#).
- GASPERINI, M., MAROZZI, G., NUGIER, F., AND VENEZIANO, G. 2011. Light-cone averaging in cosmology: Formalism and applications. *JCAP* **1107**, 008; [arXiv:\[1104.1167\]](#).

- HUNT, P. AND SARKAR, S. 2007. Multiple inflation and the WMAP glitches. 2. Data analysis and cosmological parameter extraction. *Phys. Rev.* **D76**, 123504; [arXiv:\[0706.2443\]](#).
- HUNT, P. AND SARKAR, S. 2015. Search for features in the spectrum of primordial perturbations using Planck and other datasets. *JCAP* **1512**, 12, 052; [arXiv:\[1510.03338\]](#).
- ISSERLIS, L. 1916. On certain probable errors and correlation coefficients of multiple frequency distributions with skew regression. *Biometrika* **11**, 3 (May), 185–190.
- JACKSON, A. AND MAXIMON, L. 1972. Integrals of products of bessel functions. *SIAM Journal on Mathematical Analysis* **3**, 3, 446–460.
- KOMATSU, E. AND SPERGEL, D. N. 2000. The Cosmic Microwave Background bispectrum as a test of the physics of inflation and probe of the astrophysics of the low-redshift Universe. In *Recent developments in theoretical and experimental general relativity, gravitation and relativistic field theories. Proceedings, 9th Marcel Grossmann Meeting, MG'9, Rome, Italy, July 2-8, 2000. Pts. A-C.* 2009–2012.
- KRAUSS, L., DODELSON, S., AND MEYER, S. 2010. Primordial Gravitational Waves and Cosmology. *Science* **328**, 989–992; [arXiv:\[1004.2504\]](#).
- KROESE, D. P., TAIMRE, T., AND BOTEV, Z. I. 2013. *Handbook of monte carlo methods*. Vol. 706. John Wiley & Sons.
- LESGOURGUES, J. 2011. [The cosmic linear anisotropy solving system \(class\) i: Overview](#); [arXiv:\[1104.2932\]](#).
- LEWIS, A. 2013. Efficient sampling of fast and slow cosmological parameters. *Phys. Rev.* **D87**, 103529; [arXiv:\[1304.4473\]](#).
- LEWIS, A. AND BRIDLE, S. 2002. Cosmological parameters from CMB and other data: A Monte Carlo approach. *Phys. Rev.* **D66**, 103511; [arXiv:\[astro-ph/0205436\]](#).
- LIU, H. AND JACKSON, A. D. 2016. Possible associated signal with GW150914 in the LIGO data. *JCAP* **1610**, 10, 014; [arXiv:\[1609.08346\]](#).
- LUO, X.-C. 1994. The Angular bispectrum of the cosmic microwave background. *Astrophys. J.* **427**, L71; [arXiv:\[astro-ph/9312004\]](#).
- LUSCOMBE, J. H. AND LUBAN, M. 1998. Simplified recursive algorithm for wigner 3 j and 6 j symbols. *Physical Review E* **57**, 6, 7274.
- MAJEROTTO, E. ET AL. 2012. Probing deviations from General Relativity with the Euclid spectroscopic survey. *Mon. Not. Roy. Astron. Soc.* **424**, 1392–1408; [arXiv:\[1205.6215\]](#).
- MAROZZI, G. 2015. The luminosity distance–redshift relation up to second order in the Poisson gauge with anisotropic stress. *Class. Quant. Grav.* **32**, 4, 045004; [arXiv:\[1406.1135\]](#). [Corrigendum: *Class. Quant. Grav.*32,179501(2015)].

- McDONALD, P. AND ROY, A. 2009. Clustering of dark matter tracers: generalizing bias for the coming era of precision LSS. *JCAP* **0908**, 020; [arXiv:\[0902.0991\]](#).
- McDONALD, P. AND SELJAK, U. 2009. How to measure redshift-space distortions without sample variance. *JCAP* **0910**, 007; [arXiv:\[0810.0323\]](#).
- MUKHANOV, V. 2005. *Physical foundations of cosmology*. Cambridge university press.
- MUKHANOV, V. F. 2004. CMB-slow, or how to estimate cosmological parameters by hand. *Int. J. Theor. Phys.* **43**, 623–668; [arXiv:\[astro-ph/0303072\]](#).
- MUNSHI, D., VALAGEAS, P., VAN WAERBEKE, L., AND HEAVENS, A. 2008. Cosmology with Weak Lensing Surveys. *Phys. Rept.* **462**, 67–121; [arXiv:\[astro-ph/0612667\]](#).
- NASELSKY, P., JACKSON, A. D., AND LIU, H. 2016. Understanding the LIGO GW150914 event. *JCAP* **1608**, 08, 029; [arXiv:\[1604.06211\]](#).
- NEWMAN, E. T. AND PENROSE, R. 1966. Note on the bondi-metzner-sachs group. *Journal of Mathematical Physics* **7**, 5, 863–870.
- NIELSEN, J. T. 2015. [Supernovae as cosmological probes](#); [arXiv:\[1508.07850\]](#).
- NIELSEN, J. T. AND DURRER, R. 2017. Higher order relativistic galaxy number counts: dominating terms. *JCAP* **1703**, 03, 010; [arXiv:\[1606.02113\]](#).
- NIELSEN, J. T., GUFFANTI, A., AND SARKAR, S. 2016. Marginal evidence for cosmic acceleration from Type Ia supernovae. *Sci. Rep.* **6**, 35596; [arXiv:\[1506.01354\]](#).
- PAJER, E. AND ZALDARRIAGA, M. 2013. On the Renormalization of the Effective Field Theory of Large Scale Structures. *JCAP* **1308**, 037; [arXiv:\[1301.7182\]](#).
- PYNE, T. AND CARROLL, S. M. 1996. Higher order gravitational perturbations of the cosmic microwave background. *Phys. Rev.* **D53**, 2920–2929; [arXiv:\[astro-ph/9510041\]](#).
- SARKAR, S. 2008. Is the evidence for dark energy secure? *Gen. Rel. Grav.* **40**, 269–284; [arXiv:\[0710.5307\]](#).
- SELJAK, U. AND ZALDARRIAGA, M. 1996. A Line of sight integration approach to cosmic microwave background anisotropies. *Astrophys. J.* **469**, 437–444; [arXiv:\[astro-ph/9603033\]](#).
- SENATORE, L. AND ZALDARRIAGA, M. 2014. Redshift Space Distortions in the Effective Field Theory of Large Scale Structures; [arXiv:\[1409.1225\]](#).
- SPERGEL, D. N. ET AL. 2003. First year Wilkinson Microwave Anisotropy Probe (WMAP) observations: Determination of cosmological parameters. *Astrophys. J. Suppl.* **148**, 175–194; [arXiv:\[astro-ph/0302209\]](#).
- STEINHARDT, P. J. 2004. Cosmological perturbations: Myths and facts. *Mod. Phys. Lett.* **A19**, 967–982.

- STEINHARDT, P. J. 2011. The inflation debate: Is the theory at the heart of modern cosmology deeply flawed? *Sci. Am.* **304**N4, 18–25.
- TUTUSAUS, I., LAMINE, B., DUPAYS, A., AND BLANCHARD, A. 2017. Is cosmic acceleration proven by local cosmological probes? *Astron. Astrophys.* **602**, A73; [arXiv:\[1706.05036\]](#).
- URSELL, H. 1927. The evaluation of gibbs' phase-integral for imperfect gases. *Mathematical Proceedings of the Cambridge Philosophical Society* **23**, 6 (April), 685–697.
- VARSHALOVICH, D. A., MOSKALEV, A. N., AND KHERSONSKIĬ, V. K. 1988. *Quantum Theory of Angular Momentum*. World Scientific Publishing Co. Inc., Singapore.
- WICK, G. C. 1950. The evaluation of the collision matrix. *Physical Review* **80**, 2, 268–272.
- YOO, J. AND ZALDARRIAGA, M. 2014. Beyond the Linear-Order Relativistic Effect in Galaxy Clustering: Second-Order Gauge-Invariant Formalism. *Phys.Rev.* **D90**, 023513; [arXiv:\[1406.4140\]](#).